INFORMATION TO USERS

This manuscript has been reproduced from the microfilm master. UMI films the text directly from the original or copy submitted. Thus, some thesis and dissertation copies are in typewriter face, while others may be from any type of computer printer.

The quality of this reproduction is dependent upon the quality of the copy submitted. Broken or indistinct print, colored or poor quality illustrations and photographs, print bleedthrough, substandard margins, and improper alignment can adversely affect reproduction.

In the unlikely event that the author did not send UMI a complete manuscript and there are missing pages, these will be noted. Also, if unauthorized copyright material had to be removed, a note will indicate the deletion.

Oversize materials (e.g., maps, drawings, charts) are reproduced by sectioning the original, beginning at the upper left-hand corner and continuing from left to right in equal sections with small overlaps.

Photographs included in the original manuscript have been reproduced xerographically in this copy. Higher quality 6" x 9" black and white photographic prints are available for any photographs or illustrations appearing in this copy for an additional charge. Contact UMI directly to order.

Bell & Howell Information and Learning
300 North Zeeb Road, Ann Arbor, MI 48106-1346 USA
800-521-0600

Université d'Ottawa · University of Ottawa

UNIVERSITY OF OTTAWA

Mechanisms of the Assembly of Hepatic Very Low Density Lipoprotein in Rat Hepatoma McA-RH7777 Cells

BY

Yuwei Wang

A Thesis Submitted to the School of Graduate Studies and Research
in Partial Fulfillment of the Requirements for the Degree of
DOCTOR OF PHILOSOPHY in Biochemistry

Department of Biochemistry, Microbiology and Immunology
Faculty of Medicine

Ottawa, Ontario

Abstract

The role of apolipoprotein B (apoB) and microsomal triglyceride transfer protein (MTP) in hepatic triglyceride (TG)-rich very low density lipoprotein (VLDL) assembly has been investigated. Rat hepatoma McA-RH7777 cells were used to characterize structural determinants within apoB that are required for VLDL assembly/secretion, and to define mechanisms through which MTP facilitates VLDL assembly/secretion. Working with McA-RH7777 cells stably expressing recombinant human apoB100 (representing the full-length apoB) and various carboxyl-terminally truncated apoB proteins, we found that the apoB forms equal to or shorter than apoB29 (representing the amino-terminal 29% of the full-length apoB) were unable to assemble VLDL, whereas those equal to or longer than apoB34 could. Detailed biochemical analysis using apoB100- and apoB48-transfected cells revealed that assembly of VLDL, irrespective of the apoB length, was achieved through the same general pathway. Three notable features associated with the VLDL assembly process in McA-RH7777 cells were: (a) VLDL assembly was absolutely dependent upon exogenous oleate, (b) VLDL assembly was achieved post-translationally, and (c) the hallmark of VLDL assembly was the incorporation of bulk TG. Using chemical inhibitors of MTP, we found that MTP activity was required in the assembly/secretion of TG-rich VLDL, and that the requirement of MTP activity was determined by the amount of TG utilized for lipoprotein assembly. Moreover, the accumulation and attainment of TG within microsomal lumen was a function of MTP activity. Thus, MTP plays a role in facilitating the accumulation of TG within microsomes, an event that can be separated from TG incorporation into mature VLDL but represents an indispensable requisite for the post-translational assembly of TG-enriched VLDL.

Acknowledgements

In some respects, this part is the most important of the entire dissertation, in that, completion of this work is no doubt efforts of many individuals with whom I have interacted during the tenure of my post-graduate training. Through interactions and relationships with these individuals over the past six years, I was guided, challenged, stimulated, sustained, encouraged, and finally I succeeded.

I am most indebted to Dr. Zemin Yao, my mentor and thesis advisor. Dr. Yao has contributed greatly to my personal and professional development by assisting me to navigate every course and milestone of my scientific career. He has shown me by his example and guidance the way of making long and arduous transition from an apprentice to a scientist. I can remember clearly that he spared his weekends to show me ropes in making a Maxiprep and running thin layer chromotography when I started up. I can still remember vividly the joy that emanated from rich scientific discussions with him when I became senior. I appreciate Dr. Yao's boundless patience for giving me complete freedom to develop my own ideas and interests in research. Whenever I experienced difficulties in my project, he is always available to provide me with his intellectual and moral support. It is him who has helped me to believe in myself and to believe that this research project is attainable. His uncompromising critiques and high standard in quality have enhanced this project significantly. Most importantly, he has been a true friend in my personal life, and taught me the philosophy of the life and how to collaborate and work with people. For all these, I couldn't have asked for a better mentor.

I would also like to acknowledge Dr. Khai Tran and Dr. Roger McLeod for their fruitful collaborations in this project. Khai has worked with me on a daily basis in the last two years. I really enjoyed our intellectual discussion, and appreciated greatly our struggles in overcoming the technical barriers towards our understanding the role of MTP in lipid mobilization within hepatocytes. Roger helped me to set up the experimental procedures when I started up, and shared his experimental data with me, leading to the publication of two manuscripts.

Many thanks to the people in Dr. Yao's lab: the people in Edmonton, whose excellent works have built a solid foundation for this work; and the people in Ottawa, who have provided me support in all aspects. Dr. Kerry Ko is certainly a cheerful person to work with. He has brought me much laughter, and is always available to provide critical comments whenever needed, in my manuscript preparation and my seminar presentation. I am also indebted to the fellow students Rita Kohen-Avramoglu, Robert Brown, Philip Links and Jelena Vukmirica, for their helpful ideas and comments in this project. I am grateful for the technical support from Shelley Wang and Dawn Song. Through daily excursions with Kerry, Khai and Philip, we have shared many happiness and sadness in our scientific life. Through many evenings I spent in the lab with Kerry and Robert, we developed our friendship. I look forward to scientific collaboration and friendship with these people throughout my lifetime.

I also thank all the members in the Lipoprotein and Atherosclerosis Group at the University of Ottawa Heart Institute for their efforts in creating a well-organized research

environment. I have been benefited greatly in this "open-house" research group during the tenure of my post-graduate training. Special thanks to Drs. Yves Marcel, Ross Milne, Ruth McPherson and Daniel Sparks for their generosity to share their ideas, knowledge, and expertise whenever I need them. I also acknowledge Vinita Chauhan for preparing human LDL, Xingyu Wang for helping me to perform radioimmunoassay, Tracey Neville for teaching me enzyme assay, and Vivian Franklin for purifying 1D1 IgG. I am grateful for the excellent administrative work from Anna Toma and Ann Buie.

I am thankful to Dr. Teik Ooi of Ottawa Civic Hospital, whose insightful comment in VLDL subclasses and encouragement have opened a new direction in this project. I would like to thank my graduate study committee members, Drs. Yves Marcel, Johnny Ngsee and Alex Sorisky, for their advice that leads to successful completion of this work. I acknowledge Dr. Vas Mezl who tried his best to solve my academic problems.

I acknowledge Drs. Ross Milne and Yves Marcel for providing me the monoclonal anti-human apoB antibody 1D1, Dr. David Gordon (Bristol-Myers Squibb) for the MTP inhibitors, and Dr. Larry Wong (Louisiana University) for the monoclonal antibody to rat apoB.

I would like to extend my sincere gratitude to Dr. Zemin Yao, Dr. Kerry Ko and Robert Brown for their critical reading of this thesis in a timely fashion. I thank my dissertation committee members, Drs. Mary-Ellen Harper, Ross Milne, Daniel Sparks and

Jean Vance, for their contributions and advice leading to the completion of this dissertation.

I wish to thank Dr. Zemin Yao, the Natural Sciences and Engineering Research Council of Canada, the Heart and Stroke Foundation of Canada and the School of Graduate Studies and Research at the University of Ottawa for providing me the financial support during my graduate study.

Lastly, I wish to extend my sincere gratitude to my wife Felicia, who has provided the best support I could ever ask for during the tenure of my post-graduate training. She understands me without knowing, and has shown a greatest concern for my progress. For that, saying "thank you" is never enough.

Dedications

I dedicate this thesis to my family, especially to my parents and my grandparents.

Table of Contents

List of Tables

List of Figures

Abbreviations

ADP	adenosine diphosphate
ALLN	N-acetyl-leucyl-leucyl-norleucinal
Apo	apolipoprotein
ARF	ADP ribosylation factor
ATP	adenosine triphosphate
BfA	brefeldin A
BSA	bovine serum albumin
C-terminus	carboxyl-terminus
CE	cholesteryl ester
CHO	Chinese Hamster Ovary
DG	diacylglycerol
DGAT	diacylglycerol acyl transferase
DHA	docosahexaenoic acid
DMEM	Dulbecco's modified Eagle's medium
ECL	enhanced chemiluminescence
EPA	eicosapentaenoic acid
ER	endoplasmic reticulum
ERGIC	ER-Golgi intermediate compartment
FBS	fetal bovine serum
GDP	guanosine diphosphate
GTP	guanosine triphosphate
hB48	human apoB48

hB100	human apoB100
HDL	high density lipoproteins
IDL	intermediate density lipoproteins
/MTP	large subunit of MTP
LpB	apoB-containing lipoproteins
LDL	low density lipoproteins
LV	lipovitellin
MTP	microsomal triglyceride transfer protein
N-terminus	amino-terminus
NEFA	non-esterified fatty acids
OA	oleic acid
PA	phosphatidic acid
PAGE	polyacrylamide gel electrophoresis
PBS	phosphate buffered saline
PC	phosphatidylcholine
PDI	protein disulfide isomerase
PE	phosphatidylethanolamine
PI	phosphatidylinositol
PL	phospholipid
PMME	phosphatidylmonomethylethanolamine
PS	phosphatidylserine
rB48	rat apoB48
rB100	rat apoB100

S_f	Svedberg unit
SDS	sodium dodecyl sulphate
SRP	signal recognition particle
TG	triacylglycerol
TLC	thin-layer chromatography
TRAM	translocation chain-associated membrane proteins
VLDL	very low density lipoproteins
VTG	vitellogenin

Amino acids are referred by the single letter code or the three-letter code.

A	Ala	Alanine
C	Cys	Cysteine
D	Asp	Aspartic Acid
E	Glu	Glutamic acid
F	Phe	Phenylalanine
G	Gly	Glycine
H	His	Histidine
I	Ile	Isoleucine
K	Lys	Lysine
L	Leu	Leucine
M	Met	Methionine
N	Asn	Asparagine
P	Pro	Proline

Q	Gln	Glutamine
R	Arg	Arginine
S	Ser	Serine
T	Thr	Threonine
V	Val	Valine
W	Trp	Tryptophan
Y	Tyr	Tyrosine

Chapter 1 Introduction

1.1. Introduction

Very low density lipoproteins (VLDL, d < 1.006 g/ml, refer to Table I for classification of lipoproteins) are triacylglycerol (TG)-rich particles that are produced by the liver. The function of VLDL is to transport TG from the liver to the peripheral tissues via the bloodstream. Within the bloodstream, TG associated with VLDL is hydrolyzed by the action of lipoprotein lipase. During this process, plasma VLDL is converted into intermediate density lipoproteins (IDL, d = 1.006-1.019 g/ml), and further into low density lipoproteins (LDL, d = 1.019-1.063 g/ml) (1). Plasma LDL is cleared from the bloodstream through the LDL receptor mediated endocytosis (2). The plasma concentration of all these lipoproteins, including VLDL, IDL and LDL, is positively correlated with the propensity to develop atherosclerosis (1). Since plasma VLDL particles are the precursors of IDL and LDL, hepatic production of TG-rich VLDL is a key determinant of the plasma concentration of atherogenic lipoproteins.

Assembly of TG-rich VLDL in the liver is a complicated metabolic process, and requires not only coordination in the synthesis of both the protein and lipid components of VLDL, but also protein factors that facilitate intracellular mobilization and incorporation of these components to form a large lipid-protein complex. One of the key protein components of VLDL is apolipoprotein (apo) B100. Mutations in the apoB gene in hypobetalipoproteinemia subjects result in secretion of truncated forms of the protein. In most cases, secretion of hepatic VLDL is also compromised (3). In transgenic mice,

alterations in the apoB gene, but not other apolipoprotein genes, dramatically decrease hepatic VLDL assembly and secretion (4).

Another protein, called microsomal triglyceride transfer protein (MTP), also plays a critical role in hepatic VLDL assembly. Although MTP itself is not a component of VLDL, it is an auxiliary factor that facilitates the assembly of hepatic VLDL. A defective MTP gene is the proximal cause of abetalipoproteinemia, a recessive genetic disorder in the secretion of normal apoB-containing lipoproteins (LpB) (5). [Both abetalipoproteinemia and hypobetalipoproteinemia subjects may exhibit a similar phenotype, such as malabsorption of dietary fat and of the fat-soluble vitamins (6).] Liver-specific MTP knockout in transgenic mice results in abolition of hepatic VLDL secretion (7, 8).

The mechanism responsible for hepatic TG-rich VLDL assembly has been examined extensively over the past two decades. Much progress has been made in understanding the role of apoB and MTP in recruitment of a large amount of TG (bulk TG) during VLDL assembly. In this Chapter, I will summarize our current knowledge in the following three areas. (a) The structure of apoB and MTP, and the molecular details of their interaction. (b) The biogenesis of apoB and the associated events such as initial lipidation of apoB and degradation of apoB. (c) The assembly of TG-rich VLDL, particularly the origin of TG required for VLDL assembly, the cellular localization for VLDL maturation, and the requirement of multiple protein factors (including MTP) during VLDL assembly.

1.2. Structure of apolipoprotein B and microsomal triglyceride transfer protein and their interaction

1.2.1. Apolipoprotein B

Apolipoprotein B100 is a major protein component of VLDL, IDL and LDL (1). Human apoB100 is synthesized as a protein of 4536 amino acids (Fig. 1.1*A*), assembled into VLDL in the liver, and secreted into the bloodstream. Although newly secreted VLDL also contains other apolipoproteins such as apoE and apoCs, apoB100 is the only apolipoprotein that is not transferred to other lipoprotein particles during catabolism of VLDL within plasma, and is the sole protein component present in LDL.

In humans, apoB100 is the only form of apoB that is synthesized in the liver. In rats and mice, however, apoB48, representing the amino-terminal (N-terminal) 48% of full-length apoB (Fig. 1.1*A*), is another form of apoB made in the liver. Both apoB100 and apoB48 have the ability to form VLDL, and each VLDL contains only one copy of apoB (i.e. either apoB100 or apoB48) (9). ApoB48 is also produced in the small intestine, and is associated with TG-rich chylomicrons (for review of chylomicron assembly, refer to (10)). Both apoB100 and apoB48 are derived from the same gene, and expression of apoB48 is a result of tissue-specific post-transcriptional apoB mRNA editing (11, 12). Thus, human apoB48 mRNA remains identical in structure to apoB100 mRNA except for a conversion from cytidine (C) to uridine (U) at nucleotide 6666, resulting a conversion of the first base of CAA (encoding glutamine-2153) to UAA (encoding an in-frame stop codon).

The amino acid sequence of human apoB100 has been deduced from its cDNA (13-17). Human apoB100 contains 19 potential glycosylation sites, of which 16 are glycosylated (Fig. 1.1.*B*) (18). Disruption of N-linked glycosylation of apoB with tunicamycin does not seem to affect VLDL assembly *per se* (19), but may affect apoB production (20). There are 25 cysteine residues (designated C1, C2, and so on) distributed asymmetrically within apoB100. Sixteen of the cysteine residues are involved in disulfide linkage formation, and six disulfide linkages are located in the N-terminus 500 amino acid residues (Fig. 1.1.*C*) (21). Mutagenesis studies showed that disulfide linkages formed between C2 and C4 and between C7 and C8 are required for proper folding of the N-terminus of apoB (22, 23).

One physiological function of apoB100 is to serve as a ligand for the LDL receptor. Sequence alignment demonstrates that two regions within human apoB100, spanning residues 3147-3157 (designated site A) and 3359-3367 (designated site B) show similarity to the LDL receptor binding domain of apoE (14), another ligand for the LDL receptor. [The LDL receptor-binding domain of apoE is located within a cluster of positively charged amino acids between residues 140-150 (24), which interact with negatively charged amino acid residues at the N-terminal region of the LDL receptor (2).] Comparison of primary amino acid sequence of apoB100 among different vertebrate species shows high homology of the site B, but not the site A (25).

Characterization of the secondary and tertiary structures of apoB100 has been a formidable task because of its unusually large size and extreme hydrophobicity. On the basis of primary amino acid sequence, an algorithm has predicted that human apoB100 contains 43% α-helix, 21% β-sheets, 20% random coil, and 16% β-turns (26). A computer analysis also suggested the presence of two domains of amphipathic β-strands alternating with three domains of amphipathic α-helixes within human apoB100, known as pentapartite structure NH_2-α_1-β_1-α_2-β_2-α_3-COOH (Fig. 1.1.*D*) (27). It has also been suggested that the pentapartite structure of apoB100 is conserved among nine vertebrate species (28). The α_1-helix (between B1.3 and B10.5), appears to form a globular domain with low affinity for lipids. The other two α-helix clusters, namely α_2 (between B46.4 and B56.4) and α_3 (between B89.5 and B95.6), may represent reversible lipid-binding domains. The extensive β-strands, namely β_1 (between B18.2 and B43.2) and β_2 (between B55.6 and B85.3), may represent irreversible lipid-association domains (27). The function of the five clusters of putative secondary structure within apoB remains to be defined. However, it has been proposed that the β_1 and β_2 clusters may directly bind to core lipids and provide a rigid backbone during lipoprotein assembly, whereas the α_2 and α_3 clusters may be flexible in accommodating varying amount of lipids during VLDL assembly (29). The N-terminus α_1 domain has been examined extensively and will be described in Section 1.2.3.

Using immunoelectron microscopy techniques, Chatterton *et al.* (30, 31) have determined the configuration of apoB100 on the surface of human LDL and proposed a "ribbon and bow" model. In this model, the first 89% of apoB forms a "ribbon"

encircling completely the LDL particle, with a compact configuration between B2 to B23, and a "kink" region between B41 and B50. The final 11% of apoB constitutes a "bow", stretching back and crossing over the "ribbon" at the region that encompasses the LDL receptor binding site (Fig. 1.2). Thus, the circumference of the circle made by β-strands of apoB (B23-B41, B50-B89) may determine the size of neutral lipid core (see below Section 1.3.5).

1.2.2. Microsomal triglyceride transfer protein

The microsomal triglyceride transfer protein (MTP), originally isolated from bovine liver microsomes, transfers TG, phosphatidylcholine (PC), and cholesteryl ester (CE) between lipid membranes (32). The activity of MTP is found mainly within the lumen of microsomes in both the liver and the intestine (33). The tissue distribution, subcellular localization, and lipid transfer activity of MTP imply that MTP may be involved in the assembly of TG-rich VLDL and chylomicrons.

The isolated MTP is a complex protein composed of two subunits (34): a large subunit (/MTP) with catalytic activity (97 kDa, 894 amino acid residues), and a small subunit of 55 kDa identified as protein disulfide isomerase (PDI) (35). PDI is a multifunctional protein with disulfide isomerase activity and chaperone activity (36). However, within the MTP complex, PDI does not contribute directly to the lipid transfer activity (37). Rather, PDI acts as a chaperone that contributes to the stability and function of the /MTP. Transfection studies in insect Sf9 cells showed that recombinant /MTP forms insoluble aggregates unless PDI is co-transfected, and the stable complex of the

two components is required for the activity of MTP (38). Stable interaction between PDI and /MTP may also allow the MTP complex to be retained within the endoplasmic reticulum (ER) because PDI is an ER resident protein. The KDEL sequence, found in the carboxy-terminus (C-terminus) of PDI, confers its ER retention property (39). [The KDEL sequence within an ER resident protein is specifically recognized by a receptor in the ER-Golgi intermediate compartment (ERGIC). Once bound, the ER resident protein is retrieved back to the ER compartment (40).] This ER retention sequence is absent in the entire sequence of /MTP (41). The disulfide isomerase activity of PDI may not be required for normal MTP activity, because mutation of two catalytic sites of PDI (CGHC to SGHC) does not alter the MTP lipid transfer activity (38). The molecular details of the interaction between MTP and PDI will be described in Section 1.2.3.

Our knowledge about the enzymatic property of MTP is derived mainly from *in vitro* experiments examining lipid transfer between membranes in the presence of MTP. MTP activity is commonly determined by measuring the rate of transfer of radiolabeled TG from donor membranes to acceptor membranes (5). As a lipid transfer protein, MTP promotes the exchange of TG between membranes when there are equal amounts of TG in the membranes of donor and acceptor vesicles (42). However, when the amount of TG is drastically different in the membranes, i.e., when only the donor membranes contain TG, TG can be transported from the donor to the acceptor, resulting in net TG mass transport between vesicles (42). The mode of MTP action *in vivo* has not been elucidated.

Kinetics studies show that MTP transports lipid between membranes through a shuttle mechanism (42), a process that requires a stable MTP-lipid complex as an intermediate during lipid transfer. Indeed, MTP binds up to three molecules of lipid, and forms a stable complex with a variety of lipids, including neutral lipids (TG, CE, DG, and squalene) and phospholipids (PC, PE, PS, PI and PA) (43). However, the lipid transport rate mediated by MTP is quite different among these lipid species. Under the same *in vitro* assay condition, MTP preferentially transports neutral lipids as compared to phospholipids, and the calculated initial rate of transfer of TG, CE, and DG is at least 24-, 16-, and 2.5-fold higher than that of PC, respectively (43). The preference of MTP in neutral lipid transfer raises the possibility that MTP may play a role in TG transfer during VLDL assembly.

1.2.3. Molecular details of the interaction between apolipoprotein B and microsomal triglyceride transfer protein

Early studies proposed that both apoB and *l*MTP are members of the vitellogenin gene superfamily since the primary sequence of the N-termini of apoB and of *l*MTP are homologous with that of the vitellogenin (VTG) (44, 45). This proposal is verified recently by phylogenetic analysis based on sequence alignment (46) and by database search for proteins containing more than 7 amphipathic β-sheets (47).

Vitellogenin (200 kDa, 1807 amino acid residues) is synthesized in the liver of many egg-laying animals, and is secreted into plasma as a lipid-protein complex. The complex can be taken up by proteins of the LDL-receptor superfamily in the ovary (44,

48-50). After receptor-mediated endocytosis, VTG undergoes specific cleavage into several polypeptide chains, and the lipid-binding product is referred to as lipovitellin (LV), which serves as a source of amino acids and lipid during embryogenesis. Lamprey LV contains 15% lipid (by weight) that consists of 27 molecules of phospholipid and 11 molecules of triacylglycerol (51, 52).

Crystal structure of the lamprey LV has been determined at 2.8 Å resolution (51, 53) and the amino acid residues have been assigned (54). LV contains three domains: a globular N-terminal β-barrel (amino acid residues 17-296), an extended α-helical structure (amino acid residues 297-614) and a substantial C-terminal funnel-shaped lipid-binding cavity formed by two β-pleated sheets (amino acids 615-1807) (Fig. 1.3). LV forms a homodimer, in which the β-barrel of each subunit interacts with the α-helical domain of the other subunit (54).

Coordinates of the LV have been used to model the N-termini of *l*MTP (residues 22-603) and apoB (residues 1-587) (46). The modeled *l*MTP and apoB segments show highly conserved secondary and tertiary structures. The N-terminal ~300 residues of both apoB and MTP form 3 helices and 13-stranded β-sheets; 11 of these strands form a β-barrel conformation, and some of these strands are stabilized by disulfide linkages (Fig. 1.4.*A* & *B*) (46). The next 300 residues of both *l*MTP and apoB form a double layered α-helical structure containing 17 helices (Fig. 1.4.*C* & *D*). Mutagenesis studies suggested that salt-bridge residues are required to stabilize helices 13-17 of the α-helical domains of both *l*MTP (R540-N531-E570) and apoB (R531-D524-E557) (Fig. 1.4.*E* & *F*) (46),

which in lamprey LV underlies the homodimerization interface (54). Furthermore, the salt bridge residues in /MTP, together with the surfaces of outer helices 15 and 17, form the major PDI binding sites (Fig. 1.4.*E*) (46). This is consistent with the previous observation that missense mutation of Arg540 → His in /MTP interrupts its interaction with PDI, resulting in abetalipoproteinemia (55).

The physical interaction between apoB and MTP during the assembly of LpB has been suggested (56, 57). The MTP binding sites are located within the N-terminal 18% of apoB (58), and both arginine and lysine residues within apoB18 interact directly with negatively charged residues in MTP (59). The exact number of MTP-binding sites within apoB18 is not clear. One group has reported that the amino acid residues 430-570 of apoB are crucial in MTP binding (60). Another group has shown that there are at least two potential MTP binding sites (46, 61). One site encompassing residues 1-264 (apoB5.8) interacts with the predicted β-barrel of /MTP (46). The second site is centered on residues 512-592 (apoB11-apoB13) plus flanking residues 430-511 (apoB9-apoB11) and 640-721 (apoB14-apoB16) (61). The corresponding apoB-binding site of /MTP is located within helices 13-17 of the predicted α-helical domain (61), a region in close proximity to the major PDI binding site (46). It has been postulated that during the assembly of lipoproteins, apoB displaces PDI from /MTP, and is only replaced again by PDI as lipidation progresses towards the distal parts of the secretory pathway (61).

The C-terminal lipid binding domain of lamprey LV is enriched in β-sheets (54). A triangular "lipid cavity" is lined on its two major sides by antiparallel β-sheets, namely

βA:LV and βB:LV. The bottom of the cavity is capped by a third antiparallel β-sheet, namely βD:LV. The double-layered α-helical structure containing 17 helices is located at the top of the triangular "lipid cavity". A fourth antiparallel β-sheet, namely βC:LV, is derived from the N-terminal β-barrel, and is attached to the top of βB:LV (Fig. 1.5*A*). The "lipid cavity" can accommodate approximately 38 lipid molecules (54).

On the basis of its sequence homology and motif conservation with lamprey LV, the amphipathic β-sheets within the first 1000 residues of apoB100 has been postulated to form a "lipid cavity" for self-assembly of a lipoprotein (47). It is suggested that apoB, complexed with /MTP, forms a "lipid cavity" that is surrounded by two β-sheets from apoB and one from /MTP. Such a putative tertiary structure is thought to be stabilized by the interaction between the negatively charged residues within α-helical domains of /MTP (residues 340-480) and the positively charged residues within α-helical domains of apoB (residues 477-618) (Fig. 1.5*B*) (47).

Could the "lipid cavity" model explain how lipid is recruited during LpB assembly? Although VTG, apoB and /MTP share structure motifs at their respective N-termini (46, 47), the length of their C-terminal lipid-associated domains vary profoundly (Fig. 1.6). The lipid binding capacity may be a function of the length of amphipathic β-sheets. For instance, /MTP that has the shortest amphipathic β-sheets (only about 200 amino acids in length) may form the smallest "lipid cavity" if any, and therefore may bind the least amount of lipid. In contrast, apoB that has amphipathic β-sheets over 3000 amino acids in length may form the largest "lipid cavity" and is able to accommodate a large amount of

lipid. It has been hypothesized that lipoprotein assembly is achieved through expansion of the "lipid cavity" of apoB by the co-translational addition of the amphipathic β-strands (Fig. 1.5.*C*) (47).

The above studies indicate that MTP binds to apoB, at least within its first 1000 amino acid sequence. However, demonstration of a protein-protein interaction may not explain how MTP mediates lipid transfer during VLDL assembly. It has been shown that the affinity between apoB and MTP decreases as the length of apoB increases and as the lipidation of apoB intensifies (58). Other studies, however, have shown that the requirement of MTP activity for the lipidation of apoB expands as the length of apoB increases (62). These results suggest that simply examining the protein-protein interaction between apoB and MTP may not reveal the mechanism(s) whereby MTP mediates lipid transfer onto apoB *in vivo*. In the rest of this Chapter, I will present our current understanding of the biogenesis of apoB and TG-rich VLDL, and present evidence regarding the role of MTP during the entire process of VLDL assembly.

1.3. Unique features associated with apolipoprotein B biogenesis

Most experimental evidence suggests that expression of the apoB gene is tightly controlled, and that the production of apoB is mainly regulated co-translationally or post-translationally (63-65). Some studies suggested that translocation of apoB nascent polypeptide across the ER membranes was the most critical step in regulation of apoB production (66, 67). With advanced understanding of the biogenesis of secretory proteins (for review, refer to (68, 69)), much progress has been made in unraveling the molecular

mechanism that governs apoB translocation. ApoB is an unusual secretory protein, which is intimately associated with lipid during its biogenesis. Inadequate lipid association during apoB translocation will render apoB susceptible to degradation by protease.

1.3.1. Atypical association of apolipoprotein B with endoplasmic reticulum membranes

It has been known for long that a large amount of newly synthesized apoB is tightly associated with the ER membranes (63, 70-72). This is in sharp contrast to typical secretory proteins (e.g. albumin) that are usually found mainly in the lumen of the microsomes. Furthermore, it has been shown that not only are apoB100 or apoB48 polypeptide associated with the ER membranes, they are exposed to the cytosolic side of ER membranes (73). Thus, translocation of apoB is different from that of typical secretory proteins as well. The cytosolic exposed apoB could be detected by monoclonal antibodies with epitopes at the N- or C-terminus of apoB100 (74, 75). The incompletely translocated apoB on the microsomal membranes has been observed in different hepatic cell models (75-80). Thus, apoB could be detected on the cytosolic side of the ER membranes in rat hepatocytes (75), or on the cytosolic side of the Golgi in chicken (76) and rabbit (77, 78) hepatocytes, or on the cytosolic side of the total microsomes in McA-RH7777 cells (79). In addition, a cytosolic chaperone protein Hsp70 was found associated with apoB in HepG2 cells (80). These results suggest the existence of multiple topological forms of the full-length apoB with respect to ER membranes. Some apoBs are completely translocated across the ER membranes and either in association with the inner leaflet of the ER membranes or in association with lipoproteins in the microsomal lumen.

However, some apoBs exist as a pseudo-transmembrane protein (either transiently or rather prolonged), and some apoBs may be entirely associated with the cytosolic leaflet of the ER membranes. The structural basis underlying this multiplicity of apoB topologies is unclear. Some research groups do not agree with the existence of membrane-associated apoB and claimed that it was an experimental artifact (81-83).

Attempts have been made to explain the structural basis for pseudo-transmembrane topology of apoB by several laboratories. Examining the primary sequence of apoB reveals no topogenic sequences (usually enriched in amphipathic α-helices) that confer transmembrane configuration (14, 15, 17). It has been proposed that amphipathic β-sheets of apoB may form an alternative membrane-spanning configuration, a situation similar to the transmembrane topology of porin (66). Porin is an ion-conducting channel protein in *Escherichia coli*, yet it lacks classical membrane-spanning domains. It has been suggested that the antiparallel amphipathic β-sheets form oligomer structures that allow porin to integrate into the membranes (84). Recent structure analysis suggested that the amphipathic β-sheets between B21 to B41 exhibit a 43% homology with those in porin (85). In addition, mutagenesis studies showed that putative amphipathic β-strands between B28 to B34 (within the so-called β_1 domain) indeed confer transmembrane topology of chimeric proteins containing these sequences (86). However, whether or not the amphipathic β-strands within the β_1 domain are responsible for the pseudo-transmembrane topology of apoB is still a matter of speculation (79, 87).

1.3.2. Translocon and pause transfer motif of apolipoprotein B

Like most secretory and membrane proteins, the newly synthesized apoB peptides distinguish themselves from other cytosolic proteins by a signal peptide sequence at the N-terminus. The signal peptide usually contains a positively charged N-terminal sequence, a central hydrophobic core of 7-20 amino acids, and a polar C-terminal region. The signal peptide of apoB is 27 amino acids in length. A deletion or insertion in the hydrophobic core of the 27-residue isoform results in inefficient translocation and defective secretion of apoB (88).

In mammalian cells, almost all the secretory proteins are translocated co-translationally across the ER membranes at the sites called translocons. The minimum components of a translocon are the signal recognition particle (SRP) receptor and the Sec61p complex (89). In mammalian cells, the Sec 61p complex consists of multiple subunits (89-91). The Sec61p complex must associate with ribosomes when the nascent chain-ribosome complex arrives at the ER membranes. Through this association, the ribosome induces and/or stabilizes an aqueous channel (92) and directs the alignment of the nascent peptide exit with the channel, thus ensuring continuous translocation (93). Tight association of ribosome with translocon also provides a sealed membrane barrier while the channel is in the open conformation for nascent polypeptide translocation (94). Thus, during chain elongation, the translocating polypeptide is usually not exposed to the cytosol.

Since apoB is exposed to the cytosolic side of the ER membranes during and/or after translation, this raises the possibility that there are unique sequence elements within apoB (*cis*-acting elements) that give rise to this unusual phenomenon. *In vitro* translation and translocation studies of a small segment of apoB showed that translocation of the nascent polypeptide was not continuous but rather in a step-wise manner (95, 96). In this so-called pause-transfer process, apoB exhibits stop and restart at several discrete points during chain elongation. These points of translocational pausing are suggested to be mediated by specific sequences, termed the pause transfer sequences, with a consensus motif of LKK-T----N-A (or LKK---SE) (96, 97). Sequence analysis of apoB showed that there were at least 41 candidate pause transfer sequences along the entire polypeptide (97). However, only 23 of the candidates, clustered within three regions of apoB, were found to mediate translocational pauses (98). Thus, unlike the known topogenic sequences such as the signal peptide and stop transfer sequences, whose function can be autonomously demonstrated, the topogenic manifestation of the apoB pause transfer sequence depends strongly on the context of apoB sequence (96). However as mentioned earlier on, some research laboratories do not agree with the concept of discontinuous translocation of apoB and believe that the so-called translocational pause is in fact an experimental artifact resulting from *translational* pause (99, 100).

The role of one of the pause transfer sequences in apoB translocation has been examined intensively by Lingappa and coworkers (101, 102). They observed that during a translocational pause, the junction between the ribosome and translocation channel was opened, exposing the nascent chain to the cytosol (101). [This is in contrast to the

translocation of a typical secretory protein, whereby its nascent polypeptide is not exposed to cytosol.] When the translocational pausing was relieved, and translocation of the cytosolically exposed region of the nascent chain resumed, the tight ribosome-membrane junction was reestablished (101). These results imply that the rate of translocation, the environment of nascent apoB polypeptide, and the organization of the ribosome-membrane junction may be regulated by certain *cis*-acting elements of apoB, which contain pause translocational motifs (101). Moreover, the translocation chain-associated membrane proteins (TRAM) appear to be another essential component that is required for the translocational pause (101, 102). TRAM may prevent domains that have already translocated from having access to the cytosol once the ribosome and membrane junction has been open during translocational pausing (102).

The physiological significance of translocational pausing of apoB is not known. It has been suggested that apoB translocational pausing is important for its binding to lipid during its translocation (96). However, this needs to be verified by *in vivo* experiments. Prolonged translocational pausing of apoB may result in translocational arrest (103).

1.3.3. The role of microsomal triglyceride transfer protein in apolipoprotein B translocation

The role of MTP in the translocation of apoB has been examined extensively. Initially, transfection of recombinant apoB53 cDNA into Chinese hamster ovary (CHO) cells that lack /MTP resulted in expression of apoB53 proteins (273-kDa) that could not be translocated across the ER membranes or secreted (104). Instead, an 85-kDa protein,

derived from the N-terminus of apoB53, was secreted into the medium (104). It was thus postulated that the 85-kDa species was the product of proteolysis of a translocational arrested apoB intermediate, with the N-terminal portion being translocated and the remaining C-terminal portion residing on the cytosolic surface (105). Subsequently, the 85-kDa protein was found in the plasma of abetalipoproteinemia subjects with increased (by 2000-fold) concentrations, implying that the extent of apoB translocation may be correlated to the MTP activity *in vivo* (106). Recently, it was found that co-expression of /MTP and apoB53 in CHO cells resulted in translocation of apoB53, suggesting that MTP may facilitate apoB translocation (107). Expression of /MTP in other heterologous cells transfected with apoB variants also reconstituted the assembly and secretion of LpB (108-111), and the successful reconstitution may be attributable to the role of MTP in facilitating apoB translocation (108). Inhibitors of MTP lipid transfer activity have also been shown to impair the assembly and secretion of LpB by blocking the translocation of apoB (112-114). Thus, it is believed that MTP is required for translocation of apoB (115).

However, several lines of evidence suggest that MTP may not be required for translocation of apoB across the ER membranes, at least is not required for translocation of certain N-terminal portions of apoB. In mammary derived C127 cells that lack MTP expression, transfection of truncated apoB forms (e.g. apoB41) resulted in assembly and secretion of lipoproteins (116). *In vitro* reconstitution studies have shown that translocation of apoB48 could be achieved with microsome membranes derived from either rat hepatocytes that express MTP or from dog pancreas that do not express MTP (117). Furthermore, in mice with hepatic-specific MTP knockout, plasma B48 level

(secreted from the liver) was reduced by less than 20% (8), suggesting that B48 can be translocated and secreted even in the absence of MTP activity. Thus, these results raise the possibility that the role of MTP in VLDL assembly may not simply reside in assisting apoB translocation.

1.3.4. The role of phospholipid in apolipoprotein B translocation

The lipid environment, particularly the phospholipid composition, of the ER membranes has a profound impact on translocation of apoB. Accumulation of phosphatidylmonomethylethanolamine (PMME), an otherwise quantitatively insignificant phospholipid within primary rat hepatocytes, specifically reduced the secretion of LpB (118). Vance and coworkers (119, 120) demonstrated that neither synthesis of lipid or apoB nor secretion of other proteins was affected by PMME treatment. Since PMME also inhibited the secretion of smaller apoB variants that do not normally assemble lipoprotein particles (such as apoB15), the inhibitory effect of PMME on the secretion of apoB100 and apoB48 was not caused by a defect in the assembly of apoB with a neutral lipid core (121). Trypsin protection assay showed that the defect in apoB secretion in PMME-enriched hepatocytes was the result of a specific blockade of apoB translocation into the microsomal lumen (120), and the diminished apoB translocation in PMME enriched microsomal membranes was probably caused by impaired resumption of apoB translocation after a translocation pausing (122). Clearly, phospholipid composition of ER membrane is one of the *trans*-acting elements that play a role in determining the rate of apoB translocation.

1.3.5. Formation of apolipoprotein B-containing lipoproteins during apolipoprotein B translocation

Formation of LpB, a process involving the incorporation of core lipid into apoB, initiates during translation/translocation of apoB. Metabolic labeling studies with HepG2 cells showed that when the newly synthesized apoB reached a size of 80-100 kDa, the nascent polypeptides were already engaged in lipoprotein assembly, suggesting a co-translational, co-translocational assembly mechanism (123). Similar results were also obtained by others (124). In McA-RH7777 cells, labeled apoB100 was associated with VLDL in the microsomal lumen as early as 3 min after the initiation of the labeling, and the assembly of B100-VLDL could be acutely inhibited by the cycloheximide treatment (125). Since it takes about 15-20 min to synthesize one B100 polypeptide (126), these data suggested that assembly of LpB is in close connection with synthesis and translocation of apoB nascent polypeptide. It seems that while the C-terminal portion of apoB is still being synthesized on the ribosome of the endoplasmic reticulum, the N-terminal portion has already translocated across the ER membranes and assembled a small lipoprotein particle.

Accumulating data suggest that the length of apoB plays an important role during lipoprotein assembly. In hypobetalipoproteinemia subjects, various C-terminally truncated forms of apoB100 were found predominantly in small dense plasma lipoproteins (3). Several laboratories have examined the relationship between apoB length and lipoprotein size using cells transfected with various C-terminally truncated apoB variants (123, 124, 127-129). In general, there is an inverse relationship between

apoB length and lipoprotein density (i.e., the longer the truncated apoB protein, the lower buoyant density of the lipoprotein particle), and a positive relationship between apoB length and lipoprotein core volume (i.e., the longer the truncated apoB protein, the larger the lipoprotein particle) (Fig. 1.7). Thus, apoB48 is mainly found associated with the particles with a buoyant density of 1.10 g/ml whereas apoB100 is found in the particles of density range of less than 1.03 g/ml (Fig. 1.7*A*). The calculated data indicated that every 10% decrease in length of apoB results in approximately 13% reduction in core volume of lipoproteins (129). When this linear relationship is extrapolated using apoB length as a scale, it is found that the minimum length required to assemble a lipid core is approximately 22% of apoB100 (Fig. 1.7*C*, *dotted line*) (129), almost corresponding to the starting point of the β_1 domain of apoB100. Thus, it is possible that during apoB translation/translocation, the nascent polypeptide associates initially with the inner leaflet of the ER membranes while the downstream portion of the peptide is still translating and translocating across the ER membranes. Once a portion of the polypeptide is extruded into the ER lumen, it will immediately recruit lipid to assemble a primordial lipoprotein particle. As the chain grows longer, more lipid is recruited, and the assembled particle becomes larger until the full-length apoB is released into the ER lumen (130). This co-translational/co-translocational assembly model may give rise to the phenotype of the apoB length-density relationship, and is also consistent with the aforementioned "ribbon and bow" model (Fig. 1.2) (31) and the "lipid cavity" model (Fig. 1.5) (47).

The N-terminal α_1 domain has been suggested to be important for efficient initiation of apoB lipidation. Several experimental observations indicated that apoB17,

containing only the α_1 domain of apoB, is critical for lipoprotein formation. Although the C-terminal truncated apoB forms are usually secretion-competent (123, 124, 127-129), recombinant apoB variants that lack the N-terminal sequences of apoB are often secreted poorly (79, 131). Since apoB17 has relatively low ability to bind to neutral lipids (128, 132), the proper folding of apoB17 may be essential for the initiation of lipoprotein assembly. The folding of apoB17 during the initiation of lipoprotein assembly is probably achieved through formation of clustered disulfide linkages within apoB17 (22, 23, 133). In addition, the interaction between MTP and first 1000 residues of apoB may also play a role in apoB folding (46, 47, 60, 61). However, it remains unclear how the folding of α_1 domain affect the lipidation of the downstream apoB.

1.3.6. Intracellular degradation of newly synthesized apolipoprotein B by proteasomes

The metabolic fate of the newly synthesized apoB has been investigated intensively by many research laboratories. Working with primary hepatocytes, Borchardt and Davis (134) observed that a significant amount of newly synthesized apoB disappeared from the cells, and was not quantitatively recovered from the culture medium, suggesting that some apoB polypeptides are degraded intracellularly. Subsequently, degradation of apoB was observed in other hepatic cell models, including HepG2 cells (135) and McA-RH7777 cells (129). In HepG2 cells, apoB degradation occurred even when the nascent apoBs were in their transmembrane topology (67, 105), and involved mainly the ER-localized proteases, either on the lumenal or the cytosolic side of the ER membranes

(135, 136). Recent studies demonstrated that in HepG2 cells cytosolic proteasomes were involved in apoB degradation (126, 137-140).

Proteasomes are large multi-subunit protease complexes that play an important role in degradation of ubiquitinated proteins in the cytosol of mammalian cells (141). Proteasomes are abundant in the cytoplasm and nucleus, but absent in the ER lumen. Several inhibitors have been identified to selectively block proteasome function. Among these inhibitors, the most effective and specific one is lactacystin, a fungal metabolite that modifies the threonine active site of the proteasome (142). Other less potent and less specific inhibitors, such as Acetyl-leu-leu-norleucinal (ALLN, or calpain inhibitor 1) and CBZ-leu-leu-leucinal (MG132), are peptide aldehydes that are substrate analogs, and thus competitively inhibit the chymotrypsin-like activity of the proteasome (143).

Since intracellular degradation is very active in HepG2 cells, this cell line has become a model of choice for the studies of apoB degradation (103). Over the last few years, the proteasome-mediated apoB degradation in HepG2 cells has been the subject of intense investigation. Recent evidence suggests that apoB degradation in HepG2 cells is in part mediated by the ubiquitin-proteasome pathway. In these cells, degradation of apoB is mediated by ubiquitination and dependent on ATP, and can be inhibited by proteasomal inhibitors (126, 137-139, 144). Ubiquitination/proteosomal degradation of apoB may be achieved both co-translationally (140, 145) and post-translationally (139, 140, 144). The fact that the nascent apoB polypeptide can be ubiquitinated even when its translation reaches to 50% of the full length (140, 145) suggests that degradation of apoB

may occur at the very early stage of apoB biogenesis. Currently, it is not clear if the ubiquitin/proteasome pathway for apoB degradation occurs in hepatocytes other than HepG2 cells.

In addition to the ubiquitin/proteasome pathway, other studies raised the possibility of apoB being degraded by a nonproteasomal protease such as the lumenal protease ER60 homologue (144, 146).

1.3.7. The role of oleate in the biogenesis of apolipoprotein B

As mentioned above, biogenesis of apoB is different from that of typical secretory proteins. This is probably because it is obligatory for apoB to associate with lipids during translocation. Thus, if lipidation of apoB is sufficient, translocation of apoB seems to be in close connection to its translation, similar to that of other secretory proteins. If the lipidation is insufficient, translocation of apoB will become uncoupled from its translation, rendering it susceptible to proteasomal degradation. In HepG2 cells, supplementation of oleate stimulates apoB secretion (63, 64, 147). Pulse chase studies demonstrated that oleate could effectively diminish apoB degradation in the pre-Golgi compartment and increase apoB secretion (135, 148). In contrast, protease inhibitor ALLN alone did not accelerate apoB secretion in HepG2 cells, yet it protected apoB from rapid degradation (149). An increase in apoB secretion could be manifested only when oleate was added together with ALLN (149), implying that secretion of apoB from HepG2 cells is mainly determined by the availability of oleate, not by apoB degradation. More recently, it has been shown that translocation of apoB may be affected by lipid

availability (67, 114, 145), and increasing the efficiency of apoB translocation actually decreased apoB degradation (67). Thus, it is possible that the availability of lipid is essential for maintaining continuous translocation of nascent apoB polypeptide across the ER membranes, thereby transporting apoB out of a proteasome-susceptible compartment. When lipid availability is limited, apoB translocation is impaired, and apoB is confined to this compartment and is rapidly degraded. Thus, biogenesis of apoB, unlike other secretory proteins, is tightly regulated by the intracellular lipid metabolism.

1.4. Assembly of triacylglycerol-rich very low density lipoprotein in the secretory pathway

Assembly of TG-rich VLDL particles does not follow the length-density and length-size relationship between apoB and lipoproteins (See Section 1.3.5. and Fig. 1.7). As mentioned earlier on, in rat liver both B100 and B48 have the ability to assembly TG-rich VLDL particles (9). Thus, apoB48, only half of the full length of apoB100, can assemble a lipoprotein with density and size similar to B100-VLDL. It is also known that in human plasma, VLDL particles (d < 1.006 g/ml) are heterogeneous in size and can be separated into two major classes: large $VLDL_1$ of S_f 100-400 and small $VLDL_2$ of S_f 20-100 (150). This heterogeneity may result from secretion of B100-VLDL of different sizes directly from the liver (151, 152). Thus, assembly of TG-rich VLDL is not simply governed by apoB itself.

1.4.1. Subcellular location of very low density lipoprotein maturation

Triacylglycerol-rich VLDL is assembled along the secretory pathway. However, the exact subcellular compartment where the assembly occurs is of controversy; it has been shown that VLDL maturation occurs as early as in the rough ER, or as late as in the trans-Golgi compartment. The cause for the apparent difference in the experimental results is not clear.

Evidence for VLDL maturation within rough ER came from VLDL-lipid composition study (153). In this study, it was demonstrated that apoB-containing particles, isolated from the lumen of rough ER or smooth ER or Golgi of rat hepatocytes, were of the same average size, density and lipid composition as newly secreted VLDL. These data suggested that rough ER is the site where apoB is assembled with its full complement of lipid to form a mature VLDL. A separate metabolic labeling study also demonstrated that radiolabeled B100 and B48 proteins were incorporated into VLDL fraction in the lumen of rough ER (154).

However, other experimental evidence indicated that addition of bulk lipid into apoB may not be confined to the rough ER compartment. Early electron microscopic studies showed that in perfused rat liver, formation of VLDL particles was found within the smooth-surfaced terminal ends of rough ER, but not within rough ER *proper* (155). Immunoperoxidase electron microscopic studies demonstrated that in rat hepatocytes, apoB immunostaining was found in rough ER cisternae, as well as the smooth-surfaced terminal ends of rough ER. In contrast, VLDL-sized lipid staining particles within the

smooth ER lacked the immunostaining of apoB (156). Based on these observations, Alexander *et al.* (156) proposed that VLDL-sized lipid particles lacking apoB are synthesized in smooth ER, whereas apoB polypeptides are synthesized in rough ER and become associated with the VLDL-sized lipid particles at the junction of rough and smooth ER. The mature VLDL particles are then transported through the Golgi apparatus and secreted.

Other studies suggested that a fraction of TG becomes associated with apoB in a compartment between rough ER and Golgi during VLDL assembly. In isolated rabbit (157) and rat (158, 159) livers, association of radiolabeled TG with apoB increased from rough ER lumen (only about 30% of labeled TG in rough ER) to the Golgi lumen (over 70% of labeled TG in Golgi). In chicken hepatocytes, metabolic labeling experiments showed that the Golgi apparatus was the primary site for the incorporation of bulk lipid into VLDL (72, 160). These data suggest that maturation of VLDL may not be achieved within the rough ER.

1.4.2. "One-step" assembly versus "two-step" assembly of mature very low density lipoprotein

Another unsettled issue is whether VLDL assembly is achieved through a "one-step" or "two-step" lipidation process. The "one-step" assembly process depicts that bulk TG is incorporated into apoB during its translocation, either through a concerted fashion, or through a step-wise fashion immediately after lipid-binding domains of apoB emerge from the translocational channel. In contrast, the "two-step" assembly model depicts that

apoB recruits minimal lipid during its translation/translocation, forming a small, lipid-poor primordial particle (the first step). Subsequently, bulk TG is incorporated into the primordial particle to form a mature VLDL, either by fusion with a large "apoB-free" lipid droplet or by sequential addition of lipid through the secretory pathway (the second step). Thus, in the "one-step" model, mature VLDL is formed within the rough ER. Within this scheme, formation of mature VLDL is envisioned to take place simultaneously with apoB translocation (i.e. co-translocational assembly), or even with apoB translation (i.e. co-translational assembly) (see Section 1.3.5.). In contrast, in the "two-step" model, the incorporation of bulk TG into apoB is not coupled with its translation/translocation, therefore mature VLDL may not be formed within the rough ER.

Data supporting either "one-step" or "two-step" model abound. They were obtained mostly from studies of subcellular fractionation. Thus, observations that VLDL maturation achieved in post-ER compartments (72, 155-160) propose the "two-step" model, whereas results showing VLDL maturation within rough ER (153, 154) claim the "one-step" process.

However, such a simplistic classification for a complex process like VLDL assembly may not be adequate. In a metabolic labeling study, Swift (154) has indicated that even mature VLDL within rough ER of rat liver is not assembled through a simple "one-step" lipidation. It was shown that formation of B100-VLDL in the lumen of rough ER occurred within 15 min of initial labeling, suggesting a co-translational "one-step"

assembly process. [It takes about 15-20 min to synthesize one B100 polypeptide (126)]. On the contrary, formation of B48-VLDL in the lumen of rough ER was not achieved after 30 min of the initial labeling, indicating that B48-VLDL may be formed through a "two-step" lipidation process even within the rough ER. Thus, revelation of the subcellular compartment for VLDL assembly is necessary but not sufficient to determine the lipidation step(s) of VLDL maturation.

Perhaps definitive support for the "two-step" model is the demonstration of a "precursor-product" relationship between a primordial lipid-poor particle and a mature TG-rich VLDL particle. Working with rat hepatoma McA-RH7777 cells, Borén *et al.* (125) showed an inverse relationship between secretion of apoB48-VLDL and apoB48-HDL. In these cells, secretion of apoB48-VLDL was induced only when the cells were incubated with exogenous oleate. Pulse-chase studies showed that the radiolabeled apoB48 within the microsomal lumen was first associated with lumenal dense particles (HDL-like), and later with VLDL particles in the presence of oleate supplement (125). These results suggest that lumenal apoB48-HDL is the precursor of apoB48-VLDL. However, these results became less conclusive once one realized that a significant amount of apoB48 was associated with the microsomal membranes, which might serve as a precursor for both B48-HDL and B48-VLDL. Hence, attempts have been made to isolate membrane-associated apoB.

To isolate the membrane-associated form of apoB in its native form, Rustaeus *et al.* developed an extraction method using a combination of deoxycholate (0.025%) and

carbonate treatment (161). The concentration of deoxycholate used was not supposed to affect membrane structure or lipid association with apoB (161). Using this extraction method, Stillemark *et al.* (162) demonstrated that membrane-associated B48 was of the same density as B48-HDL secreted from the cells, and that membrane-associated B48-HDL was a precursor to both secreted B48-HDL and B48-VLDL.

Assembly of B100-VLDL in McA-RH7777 cells somewhat resembles that of B48-VLDL. In this case, membrane-associated B100-HDL may act as a precursor of secreted B100-VLDL (161). Unlike B48-HDL, B100-HDL is not secretion-competent. Thus, while a significant amount of B100-HDL is found in the lumen, they were not secreted into the medium (125).

1.4.3. The role of non-esterified fatty acid in very low density lipoprotein assembly

Hepatic TG is synthesized mainly through the phosphatidic acid pathway (Fig. 1.8). Accumulating evidence suggest that it is the non-esterified fatty acids (NEFA), but not *de novo* synthesized free fatty acids from small carbohydrate-derived precursors, that are utilized for VLDL-TG formation (163-166). In the liver, there are several sources of pre-made NEFA, either from extracellular NEFA in plasma, or from intracellular hydrolysis of the cytosolic stored TG, lipoprotein remnants, or membrane phospholipids. Increased flux of plasma fatty acids from adipose tissues to the liver stimulates hepatic TG-rich VLDL production, and is often observed in familial combined hyperlipidemia and insulin-resistant subjects. In cultured rat hepatoma McA-RH7777 cells, secretion of B48-VLDL is induced only when oleate is supplemented (125). Thus, both *in vivo* and *in vitro*

data indicate that availability of extracellular NEFA is critical for hepatic TG-rich VLDL production.

Availability of extracellular NEFA, however, is not always positively associated with hepatic TG-rich VLDL production. Supplementation of some fatty acids can inhibit hepatic VLDL production. It has been recognized that feeding dietary fish oils lowers plasma TG level in human and experimental animals (167-171). The hypotriglyceridemic effect of fish oils is generally believed to be caused by a suppression of hepatic VLDL secretion mediated by the n-3 fatty acids, eicosapentaenoic acid (EPA) and docosahexaenoic acid (DHA). Since *in vitro* cell culture studies showed that TG synthesis is not altered in the presence of n-3 fatty acid (172-175), it has been postulated that a lack of TG *per se* may not be the cause for decreased VLDL assembly, but rather the amount of TG diverted for VLDL assembly is limited (176). Nevertheless, when n-3 fatty acids are fed *in vivo* via a dietary route, a decrease in TG synthesis becomes demonstrable, and this may be responsible for decreased hepatic VLDL production (169, 175, 177-179). Thus, the mechanism for the inhibitory effect of n-3 fatty acid on hepatic lipid and apoB secretion differs, depending on whether they are administered *in vivo*, via the dietary route, or *in vitro*, via direct addition to hepatocyte cultures (175).

1.4.4. The origin of triacylglycerol utilized for very low density lipoprotein assembly

Many studies indicate that the newly synthesized TG is not directly utilized "*en bloc*" for VLDL assembly. Lipid metabolic labeling experiments indicated that only about 15% of cellular TG was secreted without prior hydrolysis in chicken hepatocytes

(180). In rat hepatocytes, a maximum of 30-40% of VLDL-TG is directly made from the conventional phosphatidic acid pathway (181, 182). In contrast, at least 70% of the secreted VLDL-TG can be derived from hydrolysis of the cytosolic stored TG pool (166, 181). Thus, it is generally believed that the newly synthesized TG may not be directly utilized "*en bloc*" for VLDL assembly. Rather, the majority of the newly synthesized TG is stored temporarily in the cytosol (183). Under conditions where VLDL assembly is stimulated, these cytosolic TG may undergo a "hydrolysis-reesterification" cycle to form a "new" TG species that can be utilized for VLDL assembly (Fig. 1.9) (165, 184).

The lipase that is involved in the hydrolysis of cytosolic TG has not been characterized. The lysosomal acid lipase may not be involved since the lipolysis process is not inhibited by chloroquine (166). Several attempts have been made to determine whether a microsomal triacylglycerol hydrolase (185, 186) or a hormone-sensitive lipase (187) is involved in hydrolyzing cytosolic TG. To date the experimental data are inconclusive. It is also not clear whether the cytosolic TG is hydrolyzed primarily to DG (181, 188) or completely to glycerol and acyl moieties (Fig. 1.9) (182). In this context, it is noteworthy that the inability of HepG2 cells to form TG-rich VLDL particles (189) is probably correlated with a low rate of hydrolysis of cytosolic TG (190). Thus, the putative lipase might be defective in HepG2 cells.

The enzyme responsible for the final step in the formation of TG during the "hydrolysis-reesterification" cycle has not been defined, although the candidate enzyme is likely to be diacylglycerol acyl transferase (DGAT). Two distinct pools of DGAT

activity have been observed within the microsomal membranes of rat hepatocytes (191). In HepG2 cells, there are two distinctly localized activities of DGAT, with one major peak of high-specific-activity occurring in the smooth ER fraction (71). The two DGAT activity pools may be located at different sides of the ER membranes (192). It has been postulated that different physical locations of DGAT may underlie two different routes of intracellular synthesis of TG (163, 193, 194). The first site is responsible for *de novo* synthesis of TG, which are then transferred mainly to the cytosol. The second site is where re-esterification of TG takes place, whereby fatty acids and DG, which are released through intracellular lipolysis, are incorporated into TG. The latter pathway is probably closely linked to VLDL maturation. Obviously, more studies are needed to prove or disprove this hypothesis. Identification of the gene encoding DGAT (195) will definitely shed some light on the role of DGAT in VLDL assembly.

Membrane phospholipids have been implicated in mediating the transfer of fatty acyl moieties from cytosolic TG to VLDL-TG (193, 196). Previous studies in cultured fibroblasts and smooth muscle cells indicated the presence of enzyme machinery in mediating the transfer of fatty acyl moieties of PL into cytosolic TG (197, 198). Working with rat hepatocytes, Wiggins and Gibbons (193) found that fatty acyl moieties of PL may also be the precursor for the synthesis of VLDL-TG, possibly through PL remodeling involving a sequential coupling of phospholipase A and lysophospholipid acyltransferase activities (196). It is possible that fatty acids released during lipolysis of cytosolic TG may be shuttled across the bilayer of the ER membranes via their transient incorporation into membrane PL. Thus, the requirement of PL in VLDL assembly is not

simply limited to its structural role by providing a suitable surface lipid component to facilitate folding of apoB (124, 199) and assembly of neutral lipid core (200). More importantly, phospholipid may contribute a significant amount of fatty acyl moieties for the synthesis of lumenal TG that will be utilized for VLDL assembly, and may act as a key component in the "hydrolysis-reesterification" cycle. The involvement of PC in VLDL assembly may also provide an explanation of previous observation that active synthesis of phosphatidylcholine is required for hepatic VLDL secretion from rat hepatocytes (244).

1.4.5. Translocation of triacylglycerol across the endoplasmic reticulum membrane bilayer

Most lipids are synthesized in the cytoplasmic leaflet of the ER membranes (201), they have to be transferred to the lumenal side of the ER membranes for VLDL assembly. Triacylglycerol has a limited solubility within the amphipathic lipid bilayer of ER membranes (202). How can TG translocate across the lipid bilayer?

Translocation of apoB across the ER membranes may facilitate TG translocation. The "lipid cavity" model (Fig. 1.5) proposed by Segrest *et al.* (47) suggested that the interaction between apoB and MTP forms a "lipid cavity", through which TG can be sequestered between the membrane bilayer. Thus, the longer the apoB polypeptide is synthesized/translocated, the larger is the hydrophobic cavity within the membranes, and the more TG is recruited within the core. Translocation of TG is achieved when the nascent particle is released into the lumen. However, other studies have demonstrated that

lumenal TG moieties may exist even in the absence of apoB (158, 203, 204), suggesting that TG may be translocated across the ER membranes through a mechanism independent of apoB. It seems that other cellular factor(s) may facilitate transfer of TG across the ER membrane bilayer into microsomal lumen.

Triacylglycerol may not be always translocated across the ER membranes *en bloc* (166). It has been suggested that the amphipathic products of TG lipolysis (DG, MG and acyl chains) are much more stable and more soluble within the phospholipid bilayer than TG itself (205). Thus, it is tempting to speculate that translocation of TG is achieved through hydrolysis of TG at the cytosolic side of ER membrane, followed by translocation of the amphipathic products of TG lipolysis, and lastly reesterification of TG at the lumenal side of ER membrane. Recently, Zammit and coworkers showed that a substantial proportion of DGAT activity was found latent within the intact rat liver microsomes, indicating that the lumen-facing DGAT may be specialized for the synthesis of TG destined for secretion (192). Thus, the existence of this lumen-facing DGAT implies that DG and acyl moieties, possibly derived from hydrolysis of cytosolic TG, may be transferred across the ER membranes for synthesis of TG (194). It is not clear whether the acyl moieties are translocated across the ER membranes through putative acylcarnitines (206, 207) or through rapid flip-flop in their un-ionized form (208). Obviously, the mechanism(s) responsible for translocation of TG, either *en bloc* or through its building blocks, across the ER membranes need to be further investigated.

1.4.6. The role of microsomal triglyceride transfer protein in very low density lipoprotein assembly

In vivo studies from abetalipoproteinemia subjects (5, 41) and from liver-specific MTP knockout mice (7, 8) have provided strong evidence that MTP plays an obligatory role in VLDL assembly and secretion. However, little is known about the underlying mechanism for the MTP action. One of the functions of MTP has been shown to assist translocation of apoB across the membranes of ER ((108-111), also refer to Section 1.3.3). Based on the evidence that initial lipidation of apoB takes place during apoB translocation, some researchers postulated that MTP activity may be essential only in the early stage of apoB lipidation (113). In the recent work showing post-translational B100-VLDL assembly, the notion that MTP was required for the "early phase" of assembly but not for bulk TG incorporation at the "late phase" was reinforced (161). Since both translocation of apoB and "early phase" lipidation of apoB are the prerequisite for VLDL maturation, diminished TG-rich VLDL assembly and secretion by MTP inactivation may be a result of retarded apoB translocation and of impaired "early phase" lipidation.

Although it is plausible that MTP acts as a facilitator for apoB translocation, other studies cast some doubts on this conclusion. Experiments with cells (116) or microsomal membranes (117) that lack MTP expression have shown that apoB translocation and assembly into a primordial particle do not need MTP activity. Furthermore, emerging evidence suggests that the demand for MTP is much greater for bulk TG incorporation during VLDL assembly than that for primordial particle formation (209). In addition, in abetalipoproteinemia, fat droplets were found in the cytosol but not in the secretory

compartments (6), implying that MTP may play a role in lipid partitioning between cytosol and microsomes. The role of MTP in intracellular lipid mobilization is further supported by recent transgenic mouse studies showing that MTP inactivation resulted in decreased lipid droplet accumulation within the microsomal lumen (210). In contrast, deficiency in apoB expression in transgenic mice did not prevent microsomal lipid droplet formation, implying that mobilization of lipid into microsomes is not always accompanied with apoB translocation (203). These data raise the possibility that MTP may play a role in intracellular lipid mobilization, thereby governing the lipid availability for TG-rich VLDL assembly.

1.4.7. Effect of brefeldin A on very low density lipoprotein assembly

In addition to MTP, a brefeldin A (BfA)-sensitive factor is also required for the bulk TG incorporation into apoB (161, 211). Brefeldin A is a fungal metabolite that blocks the protein trafficking from ER to Golgi. The blockage is caused by inactivation of a guanine nucleotide exchange factor that is essential for binding (via GDP/GTP exchange) of the small ARF (ADP ribosylation factor) GTPase to membranes, a prerequisite for the formation and budding of coated vesicles (212). The effective dose of BfA to block protein trafficking is 1 μg/ml. However, in McA-RH7777 cells, assembly and secretion of B48-VLDL, but not B48-HDL, is inhibited at a low dose of BfA (0.2 μg/ml) (211). Assembly of B100-VLDL is also sensitive to the low dose of BfA (161, 211).

It is not clear how low dose BfA inhibits VLDL assembly in McA-RH7777 cells. In the presence of the low dose of BfA, both B48 (162) and B100 (161) were found in the particles of HDL-like buoyant density, and were associated with microsomal membranes. When BfA was withdrawn from the culture medium, assembly of VLDL resumed, and membrane-associated B48- or B100-containing HDL was converted into VLDL in the presence of oleate (161, 162). These experiments not only provide strong evidence showing that incorporation of bulk TG into apoB can be achieved post-translationally, but also imply that an unknown GTPase, reversibly inhibitable by low dose of BfA, is probably responsible for vesiculation of bulk TG and immature apoB particles.

1.4.8. Effect of orotic acid on very low density lipoprotein assembly

Feeding rats with a diet containing 1% of orotic acid (a pyrimidine precursor) impaired secretion of hepatic VLDL (but not HDL) with a concomitant increase in hepatic lipids resulting in fatty liver (213-216). Within the fatty hepatocytes, lipid accumulated in two forms: one located in cytosol as large lipid droplets, and the other within ER lumen as smaller droplets, forming "liposome"-like structures (217-224).

Biochemical evidence showed that neither apoB synthesis nor TG synthesis was affected in fatty hepatocytes isolated from orotic acid-fed rats. Since the membrane-bound apoB could be chased from the rough ER to the trans-Golgi membranes, the trafficking of apoB *per se* within the secretory pathway may not be affected by orotic acid treatment (225). Despite the accumulation of lipid droplets within the ER lumen and the presence of apoB, nascent VLDL particles were absent within the Golgi compartment

(223, 224), implying that there may be an impediment in the mobilization and transport of TG to the site where VLDL is assembled. Further analysis of the "liposome"-like structures showed that the "liposome" contents were profoundly deficient in apoB100 and apoB48 relative to apoE and apoC when compared with rat plasma VLDL (220). Thus, it was postulated that apoE- or apoC-containing TG-rich particles may be the putative VLDL assembly intermediates, and movement of the putative VLDL assembly intermediates out of the ER compartment may require a net acquisition of apoB to form VLDL (220).

The effect of orotic acid could be rapidly reversed or prevented by the addition of adenine or adenosine to the diet, as well as by withdrawal of orotic acid from the diet (216, 226, 227). Thus, the ER exit of the putative VLDL assembly intermediates may involve a GTP- or ATP-binding protein. The mechanism(s) for the involvement of the putative GTP- or ATP-binding protein in VLDL assembly remains to be investigated.

1.5. Thesis objective

This thesis mainly focuses on the mechanism responsible for the biogenesis of hepatic TG-rich VLDL using McA-RH77777 cells stably expressing human B100 or other C-terminally truncated apoB.

The following issues will be addressed:

(a) Can recombinant apoBs assemble TG-rich VLDL in McA-RH7777 cells? If so, what is the minimum length of apoB that is required to assemble TG-rich VLDL?

(b) Does apoB100 assemble TG-rich VLDL through the same pathway as apoB48?

(c) Is MTP required during post-translational TG-rich VLDL assembly?

(d) How is MTP involved in TG-rich VLDL assembly?

Table I.

Size, density and composition of human lipoproteins

(Adapted from (243))

	Chylomicrons	Very low density lipoproteins	Intermediate density lipoproteins	Low density lipoproteins	High density lipoproteins
Abbreviation		VLDL	IDL	LDL	HDL
Density, g/ml	< 0.95	0.95-1.006	1.006-1.019	1.019-1.063	1.063-1.210
Diameter, nm	75-2000	30-80	25-35	18-25	5-12
Composition, % dry weight					
Protein	1-2	10	18	25	33
Triacylglycerols	83	50	31	9	8
Cholesterol + cholesteryl ester	8	22	29	45	30
Phospholipids	7	18	22	21	29
Apoproteins	AI, AII				AI, AII
	B-48	B-100	B-100	B-100	
	CI, CII, CIII	CI, CII, CIII	CI, CII, CIII		CI, CII, CIII
	E	E	E		E

FIG. 1.1. Structure of human apolipoprotein B. *A*, the position of apoB amino acid residues (*top*) in comparison to the nomenclature of apoB using the centile system (*bottom*) (228). B48 refers to N-terminal 48% of full-length apoB, whereas B100 refers to the full-length apoB. The centile system of apoB will be used in this thesis. *B*, positions of the N-linked glycosylation sites within B100. There are 19 N-x-T/S sites within B100, 16 of them glycosylated (*closed*) and 3 of them unglycosylated (*open*) (15, 18). *C*, positions of cysteines within B100. Cysteines involved in disulfide linkages are connected together (21). *D*, the pentapartite model for the secondary structure of human B100 (27).

Fig. 1.1.

A. Amino acid residues and the centile system

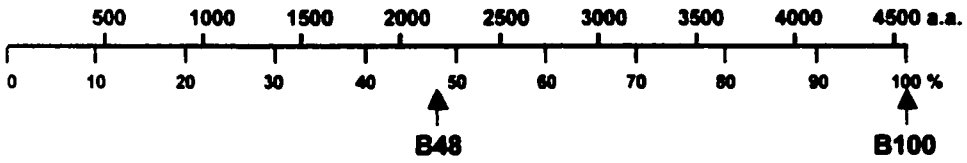

B. N-linked glycosylation sites

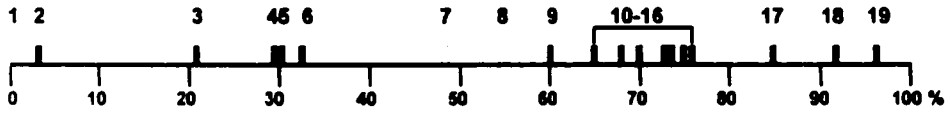

C. Disulfide linkages

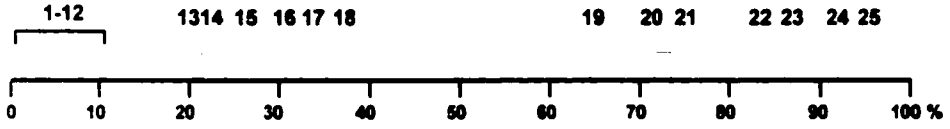

D. The pentapartite model

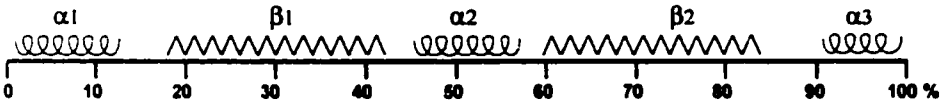

FIG. 1.2. **"Ribbon and bow" model for the conformation of apolipoprotein B100 on the low density lipoprotein surface.** *A-D*, the "ribbon" of N-terminal 89% of apoB100 on the LDL surface. These panels (from *A* to *D*) are related by sequential 90° rotations about a horizontal axis in the plane of the page. The numeric labels on the surface represent the centile nomenclature of apoB. *E*, the "bow" of apoB100. The orientation is the same as *D*. The C-terminal 11% of apoB100 moves "backward" from B89 into one hemisphere (at B92), and then crosses the ribbon near the LDL-receptor binding site and terminates in the other hemisphere (at B100) (adapted from (31)).

Fig. 1.2.

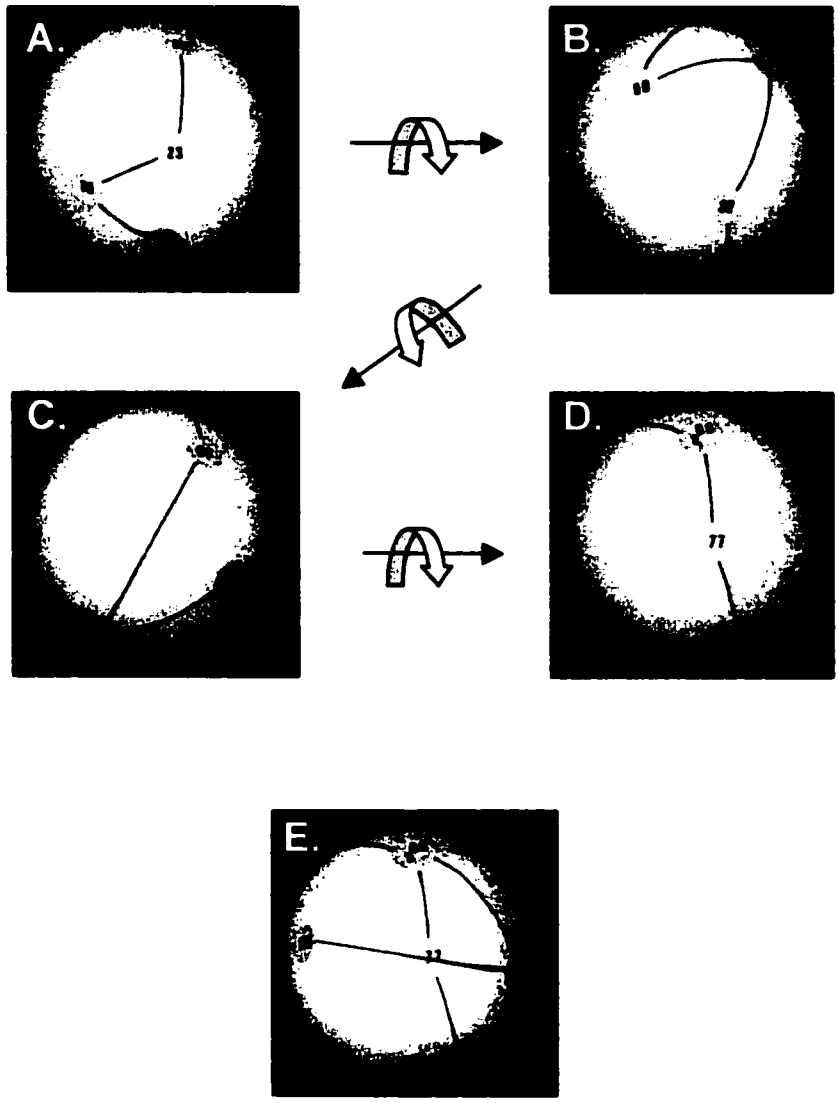

FIG. 1.3. **Ribbon diagrams of the lamprey lipovitellin monomer.** *A*, the view looking from the side of the lipid cavity. *B*, the view looking down into the lipid cavity from the widened opening. The cartoon is color-coded to show the three domains of the LV. (The atomic coordinates for lipovitellin were obtained from the Protein Data Bank, Brookhaven, with accession code 1LLV. The models were prepared using the program Rasmol.)

Fig. 1.3.

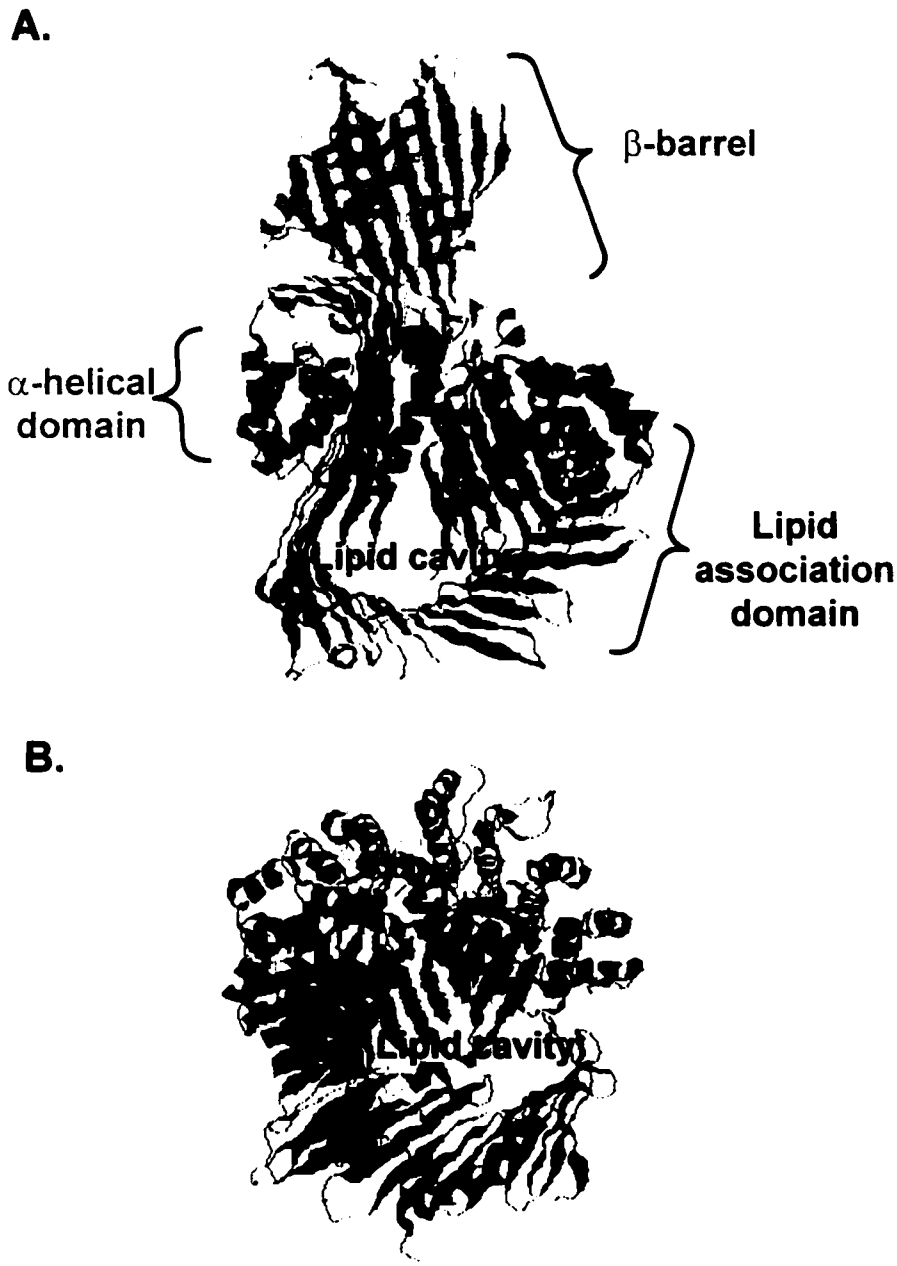

FIG. 1.4. **Molecular models of MTP and apoB based on the atomic coordinates of lamprey lipovitellin.** *A*, the N-terminal β-barrel of MTP. *B*, the N-terminal β-barrel of apoB. *C*, the predicted α-helical domain of MTP. *D*, the α-helical domain of apoB. *E*, expanded view of helices 13-17 of MTP showing the predicted buried salt bridge R540-N531-E570 in red) and PDI-binding residues (Y554, M555, K558, I592 in dark green). *F*, expanded view of the R531-E557-D524 buried salt bridge of apoB. In *A* to *F*, α-helices are depicted as blue cylinders, disulfide groups are red, loops are gray and β-strands are yellow, except those that correspond to the homodimerization interface of lamprey LV, which are shown in green (adapted from (46)).

Fig. 1.4.

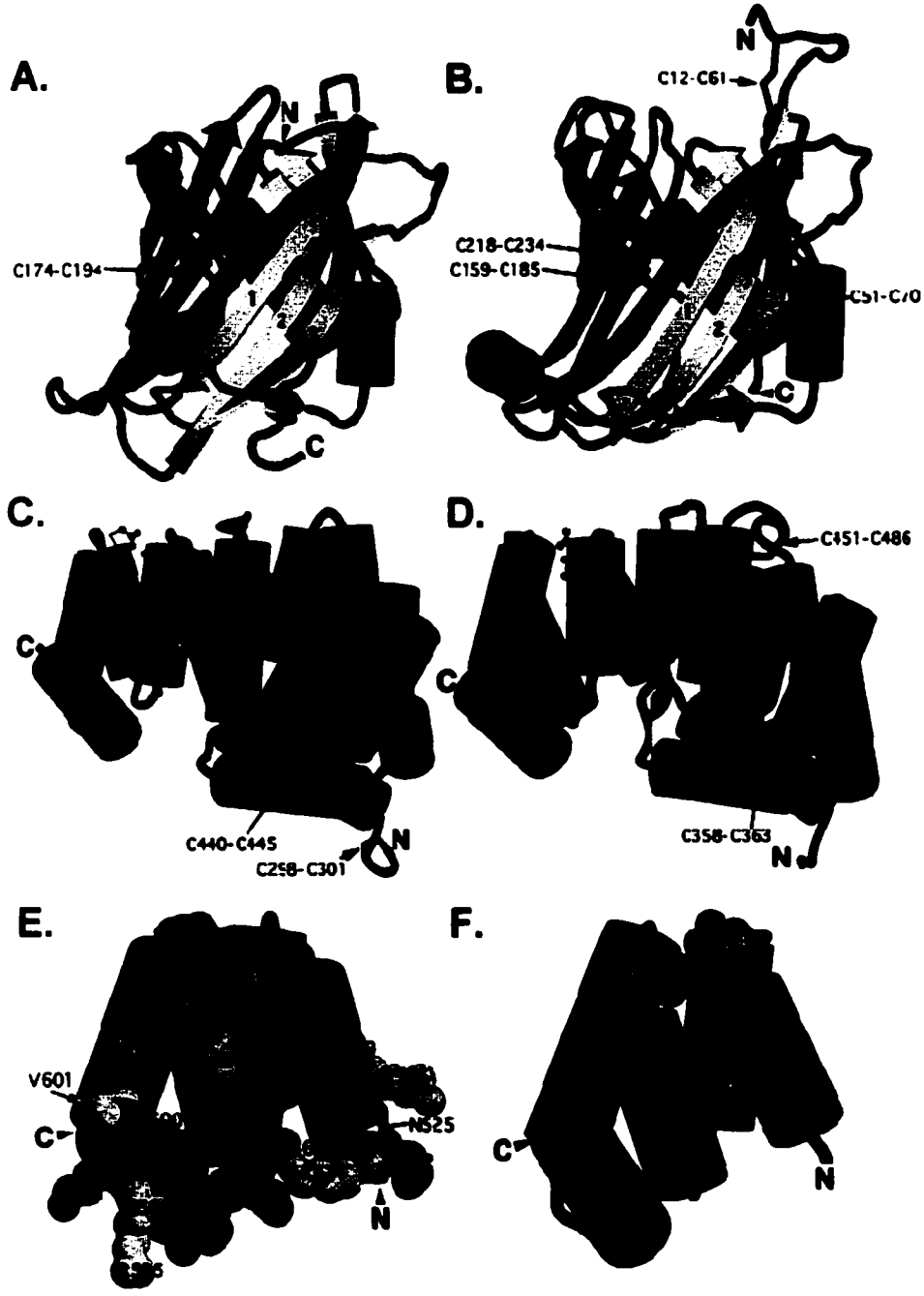
A.
N
C174-C194
C
B.
N
C12-C61
C218-C234
C159-C185
C
C.
C
C440-C445
C258-C301
N
D.
C451-C486
C
C358-C363
N
E.
V601
C
N525
N
F.
C
N

FIG. 1.5. **"Lipid cavity" model for assembly of apolipoprotein B-containing lipoprotein particles.** *A*, model of the structure of the lamprey LV "lipid cavity" viewed from above. Green circles represent phospholipid headgroups. The protein structural schematics in blue indicate the relative positions of the β sheets, βC:LV, βA:LV, βB:LV, and βD:LV, and the α helical cluster, α:LV (cylinders for α helixes, and arrows for antiparallel β sheets). *B*, model of the proposed hApoB "lipid cavity" viewed from above. To complete the "lipid cavity" (compare with *A*), βA:B and βB:B require the amphipathic β strand cluster βB:MTP and the a helical cluster α:MTP from hMTP. The protein structural schematics are color coded, blue for hApoB and red for hMTP. Notice that the portion of α:MTP that lines the lipid cavity (negatively charged) binds to the positively charged N-terminal portion of the α:B domain of hApoB. *C*, an incomplete "lipid pocket" is formed by amphipathic β strands (blue dashes) located in the α_1 domain of hApoB. MTP is required for this pocket to fill with lipid (yellow, neutral lipid; green, phospholipid head groups; black, fatty acyl chains), perhaps acting as a co-structural element to complete the pocket (see *B*). Once the pocket is filled, additional amphipathic β strands from the β_1 domain of hApoB are co-translationally added, allowing the "lipid cavity" to expand until defined lipoprotein particles with HDL, then VLDL density result (adapted from (47)).

Fig. 1.5.

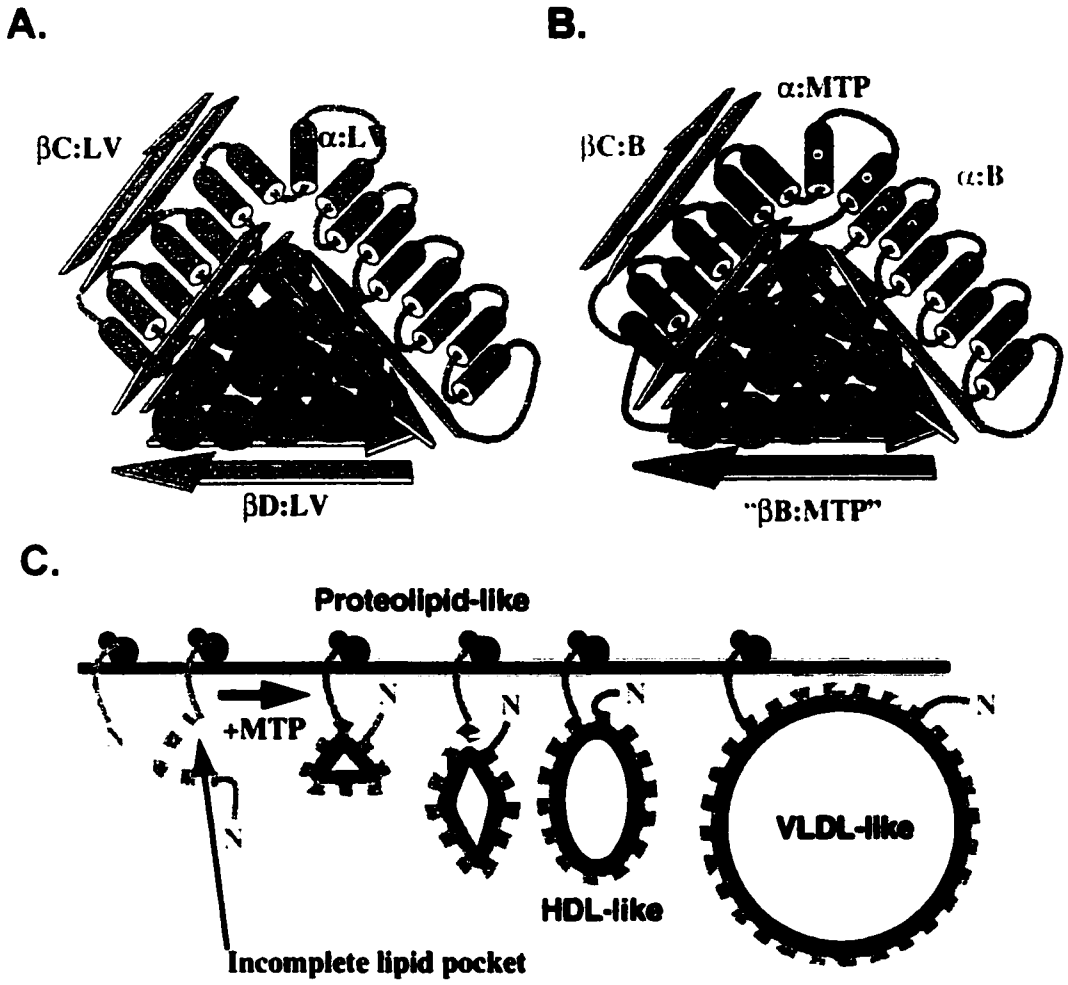
A.
βC:LV
α:LV
βD:LV
B.
α:MTP
βC:B
α:B
"βB:MTP"
C.
Proteolipid-like
+MTP
N
N
N
N
N
VLDL-like
HDL-like
Incomplete lipid pocket

FIG. 1.6. **Comparison of the length of primary sequence responsible for the lipid association domain among apolipoprotein B (apoB), vitellogenin (VTG) and microsomal triglyceride transfer protein (MTP)** (adapted from (61)).

Fig. 1.6.

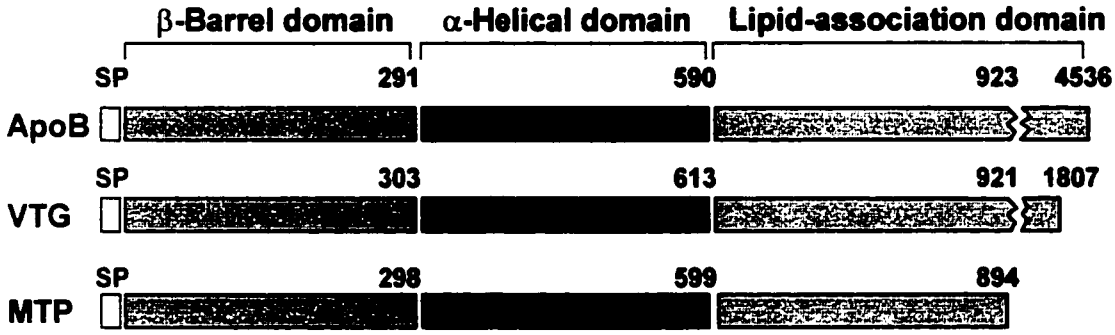
β-Barrel domain
α-Helical domain
Lipid-association domain
SP
291
590
923
4536
ApoB
SP
303
613
921
1807
VTG
SP
298
599
894
MTP

FIG. 1.7. **The buoyant density and the size of lipoproteins containing apolipoprotein B is a function of apolipoprotein B length.** *A*, immunoblots of human apoB proteins associated with lipoproteins secreted from transfected McA-RH7777 cells (without oleate supplement). Lipoproteins from conditioned media were fractionated by a continuous density gradient ultracentrifugation, denatured and resolved by SDS-PAGE. The arrows indicate peak fractions of lipoproteins. *B*, medium lipoproteins were resolved by non-denaturing polyacrylamide gradient gel electrophoresis (3-10%) and human apoB were visualized by immunoblotting. *C*, the relationship between the buoyant density and the core volume of lipoprotein and the apoB length. Each particle contains C-terminally truncated apoB, the length of which is indicated by X-axis. The size of particle increases with the apoB length, as illustrated by the size of circles in the cartoon. Increasing truncation of the C-terminus of apoB increases the buoyant density (left Y-axis), but decreases the core volume (right Y-axis), of the particles (adapted from (229)).

Fig. 1.7.

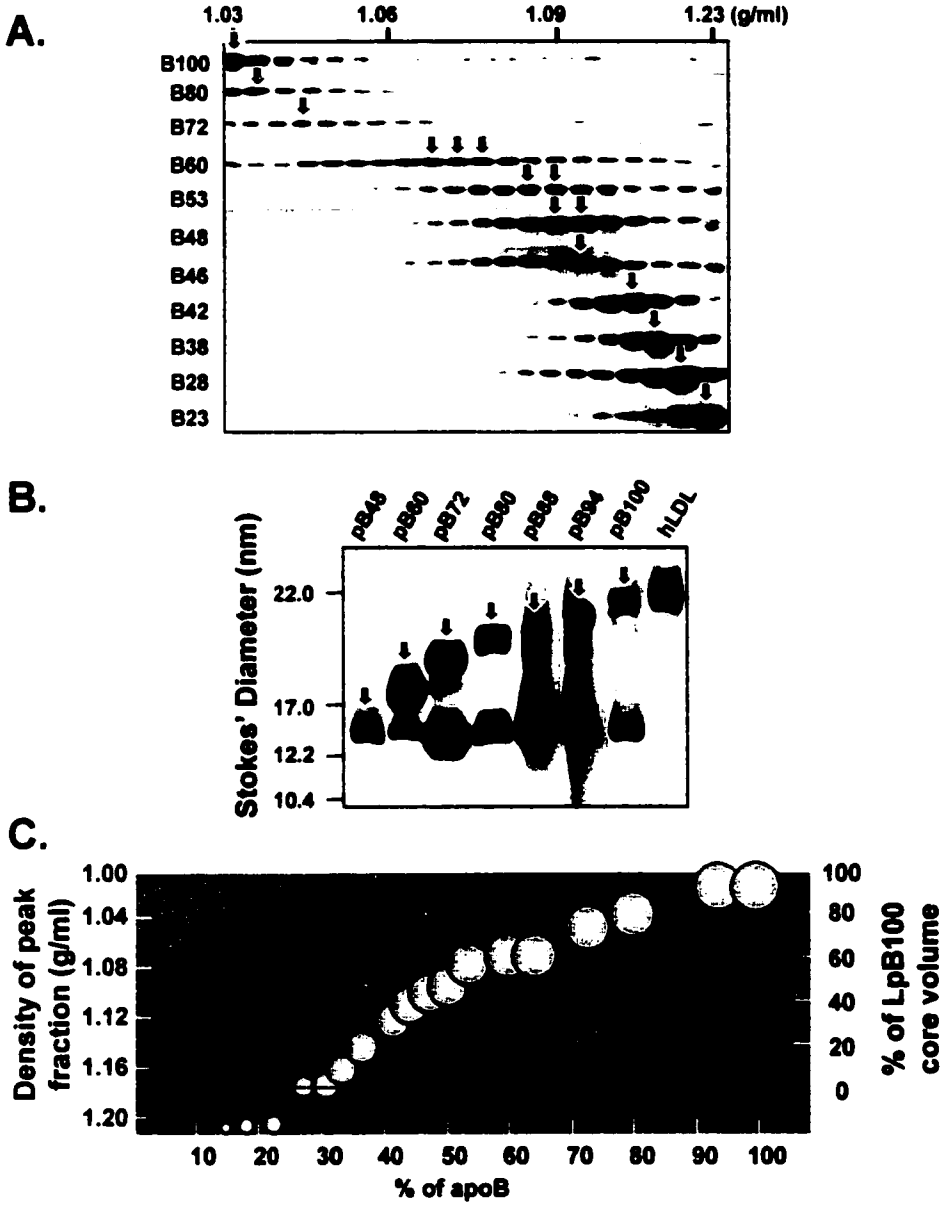
A.
1.03
1.06
1.09
1.23 (g/ml)
B100
B80
B72
B60
B53
B48
B46
B42
B38
B28
B23
B.
pB48
pB60
pB72
pB90
pB98
pB94
pB100
hLDL
Stokes' Diameter (nm)
22.0
17.0
12.2
10.4
C.
Density of peak fraction (g/ml)
1.00
1.04
1.08
1.12
1.16
1.20
10
20
30
40
50
60
70
80
90
100
% of apoB
100
80
60
40
20
0
% of LpB100 core volume

FIG. 1.8. **Phosphatidic acid pathway for biosynthesis of triacylglycerol in hepatocytes.** Notice that both glycerol and fatty acid (such as oleate) are the precursors for triacylglycerol.

Fig. 1.8.

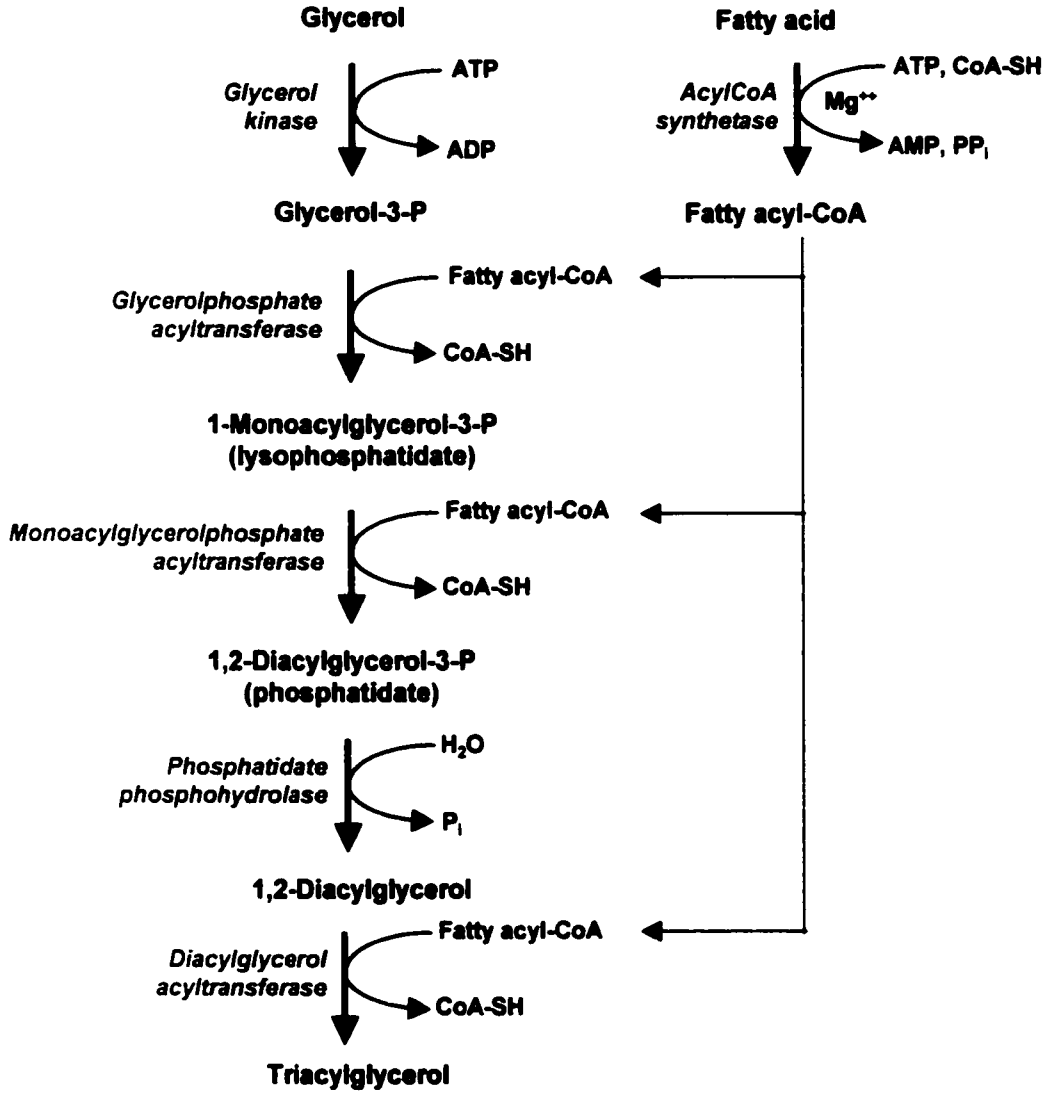
Glycerol
Fatty acid
Glycerol kinase
ATP
ADP
AcylCoA synthetase
ATP, CoA-SH
Mg++
AMP, PPi
Glycerol-3-P
Fatty acyl-CoA
Glycerolphosphate acyltransferase
Fatty acyl-CoA
CoA-SH
1-Monoacylglycerol-3-P (lysophosphatidate)
Monoacylglycerolphosphate acyltransferase
Fatty acyl-CoA
CoA-SH
1,2-Diacylglycerol-3-P (phosphatidate)
Phosphatidate phosphohydrolase
H2O
Pi
1,2-Diacylglycerol
Diacylglycerol acyltransferase
Fatty acyl-CoA
CoA-SH
Triacylglycerol

FIG. 1.9. **Putative pathways for hydrolysis and reesterification of cytosolic triacylglycerol during very low density lipoprotein assembly.** The newly synthesized triacylglycerol is considered to be partitioned between association with apoB to form nascent particles and the formation of cytosolic TG. The latter is hydrolyzed to form partial glycerides (either diacylglycerol or monoacylglycerol) and fatty acyl-CoA through the action of unknown hydrolase. Triacylglycerol can be synthesized from the remodeled DG to be incorporated into VLDL, although the enzymes responsible for reesterification process remain to be defined (adapted from (194)).

Fig. 1.9.

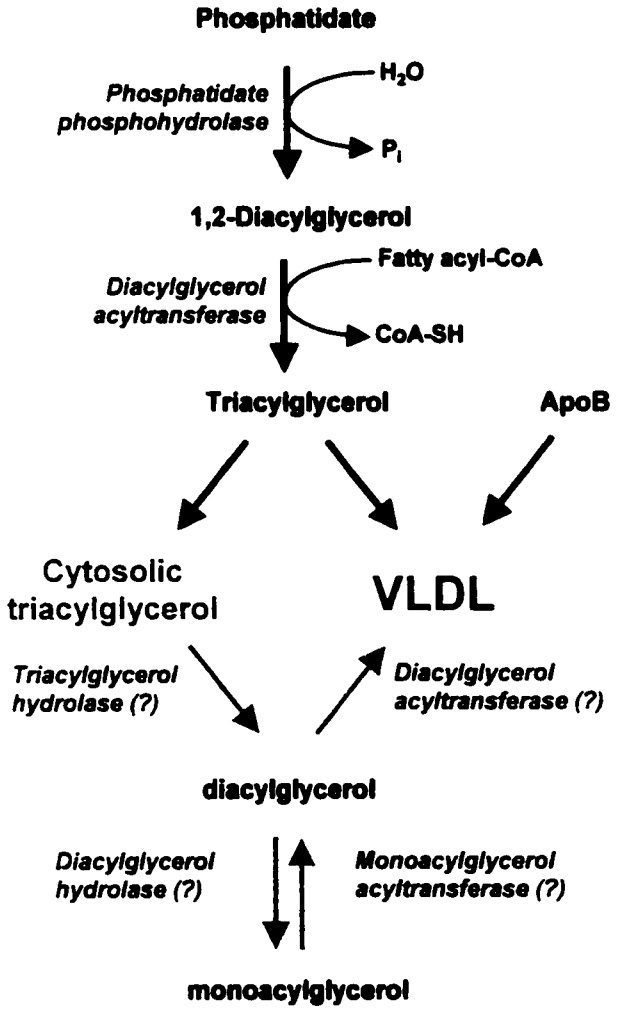
Phosphatidate
Phosphatidate phosphohydrolase
H_2O
P_i
1,2-Diacylglycerol
Diacylglycerol acyltransferase
Fatty acyl-CoA
CoA-SH
Triacylglycerol
ApoB
Cytosolic triacylglycerol
VLDL
Triacylglycerol hydrolase (?)
Diacylglycerol acyltransferase (?)
diacylglycerol
Diacylglycerol hydrolase (?)
Monoacylglycerol acyltransferase (?)
monoacylglycerol

Chapter 2 Material and Methods

Materials - Dulbecco's modified Eagle's medium (DMEM), fetal bovine serum (FBS), horse serum and neomycin analog G418 were obtained from Life Technologies Inc. Reagents for polyacrylamide gel electrophoresis (PAGE) and nitrocellulose membrane were obtained from Bio-Rad. Sheep anti-human apoB and apoA-I antiserum, the ECL immunodetection system, trypsin and soybean trypsin inhibitor were obtained from Boehringer Mannheim. CNBr-activated Sepharose 4B beads and protein A-Sepharose CL-4B beads were obtained from Pharmacia LKB Biotechnology Inc. ProMix™ ([^{35}S]methionine/cysteine, 1000 Ci/mmol), [2-^{3}H]glycerol (1 Ci/mmol), [^{3}H]oleic acid (9 Ci/mmol), [1-^{14}C]oleic acid, glycerol tri[1-^{14}C]oleate (80 mCi/mmol), Na^{125}I (100 mCi/ml), and peroxidase-conjugated anti-mouse immunoglobulin G antibody were obtained from Amersham Pharmacia Biotech Ltd. Oleic acid, fatty acid free bovine serum albumin, and standard lipids were obtained from Sigma. N-acetyl-leucyl-leucyl-norleucinal (ALLN) was obtained from Biomol. Silica Gel 60 thin-layer chromatography (TLC) plates and organic solvents used for TLC were obtained from BDH Chemicals. Brefeldin A was obtained from Epicenter Technologies. MTP inhibitors BMS-192951 and BMS-197636 (designated compound 7) (230) were gifts of D. Gordon (Bristol-Myers Squibb). Monoclonal antibodies specific for human apoB (1D1, Bsol14, 3E5) or rat apoB (LRB220) were obtained from R. Milne, Y. Marcel (University of Ottawa Heart Institute) and L. Wong (Louisiana State University), respectively.

Cell Culture and Stock Solution – Rat hepatoma McA-RH7777 cells stably expressing human apoB variants, i.e., hB29, hB34, hB37, hB42, hB48, hB60, hB72, hB80 and

hB100 (129), were cultured in DMEM containing 10% (v/v) FBS, 10% (v/v) horse serum and 200 μg/ml G418 in 100-mm dishes. Cells were split in a ratio of 1:8 every three days (defined as one passage). For experiments, cells were grown no more than 20 passages after revival from liquid nitrogen.

All experiments, except for subcellular fractionation studies, were carried out in 60-mm Primaria dishes. Cells were prepared one or two days before experiments so that cell confluency was 100% (about 1 mg protein/dish) on the day of experiment. For subcellular fractionation studies, 100-mm Falcon dishes were used, and the confluency of the cells was 100% (about 4 mg protein/dish) on the day of experiment.

A stock solution of BfA (5 mg/ml) was prepared in absolute ethanol. MTP inhibitors BMS-192951 (20 mM) and BMS-197636 (20 mM) were prepared in dimethylsulfoxide.

Metabolic Labeling – Procedures for metabolic labeling with [^{35}S]methionine, [^{3}H]glycerol, [^{3}H]oleate, or [^{14}C]oleate are described in the figure legends.

Ultracentrifugation of Lipoproteins – Three ultracentrifugation methods were used to separate lipoproteins. (i) Sucrose density gradient ultracentrifugation. The conditioned media were collected, diluted to 5 ml with phosphate-buffered saline (pH 7.4), and mixed with 0.655 g sucrose for a final concentration of 12.5% (w/v). The samples were then subjected to ultracentrifugation in a sucrose density gradient. Briefly, the centrifuge tube

was loaded from the bottom to the top: 2.0 ml 47% sucrose, 2.0 ml of 25% sucrose, 5.0 ml of the sample in 12.5% sucrose, 3 ml phosphate-buffered saline (pH 7.4). The gradient was formed after 65 h centrifugation at 35,000 rpm in a Beckman SW41 rotor at 12 °C. Twelve fractions (1 ml each) were collected from the top of the centrifuge tube, of which fractions 1 and 2 (the top two ml) represent VLDL (d < 1.02 g/ml) and fractions 8-10 (from the top of the gradient) represent lipoproteins of densities similar to that of HDL (d = 1.08 – 1.13 g/ml). (ii) Sequential flotation ultracentrifugation. The conditioned media were collected, diluted to 5 ml with phosphate-buffered saline (pH 7.4), and adjusted to d = 1.02 g/ml with 0.1 g KBr. The samples were loaded into quick-seal tubes, and subjected to ultracentrifugation in a Beckman TLA100.4 rotor at 100,000 rpm (12 °C, 4 h). After centrifugation, the tubes were sliced to separate the top fraction (1 ml, d < 1.02 g/ml) from the bottom fraction (4 ml, d > 1.02 g/ml). (iii) Cumulative rate flotation ultracentrifugation. The samples (conditioned media or the lumenal contents of microsomes) were collected, diluted to 4 ml with phosphate-buffered saline (pH 7.4), and adjusted to d = 1.10 g/ml with 0.56 g KBr. The samples were then loaded onto the bottom of Beckman SW40 centrifuge tubes, and overlaid with 3 ml of d = 1.065 g/ml NaBr, 3 ml of d = 1.02 g/ml NaBr, and 3 ml of d = 1.006 g/ml NaCl. After ultracentrifugation (40,000 rpm, 20 °C, 148 min), $VLDL_1$ (S_f > 100) was collected from the top 1 ml of the gradient. After an additional ultracentrifugation (37,000 rpm, 15 °C, 18 h), other lipoproteins were collected from top to bottom into 12 fractions (1 ml each). Of the 12 fractions, the top two fractions represent $VLDL_2$ (S_f 20-100).

Analysis of ApoB Proteins – ApoB proteins were quantitatively immunoprecipitated with sheep anti-human apoB polyclonal antibody (Boehringer Mannheim). The anti-apoB polyclonal antibody cross-reacted with both rat apoB100 and rat apoB48. The immunocomplexes were recovered by protein A-Sepharose CL-4B. ApoB proteins were eluted from the beads, and subjected to electrophoresis on 5% (w/v) or 3-15% (w/v) gradient polyacrylamide gels with 0.1% (w/v) SDS. For radiolabeled apoB proteins, the gels were treated with Amplify (Amersham Corp.) for 30 min, dried, and apoB proteins were detected by fluorography. For non-radiolabeled apoB proteins, they were analyzed by immunoblotting. Briefly, after electrophoresis, apoB proteins were transferred onto nitrocellulose membranes at 125V for 6 h with a transfer buffer (190 mM glycine, 25 mM Tris base, 20% methanol) at −10 °C, and detected with 1D1 for human apoB or with LRB220 for rat apoB using ECL.

Non-denaturing Gradient Gel Electrophoresis – Conditioned media were fractionated into VLDL (d < 1.02 g/ml) and HDL (d = 1.06 - 1.21 g/ml) by sequential flotation ultracentrifugation, or into $VLDL_1$ (S_f > 100) and $VLDL_2$ (S_f 20 -100) by cumulative rate flotation ultracentrifugation. Each fraction was further concentrated to 200 µl by centrifugation. The concentrated samples (20 µl) were subjected to electrophoresis on 2-8% (w/v) polyacrylamide gradient gels under non-denaturing conditions. The electrophoresis was performed at 125 V for 32 h with a recirculating buffer solution which contained 90 mM Tris base, 90 mM boric acid, and 2 mM EDTA, pH8.0. Human LDL (22 nm), thyroglobulin (17 nm) and ferritin (12.2 nm) were used as size markers for determination of particle diameter. Proteins were transferred to nitrocellulose membrane

for 30 h with a transfer buffer (190 mM glycine, 25 mM Tris base, 20% methanol) being replaced once during transfer, and apoB proteins were analyzed by immunoblotting.

Immunoaffinity Purification of Lipoproteins Containing ApoB and Lipid Analysis- Monoclonal antibody 1D1 (4 mg) was coupled to CNBr-activated Sepharose 4B beads (1 g) according to the manufacturer's instructions. For human B48-transfected cells, twelve fractions obtained from sucrose gradient ultracentrifugation of the conditioned media were mixed with bovine serum albumin (final concentration 1%) and 100 µl of 1D1-affinity beads for 16 h at 4 °C to recover hB48-lipoproteins. After hB48-lipoproteins were precipitated, the supernatant was subsequently mixed with an anti-human apoB polyclonal antibody (Boehringer Mannheim, this antibody cross-reacts with rat apoB) to recover lipoproteins containing endogenous rat apoB100. Immunocomplexes with either hB48- or rB100-lipoproteins were washed five times with 1 ml of phosphate-buffered saline by centrifugation. Since hB48- and rB100-lipoproteins were mostly confined to fractions 1 and 2 (VLDL, $d < 1.02$ g/ml) and 8-10 (HDL, $d = 1.08$-1.13 g/ml) in the sucrose density gradient, in some cases only these two combined fractions were subjected to immunoprecipitation to recover hB48-VLDL, rB100-VLDL, and hB48-HDL particles. The recovery of hB48-VLDL from the conditioned medium by immunoaffinity purification was greater than 90%, and the purified hB48-VLDL contained less than 15% endogenous rB100-VLDL as determined by Western blot analysis and by quantification of ^{35}S-labeled apoBs (data not shown).

For human B100-transfected cells, the conditioned media were subjected to cumulative rate flotation ultracentrifugation to isolate $VLDL_1$ ($S_f > 100$) and $VLDL_2$ (S_f 20-100) fractions. Human B100-$VLDL_1$ and hB100-$VLDL_2$ were purified from these two fractions using 1D1-affinity beads. After hB100-lipoproteins were precipitated, the supernatant was subsequently mixed with an anti-human apoB polyclonal antibody to recover rB100-$VLDL_1$ and rB100-$VLDL_2$.

Lipids associated with the purified lipoprotein particles were extracted by chloroform/methanol. Separation of phospholipids and neutral lipids was performed on silica gel 60 plates as described (231) using egg yolk lipids as a carrier. The radioactivity associated with individual lipid species was quantified by liquid scintillation counting (Wallac 1409 counter).

Radioimmunoassay - Solid phase radioimmunoassay was performed in Immulon II removawells (Dynatech Laboratories, Alexandria, VA). The wells were coated with 100 µl of 1D1 (10 µg/ml of purified immunoglobulins in 5 mM glycine, pH 9.2) for 16 h and subsequently saturated by incubation with 125 µl of 1% BSA in PBS, pH 7.4 (PBS-BSA) for 1 h. Human LDL and medium VLDL ($d < 1.02$ g/ml) were appropriately diluted in PBS-BSA as indicated in the figure legends, and aliquots (100 µl) of the samples were loaded into the coated wells that had been washed with 0.15 M NaCl containing 0.025% Tween 20. After overnight incubation, the wells were rinsed with the Tween-saline solution and incubated with 10 ng ^{125}I-labeled immunoglobulins (*i.e.* 1D1, Bsol 14, 3F5, or LRB220) in 1% PBS-BSA (specific activity: 10,000 cpm/ng) for another overnight

period. Finally, the wells were rinsed with the Tween-saline solution and radioactivity was quantified by counting. The epitopes for Bsol 14, 1D1, and 3F5 are located within amino acids 186-670, 474-539, and 2835-2922, respectively, of human apoB100 (232). Antibody Bsol 14, which does not compete with 1D1 for binding to LDL, was used to show the lack of spatial constraint between 1D1 and the captured VLDL particle that could potentially interfere with antibody-antigen binding.

MTP Activity Assay – The TG transfer activity of MTP was measured using [^{14}C]triolein and the deoxycholate extract of total cell homogenate according to the published protocol (5). Since the extensive dialysis required for the deoxycholate extraction precluded the assessment of BMS-197636 (a reversible inhibitor) effect on MTP, an alternative protocol (referred to as sonication extraction) was developed in which the cell homogenate was sonicated for 2 min at 4 °C. After centrifugation (400,000 × *g*, 16 min) of the sample, the supernatant that contained the MTP activity was used for TG transfer assay. The MTP activity in McA-RH7777 cells measured by the two protocols was comparable (data not shown).

Subcellular Fractionation – Metabolically labeled cells (100-mm dish) were suspended in 2 ml of Tris-sucrose buffer (10 mM Tris-HCl, pH 7.4, and 250 mM sucrose) that was supplemented with protease inhibitors (0.1 mM leupeptin, 0.1 mM phenylmethylsulfonyl fluoride, 100 unit/ml aprotonin, and 40 μg/ml ALLN). The cells were homogenized using a ball-bearing homogenizer (20 passages) (79), and the postnuclear supernatant was obtained by centrifugation (10,000 × *g*, 4 °C, 10 min). Heavy microsomes were isolated

from the postnuclear supernatant by centrifugation using a microfuge (16,000 × *g*, 4 °C, 15 min), and subsequently the light microsomes and cytosol were separated by centrifugation using a Beckman TLA-100.4 rotor (400,000 × *g*, 4 °C, 16 min). The heavy microsomes were enriched with ribosomal RNA as determined by ethidium bromide staining of total RNA separated by agarose gel electrophoresis. In some experiments, the heavy and light microsomes were combined (referred to as total microsomes).

Trypsin Digestion – Heavy microsomes were resuspended in 200 µl of Tris-sucrose buffer using a 25 G needle (5 passages). Aliquots (60 µl) of the samples were incubated (30 min on ice) with or without 50 µg/ml of trypsin and 1% (v/v) of Triton X-100. Trypsin digestion was terminated by the addition of soybean trypsin inhibitor (final concentration of 0.5 mg/ml). The samples were solubilized with an equal volume of lysis buffer [1% (v/v) Triton X-100, 1% (w/v) deoxycholate, and 2% (w/v) SDS] for 16 h and diluted to 0.2% (w/v) SDS prior to immunoprecipitation with an anti-apoB antiserum (Boehringer Mannheim). [^{35}S]ApoB was analyzed by PAGE/fluorography as described above.

Sodium Carbonate Treatment – The total microsome pellet, obtained from centrifugation (400,000 × *g*, 4 °C, 16 min) of postnuclear supernatant derived from approximately 2 dishes (100 mm) of cells, were rinsed twice with (to minimize cytosol contamination) and resuspended in 2 ml Tris-sucrose buffer. The microsome samples were mixed with equal volume of 0.2 mM sodium carbonate, pH 12.4 (the final concentration of sodium carbonate was 0.1 mM and pH of which was 11.3) using a nutator™ (a mechanical

rocker) for 30 min at room temperature to release lumenal contents. The lumenal contents were separated from microsomal membranes by ultracentrifugation (400,000 × *g*, 4 °C, 16 min).

Analysis of Intracellular Lipids – [^{3}H]Lipids were extracted with $CHCl_3/CH_3OH/H_2O$ (4:2:3; by volume) from cytosol, microsomal membrane, and microsomal lumen. and separated by TLC on Silica gel 60 plates using egg yolk lipids as a carrier, as described previously (231). The radioactivity associated with individual lipid species was quantified by liquid scintillation counting (Wallac 1409 counter). The recovery of [^{3}H]TG was nearly 100% for cytosol, microsomal membrane, and microsomal contents as determined by monitoring radioactivity associated with each fraction in comparison to that associated with total postnuclear supernatant.

Other Assays - Protein (233) and TG mass (234) were determined by published methods. Phosphatidylcholine (PC) mass was quantified using an assay kit (Boehringer Mannheim) according to the manufacturer's instruction.

Chapter 3 Results

3.1. Assembly of human B48-VLDL in transfected McA-RH7777 cells

In rat hepatoma McA-RH7777 cells, assembly and secretion of endogenous rat B48-VLDL can be induced by oleate in the presence of DMEM + 20% serum (125). Assembly of B48-VLDL has been postulated to undergo a two-step lipidation process: in the first step lipidation, a primordial particle with the buoyant density of HDL (d = 1.063-1.21 g/ml) is formed during or immediately after translation of apoB48 nascent polypeptide. In the presence of sufficient lipid supply, a second step lipidation occurs whereby bulk lipid is incorporated into the core of the primordial particle to form mature VLDL (125, 162). Thus, McA-RH7777 cells retain the ability to assemble VLDL.

Based on the above results, we raised the following questions: (a) Does human apoB48 also have the ability to assemble TG-rich VLDL in McA-RH7777 cells? (b) What is the minimum length of human apoB that is required for the assembly of TG-rich VLDL? We chose transfected McA-RH7777 cells as the cell model for the following reasons: (a) McA-RH7777 is the only available hepatoma cell line that produces authentic VLDL (i.e. d < 1.006 g/ml). (b) Although the level of endogenous apoB expression is low in McA-RH7777 cells, these cells are suitable for stable transfection with recombinant human apoBs. Such a system makes it possible to address the effect of apoB length on VLDL assembly. (c) In human B48-transfected McA-RH7777 cells, overexpression of human apoB48 (hB48) suppresses endogenous rat apoB48 (rB48) expression (235), therefore the assembly of human B48-VLDL (hB48-VLDL) can be examined in this cell line without any interference from rat B48-VLDL (rB48-VLDL).

3.1.1. Oleate-induced assembly and secretion of human B48-VLDL in human B48-transfected McA-RH7777 cells

In human B48-transfected McA-RH7777 cells, secretion of hB48-VLDL, like that of rB48-VLDL, was dependent entirely on oleate supplementation (Fig. 3.1.1.*A*). In the absence of oleate, hB48 was secreted primarily as HDL (Fig. 3.1.1.*A*). Formation of hB48-VLDL was achieved within the cells, but not through nonspecific association of exogenous oleate with secreted hB48-HDL, since formation of hB48-VLDL was not observed when oleate was mixed with conditioned media containing only hB48-HDL (data not shown). Oleate also stimulated rB100-VLDL secretion (Fig. 3.1.1.*B*). However, it was not clear whether the increased rB100-VLDL secretion was accompanied with a decrease in the buoyant density of the particles since the sucrose density gradient could not resolve particles with density less than 1.02 g/ml (Fig. 3.1.1.*C*).

Secretion of hB48-VLDL was stimulated by oleate in a time-dependent manner. When human B48-transfected cells were continuously labeled with [^{35}S]methionine/cysteine in the absence (Fig. 3.1.2.*A*) or presence (Fig. 3.1.2.*B*) of 0.4 mM oleate for up to 6 h, secretion of [^{35}S]hB48-VLDL was stimulated more than 10-fold by oleate (Fig. 3.1.2.*C*, *left* panel), while secretion of [^{35}S]rB100-VLDL was stimulated 4-fold by oleate (Fig. 3.1.2.*C*, *right* panel). Oleate had no effect on [^{35}S]hB48-HDL secretion (Fig. 3.1.2.*C*, *middle* panel).

Secretion of hB48-VLDL was also stimulated by oleate in a dose-dependent manner (Fig. 3.1.3). Incremental increases in exogenous oleate concentration, from 0 to 0.4 mM, gradually increased secretion of the amount of [^{35}S]hB48 and [^{35}S]rB100 associated with VLDL, while altered secretion of [^{35}S]hB48-HDL to a less extent. At 0.8 mM oleate, secretion of both [^{35}S]hB48 and [^{35}S]rB100 decreased, probably due to cytotoxicity of high dose of oleate. Therefore, 0.4 mM oleate was used in the subsequent experiments.

3.1.2. Characterization of human B48-VLDL

The size of secreted hB48-VLDL from McA-RH7777 cells is comparable to that of authentic human plasma VLDL (Fig. 3.1.4, compare *lane 2* with *lane 8*). In the absence of oleate (*lanes 1 & 3*), human apoB48 was secreted only as HDL with a diameter of 13 nm. Thus, there is a quantum leap in the particle size of apoB48-associated particles from HDL to VLDL, reflecting an enlargement of neutral lipid core. Oleate had little effect on the size of the majority of rB100-VLDL, although a slight increase in particle size was observed with a small portion of rB100-VLDL in the presence of oleate (*lanes 5 & 6*).

To examine the incorporation of lipid into VLDL, we have monitored intracellular synthesis of lipid and utilization of lipid for VLDL assembly/secretion. The intracellular lipid synthesis was determined by incubation of human B48-transfected cells with [^{3}H]glycerol for up to 4 h. As shown in Fig. 3.1.5.*A*, oleate supplementation (0.4 mM oleate) increased [^{3}H]glycerol incorporation (> 10-fold) into cell TG but had less effect on the incorporation of [^{3}H]glycerol into cell PC (about 2-fold), suggesting that TG synthesis is dramatically enhanced by oleate treatment. At the end of 4 h labeling,

secretion of [^{3}H]TG associated with both hB48-VLDL and rB100-VLDL (d < 1.02 g/ml) was also significantly increased (16-fold and 4-fold, respectively) by oleate, whereas secretion of [^{3}H]TG associated with hB48-HDL was increased by 2-fold (Fig. 3.1.5.*B*, *left* panels). Oleate increased incorporation of [^{3}H]PC into hB48-VLDL and rB100-VLDL, but not hB48-HDL (Fig. 3.1.5.*B*, *right* panels). Thus, utilization of newly labeled lipid for the assembly and secretion of both hB48-VLDL and rB100-VLDL is stimulated upon oleate supplementation.

In comparison to hB48-HDL, the hB48-VLDL particle is enriched in TG within the core. For example, in 4 h oleate-treated conditioned media, the ratio of apoB48 proteins associated with VLDL over HDL was 2:3 (Fig. 3.1.2.*C*), and the ratio of TG associated with VLDL over HDL was 10:1 (Fig. 3.1.5.*B*). Therefore, the amount of TG per hB48-VLDL particle was approximately 15 fold more than that of hB48-HDL. This corresponded to a 2.5-fold increase in particle diameter; since the diameter of hB48-HDL is around 13 nm (Fig. 3.1.4), it is estimated that the diameter of hB48-VLDL is about 32.5 nm.

We also performed lipid pulse chase experiments to examine the incorporation of pre-existing TG into VLDL. In this experiment, human B48-transfected cells were labeled with [^{3}H]oleate for 4 h under basal conditions (*i.e.* DMEM plus 20% serum). The cells were then immediately incubated with or without 0.4 mM oleate for up to 4 h. Lipids associated with both cell and secreted apoB-containing particles were analyzed. A representative experiment, shown in Fig. 3.1.6.*A*, indicated that oleate supplementation

during the 4 h chase increased cell [^{3}H]TG by 1.3-fold and decreased [^{3}H]PC by 34%. Oleate-stimulated [^{3}H]PC turnover and [^{3}H]TG formation was also observed in other McA-RH7777 cells (both wildtype and human apoB-transfected cells) and CHO cells, but not in HepG2 cells or COS-7 cells (data not shown). These data indicate that oleate may enhance the PC turnover in McA-RH7777 cells, and the products from PC turnover (either acyl chains or acylglycerol moieties) may be utilized for TG formation during the oleate-supplemented chase, as described by Gibbons and associates (196). At the end of 4-h chase, oleate increased incorporation of [^{3}H]TG into hB48-VLDL more than 6-fold (Fig. 3.1.6.*B*, *left* panel), and concomitantly decreased [^{3}H]TG associated with hB48-HDL by 2-fold (Fig. 3.1.6.*B*, *middle* panel). In contrast, incorporation of [^{3}H]TG into rB100-VLDL (d < 1.02 g/ml) was not affected by oleate (Fig. 3.1.6.*B*, *right* panel). Thus, pre-labeled [^{3}H]TG, either derived from phospholipid remodeling or from pre-existing TG *en bloc*, is recruited in bulk for hB48-VLDL assembly, but not for rB100-VLDL assembly. The incorporation of bulk TG into human apoB48 is the hallmark for hB48-VLDL assembly, regardless of the origin of TG.

The apolipoprotein stoichiometry of hB48-VLDL was analyzed by solid-phase radioimmunoassay (Fig. 3.1.7.*A*) and compared to that of human plasma LDL (Fig. 3.1.7.*B*). Human B48-VLDL was isolated from overnight conditioned media, and was immobilized by 1D1 on a solid phase. ^{125}I-1D1 in the liquid phase was not able to bind to immobilized hB48-VLDL. This was not caused by steric hindrance of VLDL particles since ^{125}I-Bsol14 with its epitope in the vicinity of 1D1 (Fig. 3.1.7.*C*) could effectively bind to immobilized hB48-VLDL (Fig. 3.1.7.*A*). These data suggested that there is only

one 1D1-epitope on each of hB48-VLDL particles, i.e. one copy of human apoB48 per VLDL particle. ^{125}I-3F5, with an epitope in the C-terminal of human apoB100 (Fig. 3.1.7.*C*) could bind to human LDL, but not hB48-VLDL.

3.1.3. Post-translational assembly and secretion of B48-VLDL

Previous studies from Olofsson's group (125) demonstrated that assembly of rat B48-VLDL was achieved post-translationally in McA-RH7777 cells. The effect of oleate on pre-made human apoB48 was examined by pulse-chase analysis. In human B48-transfected McA-RH7777 cells, the decay of both cellular [^{35}S]B100 and [^{35}S]B48 was not affected by oleate (Fig. 3.1.8.*A*). However, addition of oleate during the chase stimulated incorporation of prelabeled [^{35}S]hB48 into VLDL at 2 h chase (Fig. 3.1.8.*B*). Oleate had less effect on [^{35}S]hB48-HDL secretion (less than 2-fold increase) (Fig. 3.1.8.*C*). These data suggested that like rat B48-VLDL, formation and secretion of human B48-VLDL could be achieved post-translationally.

3.1.4. Oleate-induced secretion of VLDL containing carboxyl-terminally truncated apolipoprotein B variants shorter than apoB48

To determine the minimum length of human apoB that is required for VLDL assembly, we examined VLDL assembly in McA-RH7777 cells stably expressing human apo-B29, -B34, -B37, and -B42 (Fig. 3.1.9.*A*). Under standard cell culture conditions (i.e. DMEM containing 20% serum), all of the secreted h-apoBs were associated with HDL (*d* = 1.08-1.18 g/ml) species (Fig. 3.1.9.*B*). When culture media were supplemented with oleate (0.4 mM), VLDL formation could be observed with apo-B42, -B37, and -B34,

indicating that the ability to assemble VLDL was not severely affected by the truncation (although VLDL formation by apoB34 was compromised) (Fig. 3.1.9.*C*). In contrast, formation of VLDL was entirely abolished by truncation to apoB29. None of the truncations affected the secretion of apoBs as HDL (Fig. 3.1.9.*C*).

Sequential flotation of the secreted lipoproteins confirmed that hB34, hB37, and hB42 indeed formed VLDL (d < 1.006 g/ml) (data not shown). Analysis of the size of hB34-VLDL by nondenaturing gradient gel electrophoresis (2-8%) showed a size similar to that of hB48-VLDL (Fig. 3.1.10). Taken together, these data are reminiscent of observations in human hypobetalipoproteinemia subjects, whereby apoB37 or longer, but not apo-B31 and -B32.5, are found associated with VLDL in plasma (3). Thus, these results provide *in vitro* evidence that the lipid-recruiting sequences for VLDL formation most likely reside beyond the N-terminal 30% of apoB100.

3.1.5. Conclusion

In conclusion, human apoB48, like rat apoB48, has the ability to assemble authentic TG-rich VLDL, as determined by its buoyant density, size and lipid composition. Human B48-VLDL, like rB48-VLDL (9), contains only one copy of apoB48. The minimum length of apoB that is required to assemble VLDL is beyond the N-terminal 30% of human apoB100. Incorporation of bulk TG into apoB48 is the hallmark for post-translational TG-rich B48-VLDL assembly.

FIG. 3.1.1. **Oleate-induced formation of human apoB48-VLDL in McA-RH7777 cells.** Human B48-transfected cells were treated with or without 0.4 mM oleate in 20% serum-containing media for 6 h. The conditioned media were fractionated into 12 fractions in a sucrose density gradient. ApoBs in each fraction were recovered by immunoprecipitation, resolved by 5% SDS-PAGE, and visualized by immunoblotting. *A*, immunoblot with monoclonal antibody 1D1 against human B48. *B*, immunoblot with polyclonal antibody against rat B100. *C*, sucrose density gradient profile. Experiments were repeated five times and similar results were obtained.

Fig. 3.1.1.

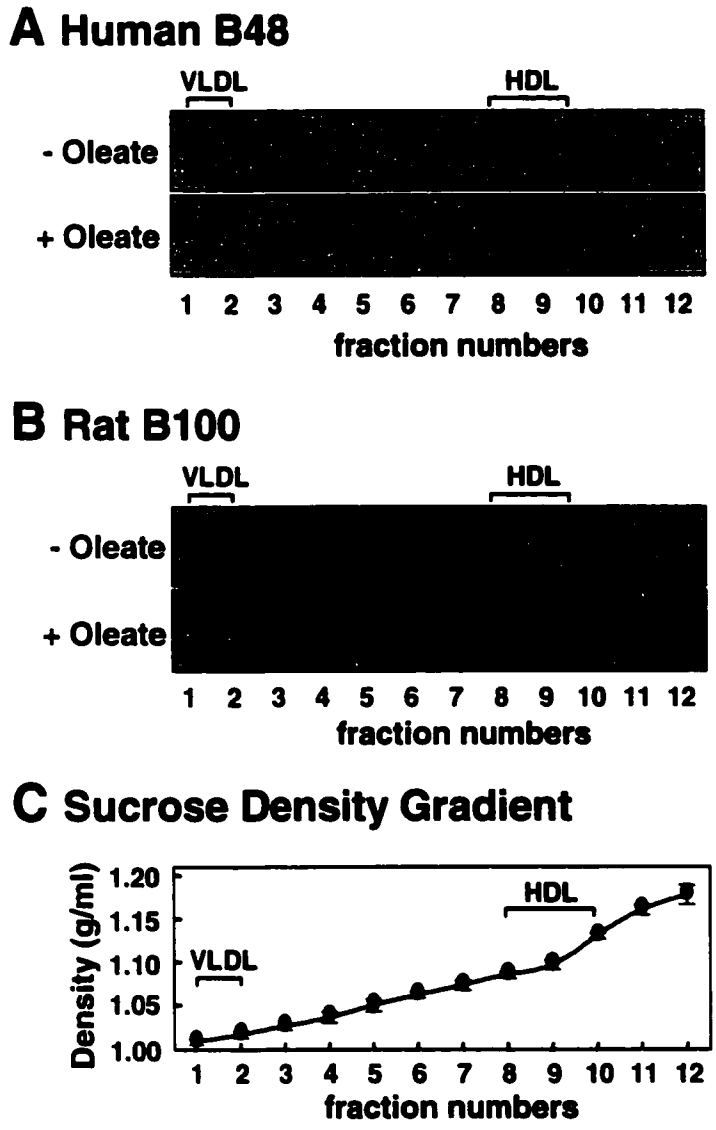
A Human B48
VLDL
HDL
- Oleate
+ Oleate
1 2 3 4 5 6 7 8 9 10 11 12
fraction numbers
B Rat B100
VLDL
HDL
- Oleate
+ Oleate
1 2 3 4 5 6 7 8 9 10 11 12
fraction numbers
C Sucrose Density Gradient
Density (g/ml)
1.20
1.15
1.10
1.05
1.00
VLDL
HDL
1 2 3 4 5 6 7 8 9 10 11 12
fraction numbers

FIG. 3.1.2. **Time course of oleate-stimulated human B48- and rat B100-VLDL secretion.** Human B48-transfected cells were labeled with 400 μCi [^{35}S]methionine/cysteine in 20% serum-containing medium in the absence (*A*) or presence (*B*) of 0.4 mM oleate for up to 6 h. The conditioned media were fractionated into 12 fractions by ultracentrifugation in a sucrose density gradient. The [^{35}S]apoB in each fraction was recovered by immunoprecipitation, separated by SDS-PAGE, and visualized by fluorography. *C*, radioactivity associated with human B48-VLDL (combined from fractions 1-2), human B48-HDL (fractions 8-10), and rat B100-VLDL (fractions 1-2) was quantified by scintillation counting. Repetition of the experiments yielded similar results. *Open circle*: no oleate; *closed circle*: with oleate.

Fig. 3.1.2.

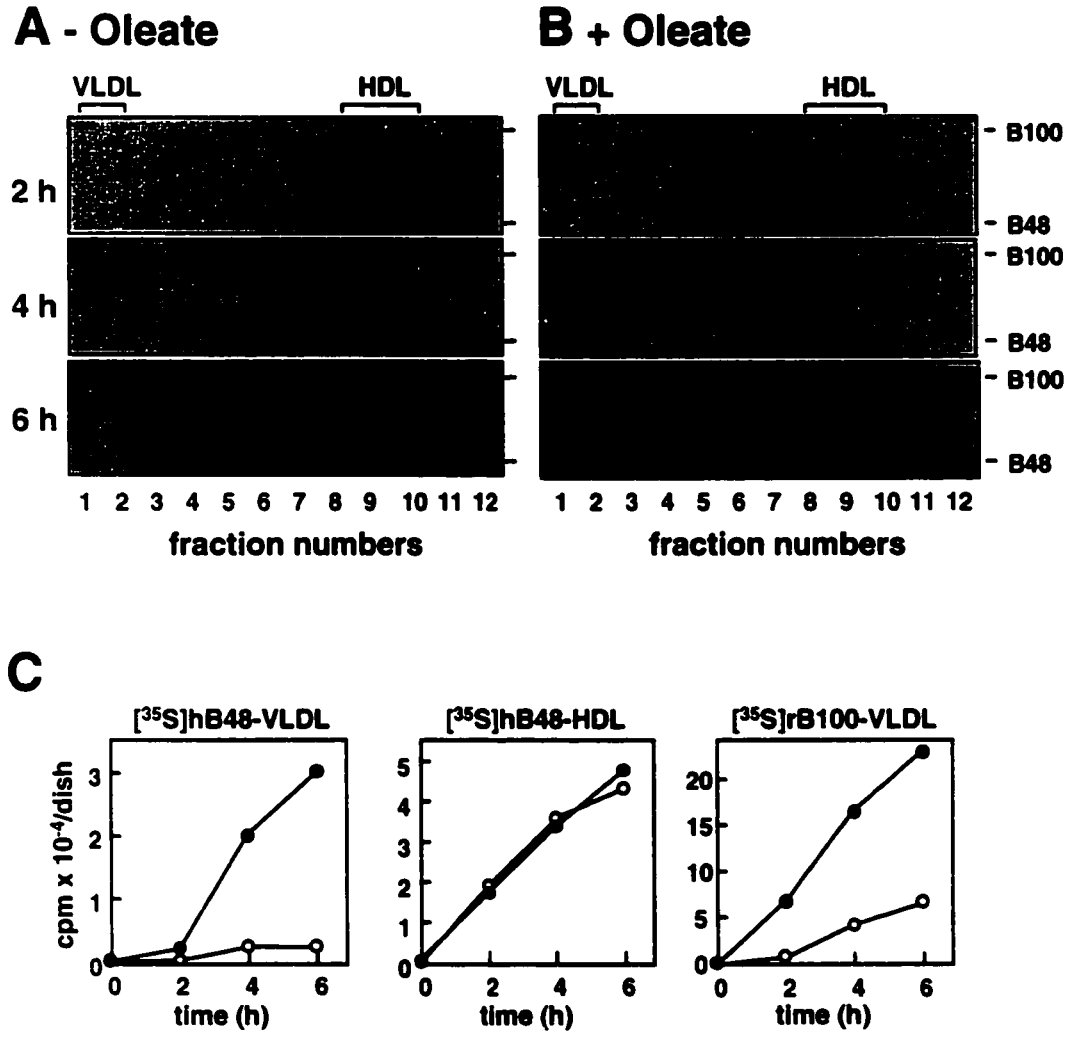
A - Oleate
B + Oleate
VLDL
HDL
2 h
4 h
6 h
B100
B48
1 2 3 4 5 6 7 8 9 10 11 12
fraction numbers
C
[35S]hB48-VLDL
[35S]hB48-HDL
[35S]rB100-VLDL
cpm x 10-4/dish
time (h)

FIG. 3.1.3. **The effect of oleate dose on human B48- and rat B100-VLDL secretion.** *A*, human B48-transfected cells were labeled with 400 μCi [^{35}S]methionine in 20% serum-containing media for 6 h in the presence of oleate with incremental concentration (0 to 0.8 mM). The conditioned media were subjected to sucrose density gradient ultracentrifugation into 12 fractions. [^{35}S]apoBs were recovered from each fraction by immunoprecipitation, resolved by 5% SDS-PAGE, and visualized by fluorography. *B*, radioactivity associated with human B48-VLDL (combined from fractions 1-2), human B48-HDL (fractions 8-10), and rat B100-VLDL (fractions 1-2) was quantified by scintillation counting. Repetition of the experiments yielded similar results.

Fig. 3.1.3.

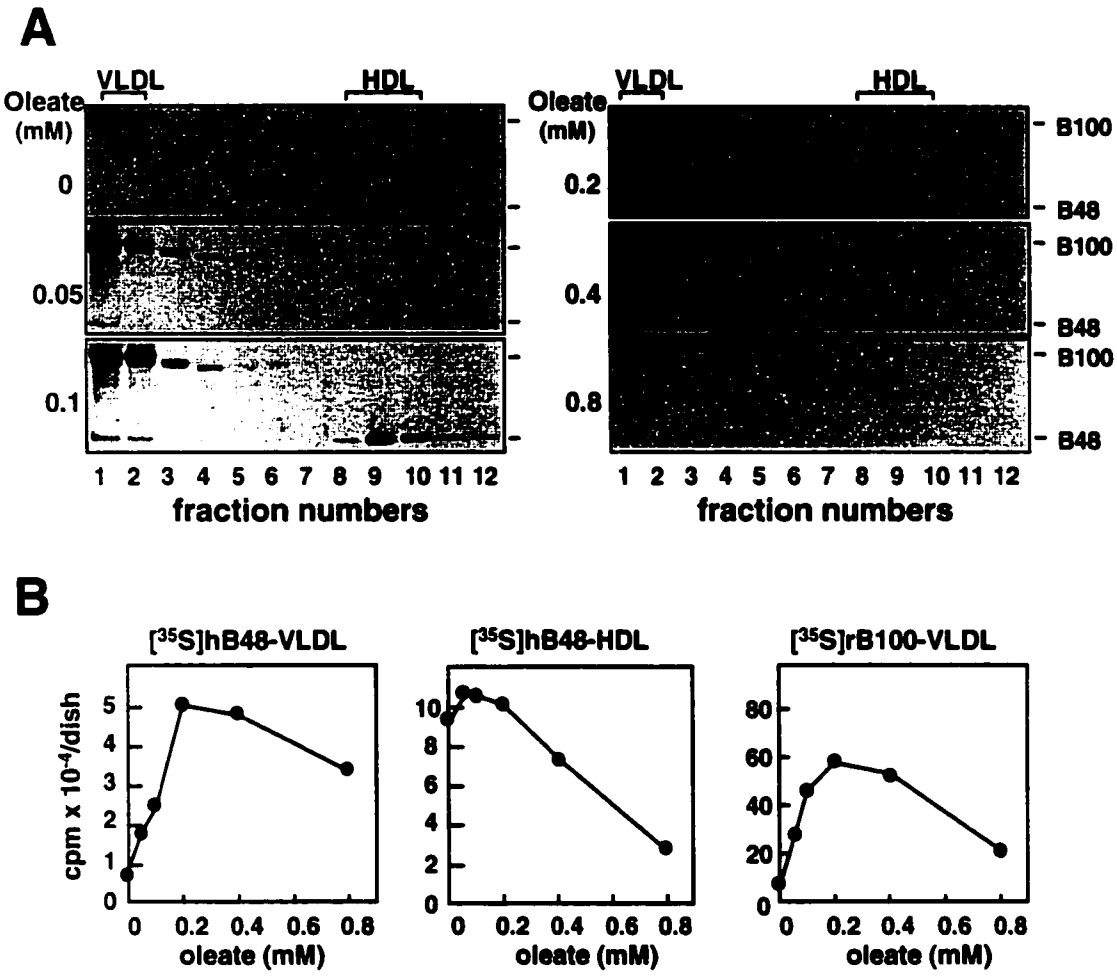
A
VLDL
HDL
Oleate (mM)
0
0.05
0.1
0.2
0.4
0.8
B100
B48
1 2 3 4 5 6 7 8 9 10 11 12
fraction numbers
B
[35S]hB48-VLDL
[35S]hB48-HDL
[35S]rB100-VLDL
cpm x 10-4/dish
oleate (mM)

FIG. 3.1.4. **Gradient gel electrophoresis of secreted human B48- and rat B100-containing lipoproteins.** Human B48-transfected cells were incubated with or without 0.4 mM oleate in 20% serum-containing media for 20 h. The conditioned media were ultracentrifugally separated into VLDL (d < 1.02 g/ml) and HDL (d > 1.02 g/ml) fractions, followed by gradient polyacrylamide gel (2-8 %) electrophoresis under non-denaturing conditions and immunoblotting for hB48 and rB100, respectively. Positions of markers are indicated on the *left*: human LDL, 22 nm; thyroglobulin, 17 nm; ferritin, 12.2 nm. Normolipidemic VLDL (*hVLDL*) and LDL (*hLDL*) were used as lipoprotein standards. Repetition of the experiments three times yielded similar results.

Fig. 3.1.4.

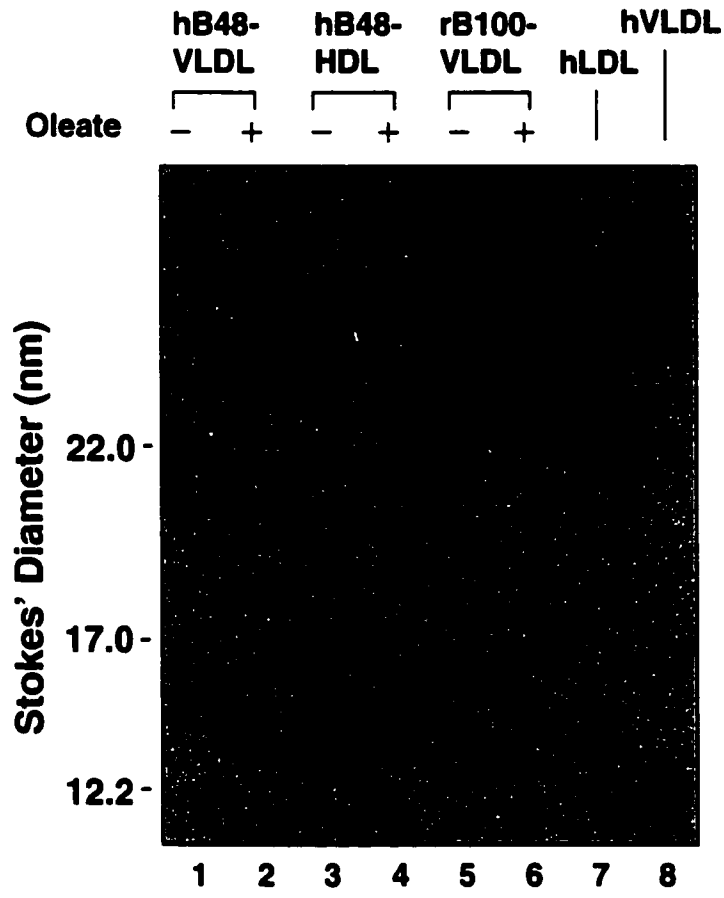
hB48-
VLDL
hB48-
HDL
rB100-
VLDL
hLDL
hVLDL
Oleate
– + – + – +
Stokes' Diameter (nm)
22.0
17.0
12.2
1 2 3 4 5 6 7 8

FIG. 3.1.5. **Continuous labeling analysis of lipids associated with apoB-containing particles from human B48-transfected cells.** Human B48-transfected cells were pulsed labeled with 30 μCi [^{3}H]glycerol in the absence or presence of 0.4 mM oleate for up to 4 h. [^{3}H]glycerol-labeled cell lipids were extracted and quantified (*A*). The conditioned media were subjected to sucrose gradient ultracentrifugation. Human B48-VLDL, human B48-HDL and rat B100-VLDL were immunoprecipitated under non-denaturing condition, and [^{3}H]glycerol-labeled TG and PC associated with these particles were quantified (*B*). Repetition of the experiments yielded similar results. *Open square*: no oleate; *closed square*: with oleate.

Fig. 3.1.5.

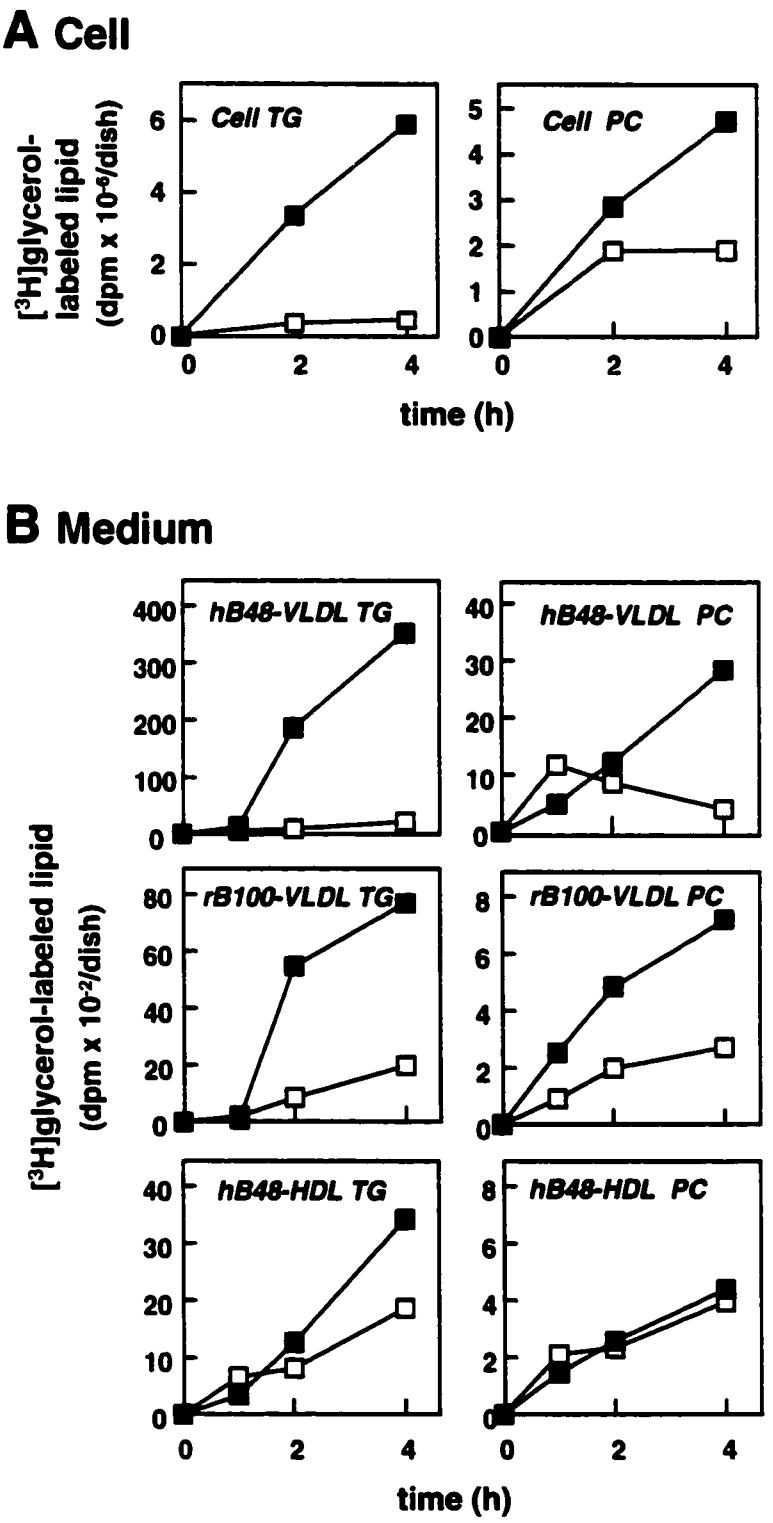
A Cell
[3H]glycerol-labeled lipid (dpm x 10-4/dish)
Cell TG
Cell PC
time (h)
B Medium
[3H]glycerol-labeled lipid (dpm x 10-2/dish)
hB48-VLDL TG
hB48-VLDL PC
rB100-VLDL TG
rB100-VLDL PC
hB48-HDL TG
hB48-HDL PC
time (h)

FIG. 3.1.6. **Pulse-chase analysis of lipids associated with apoB-containing particles from human B48-transfected cells.** Human B48-transfected cells were pulsed labeled with 10 μCi [^{3}H]oleate in the absence of oleate for 4 h, and chased in the presence or absence of 0.4 mM oleate for up to 4 h. [^{3}H]oleate-labeled cell lipids were extracted and quantified (*A*). The conditioned media were fractionated by sucrose gradient ultracentrifugation, [^{3}H]oleate-labeled TG associated with hB48-VLDL, hB48-HDL and rB100-VLDL were quantified (*B*). Repetition of the experiments with [^{14}C]oleate yielded similar results. *Open square*: no oleate; *closed square*: with oleate. In two separate experiments, only the radioactivity associated with cell lipids and medium VLDL lipids at 4 h time-point was measured, and similar results as shown in this figure (4 h time-point) were obtained.

Fig. 3.1.6.

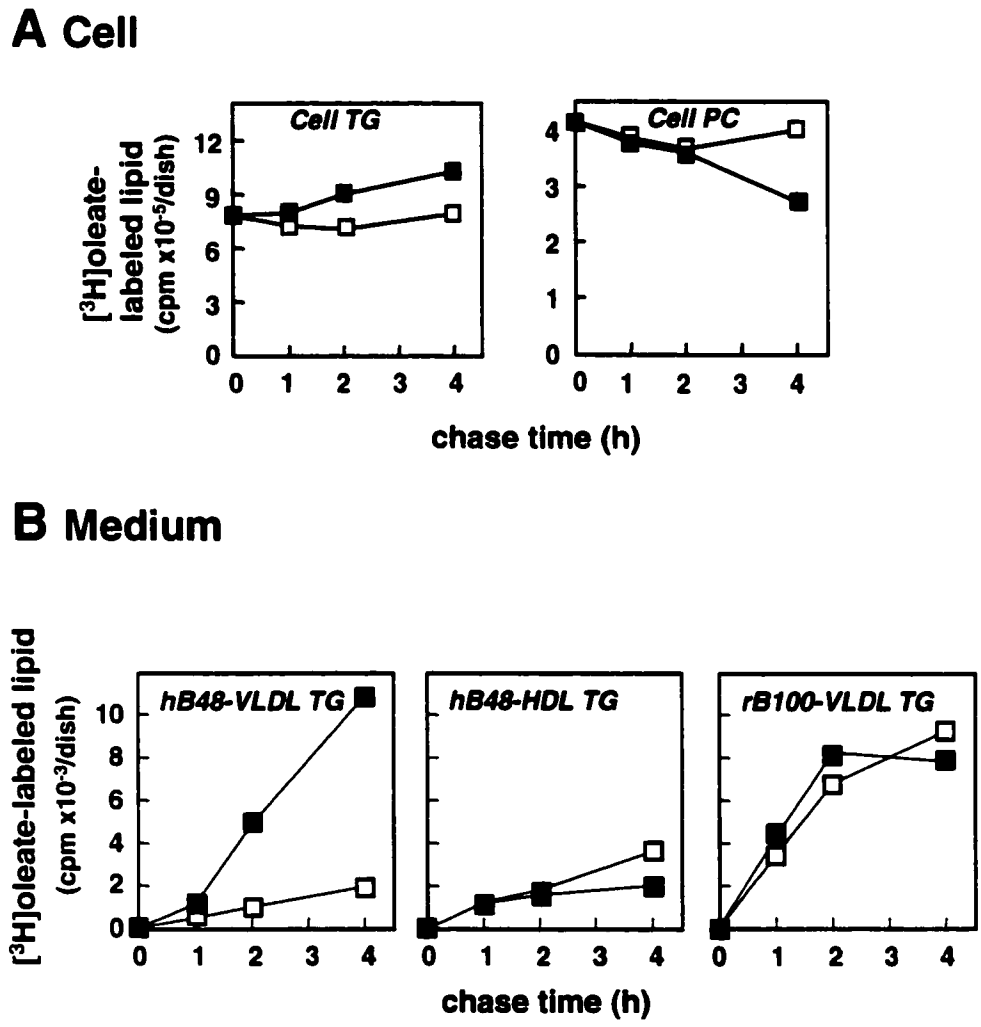
A Cell
Cell TG
Cell PC
[3H]oleate-labeled lipid (cpm x10-5/dish)
chase time (h)
B Medium
hB48-VLDL TG
hB48-HDL TG
rB100-VLDL TG
[3H]oleate-labeled lipid (cpm x10-3/dish)
chase time (h)

FIG. 3.1.7. **Radioimmunoassay of human B48-VLDL.** *A*, the conditioned media from human B48-transfected cells incubated with 0.4 mM oleate for 20 h were collected, and subjected to ultracentrifugation to isolate VLDL fractions ($d < 1.02$ g/ml). Human B48-VLDL in serial dilution (X-axis) was immobilized by 1 μg 1D1 IgG in Immulon II removawells, rinsed, and incubated with 10 ng ^{125}I-labeled immunoglobulins (*i.e.* 1D1, Bsol 14, 3F5, or LRB220) in 1% PBS-BSA (specific activity: 10,000 cpm/ng) overnight. After rinse, the radioactivity in each well was quantified by counting. *B*, human LDL isolated from normalipidemic plasma was used as control. *C*, the epitopes for Bsol14, 1D1, and 3F5 are located within amino acids 186-670, 474-539, and 2835-2922, respectively, of human apoB100. The experiment was repeated twice with similar results.

Fig. 3.1.7.

A RIA of hB48-VLDL

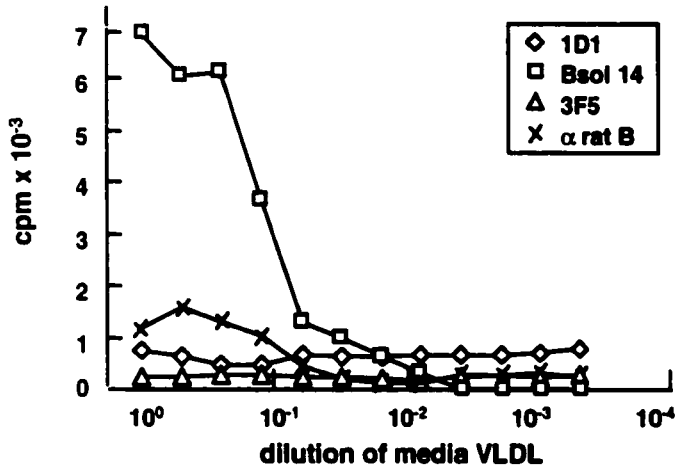

B RIA of hLDL

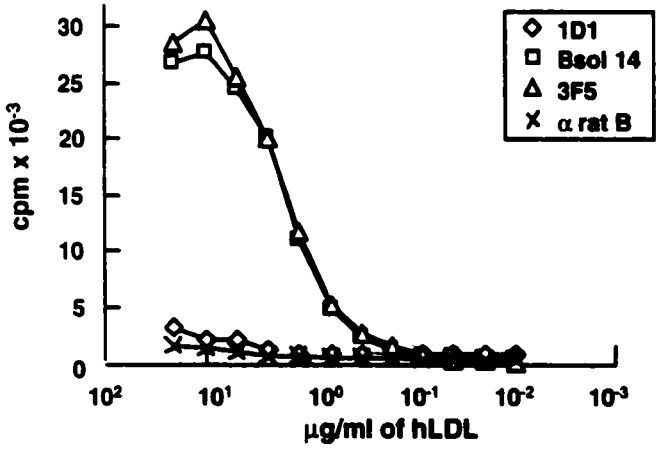

C Epitope Map

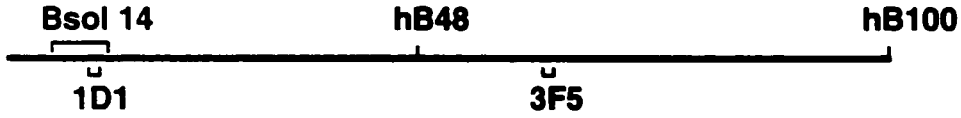

FIG. 3.1.8. **Pulse-chase analysis of secreted human B48- and rat B100-associated lipoproteins.** Human B48-transfected cells were labeled with 400 μCi [^{35}S]methionine without oleate for 0.5 h, washed, and incubated with (*closed square*) or without (*open square*) 0.4 mM oleate for up to 4 h. Cells (*A*) were immediately lysed in 1% SDS-RIPA. The conditioned media were separated into VLDL ($d < 1.02$ g/ml) (*B*) and HDL ($d > 1.02$ g/ml) (*C*) fractions. [^{35}S]apoBs were immunoprecipitated from cells, VLDL and HDL fractions, resolved by SDS-PAGE and visualized by fluorography. The intensity of the bands was quantified by scanning densitometry using One-D scan software. Repetition of the same experiment twice yielded similar results.

Fig. 3.1.8.

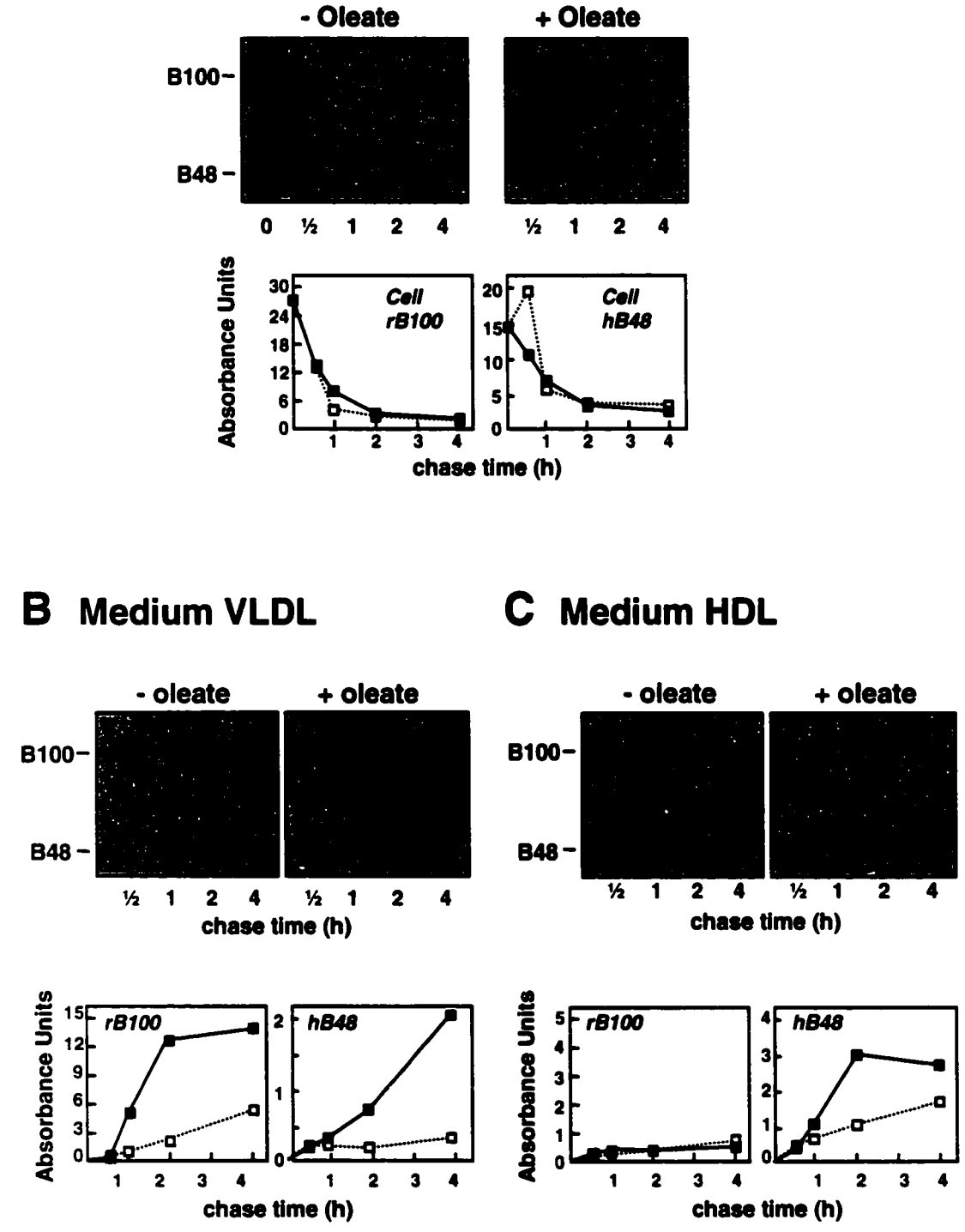
A Cell
- Oleate
+ Oleate
B100
B48
0 ½ 1 2 4
½ 1 2 4
Absorbance Units
Cell rB100
Cell hB48
chase time (h)
B Medium VLDL
- oleate
+ oleate
B100
B48
½ 1 2 4 ½ 1 2 4
chase time (h)
rB100
hB48
Absorbance Units
chase time (h)
C Medium HDL
- oleate
+ oleate
B100
B48
½ 1 2 4 ½ 1 2 4
chase time (h)
rB100
hB48
Absorbance Units
chase time (h)

FIG. 3.1.9. **Oleate-induced secretion of VLDL containing truncated human apolipoprotein B shorter than apoB48.** *A*, schematic diagram of C-terminally truncated human apoBs, represented by *solid bars*. McA-RH7777 cells transfected with human apoB variants were incubated in the absence (*B*) or presence (*C*) of 0.4 mM oleate for 6 h. The condition media were fractionated into 12 fractions in a sucrose density gradient. ApoBs in each fraction were recovered by immunoprecipitation, resolved by 5% SDS-PAGE, and visualized by immunoblotting using 1D1. Repetition of the experiments yielded similar results.

Fig. 3.1.9.

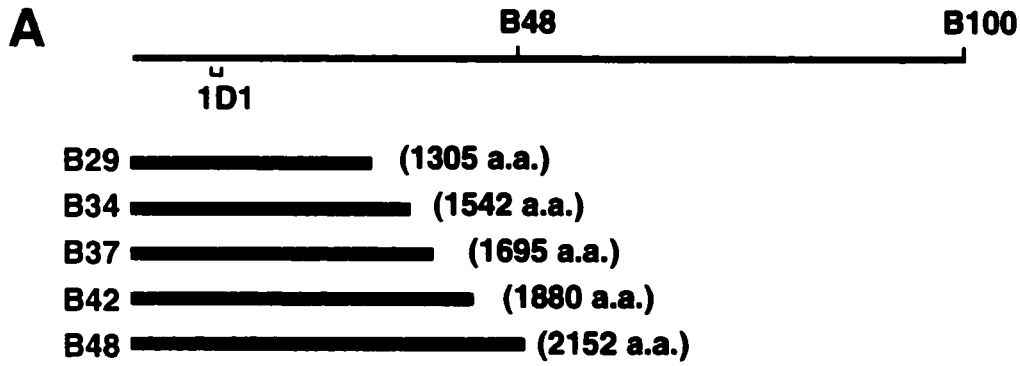
A
B48
B100
1D1
B29 (1305 a.a.)
B34 (1542 a.a.)
B37 (1695 a.a.)
B42 (1880 a.a.)
B48 (2152 a.a.)

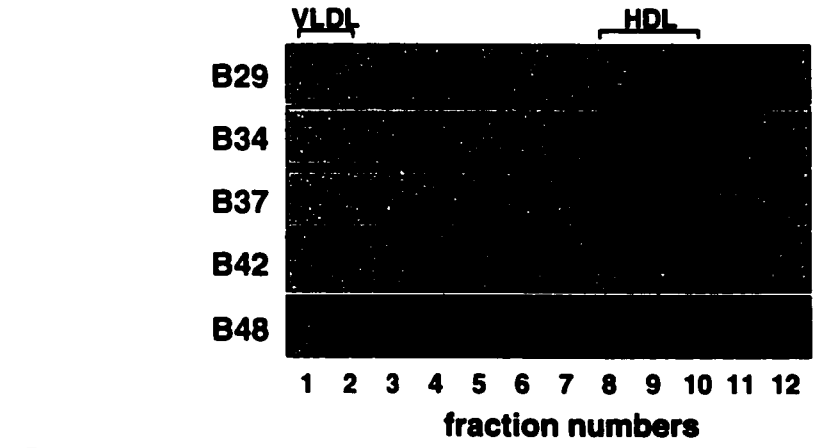
B - Oleate
VLDL
HDL
B29
B34
B37
B42
B48
1 2 3 4 5 6 7 8 9 10 11 12
fraction numbers

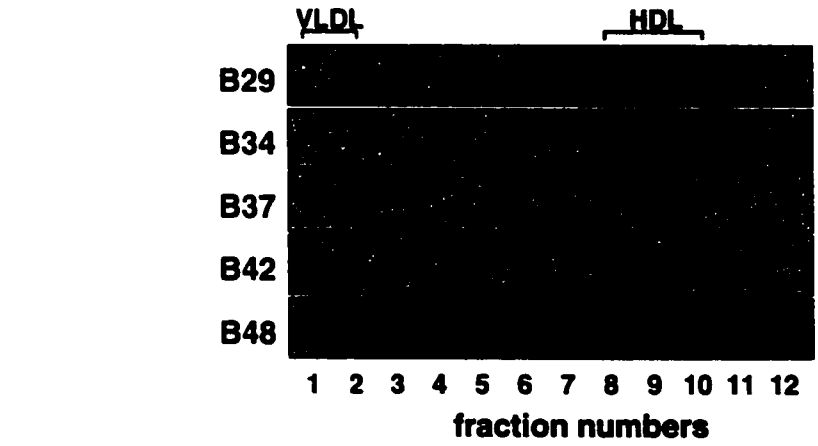
C + Oleate
VLDL
HDL
B29
B34
B37
B42
B48
1 2 3 4 5 6 7 8 9 10 11 12
fraction numbers

FIG. 3.1.10. **Gradient gel electrophoresis of secreted human B48- and human B34-containing lipoproteins.** McA-RH7777 cells transfected with human B48 or B34 were incubated with 0.4 mM oleate for 20 h. The conditioned media were ultracentrifugally separated into VLDL (d < 1.02 g/ml) and HDL (d > 1.02 g/ml) fractions, followed by gradient polyacrylamide gel (2-8 %) electrophoresis under non-denaturing conditions and immunoblotting. Positions of markers are indicated on the *left*: human LDL, 22 nm; thyroglobulin, 17 nm; ferritin, 12.2 nm. Normolipidemic LDL (*hLDL*) was used as lipoprotein standard. The experiment was performed once.

Fig. 3.1.10.

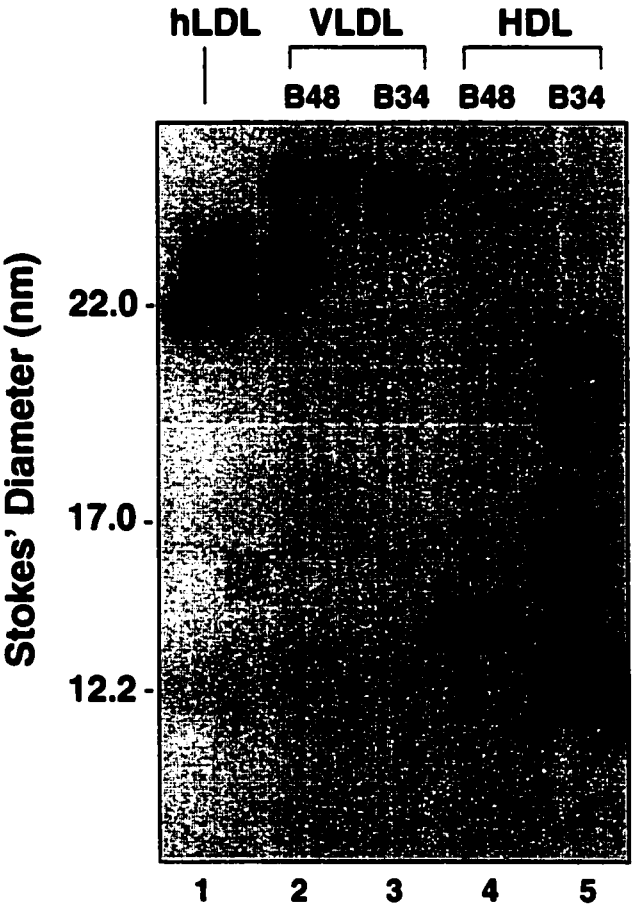
hLDL
VLDL
HDL
B48
B34
B48
B34
Stokes' Diameter (nm)
22.0
17.0
12.2
1
2
3
4
5

3.2. Assembly of human B100-VLDL in transfected McA-RH7777 cells

Compared to assembly of B48-VLDL, relatively little is known about the mechanism(s) for assembly of B100-VLDL. Attempts have been made to understand the pathway for B100-VLDL assembly (123, 125, 211), and the results remain controversial: evidence in favor of the co-translational assembly comes from observations that B100-VLDL can be detected as early as three minutes after initiation of labeling (125); evidence for the post-translational assembly comes from the observations that membrane-bound apoB100 in its HDL form accumulated during BfA treatment can be converted into B100-VLDL after BfA withdrawal (211). However, the nature of B100-VLDL in these two studies is not clear. In plasma, B100-VLDL particles secreted from the liver are heterogeneous, varying in size and lipid composition. At least two different subclasses, large TG-rich B100-VLDL$_1$ (S_f > 100) and small B100-VLDL$_2$ (S_f 20-100), have been characterized (151, 152). The mechanisms responsible for formation of B100-VLDL$_1$ and B100-VLDL$_2$ will be investigated.

3.2.1. Oleate-induced secretion of VLDL containing carboxyl-terminally truncated apolipoprotein B variants longer than apoB48

First, we analyzed the effect of oleate on the assembly/secretion of VLDL in McA-RH7777 cells stably expressing human apo-B64, -B72, -B80 or -B100 (Fig. 3.2.1.*A*). Under basal culture conditions (*i.e.* DMEM + 20% serum), the buoyant density of secreted apoB-lipoproteins, as expected, was inversely related to apoB length. Thus, apoB64, apoB72, and apoB80/apoB100 were found predominantly in fractions with densities resembling those of HDL, LDL, and VLDL, respectively (Fig. 3.2.1.*B*, panels

labeled *–OA*). Upon oleate supplementation, all apoB forms could be recovered in VLDL fraction (Fig. 3.2.1.*B*, panels labeled *+OA*). However, the enlargement of lipoprotein size was readily demonstrable for apoB64 and apoB72 by ultracentrifugation in a sucrose density gradient, but it was less evident for apoB80 and apoB100 because these proteins were already observed in VLDL (d < 1.02 g/ml) fraction even in the absence of oleate. Thus, in the following experiments, an alternative method was used to resolve VLDL particles of different sizes.

3.2.2. Oleate-induced assembly and secretion of triacylglycerol-rich B100-VLDL$_1$

We used cumulative rate flotation technique to resolve lipoproteins into VLDL$_1$ (S_f > 100), VLDL$_2$ (S_f 20-100), IDL/LDL, and HDL. In human B100-transfected McA-RH7777 cells, assembly and secretion of [^{35}S]B100-VLDL$_1$ were induced by oleate (Fig. 3.2.2, *+OA*). Oleate also increased secretion of [^{35}S]B100-VLDL$_2$ by more than 3-fold (Fig. 3.2.2, *+OA*). In the absence of oleate, [^{35}S]B100 was secreted as VLDL$_2$ and IDL/LDL (Fig. 3.2.2, *-OA*). Western blot analysis confirmed that both recombinant human B100 and endogenous rat B100 could assemble VLDL$_1$ in response to oleate supplementation (data not shown). Thus, oleate not only increases the number of VLDL particles as indicated by the increase in B100 secretion, but also increases the size of VLDL particles as shown by the secretion of VLDL with low buoyant densities.

The size of hB100-VLDL$_1$ is indeed larger than that of hB100-VLDL$_2$, as analyzed by gradient gel electrophoresis under non-denaturing conditions (Fig. 3.2.3, *lanes 1-6*). In addition, secretion of hB100-VLDL$_1$ was induced by oleate in a dose dependent manner

(from 0.1 to 0.4 mM) with maximum stimulation at 0.4 mM. Similar oleate dose effect was observed for rB100-VLDL$_1$ secretion (data not shown).

Lipid composition of B100-VLDL$_1$ and -VLDL$_2$ (both human and rat) secreted from human B100-transfected McA-RH7777 cells was also analyzed. The B100-VLDL$_1$ contained ~25% of total secreted [^{35}S]B100 and contained 74% and 65% of respective total [^{3}H]TG and [^{3}H]PC associated with B100 (Table II). As a result, the ratios of [^{3}H]TG/[^{35}S]B100 and [^{3}H]PC/[^{35}S]B100 in VLDL$_1$ are 8- and 5-fold, respectively, greater than those in VLDL$_2$. Thus, the oleate-induced size enlargement of B100-VLDL (equivalent to a 2-fold increase in diameter) was accompanied with bulk TG incorporation, which was observable only after VLDL$_1$ and VLDL$_2$ were resolved. These data are reminiscent of the difference in lipid composition of B48-VLDL in comparison to that of B48-HDL (refer to Section 3.1.2.).

To determine the kinetics of lipid incorporation into B100-VLDL$_1$ and B100-VLDL$_2$, we performed the following two lipid labeling experiments. In the first experiment, human B100-transfected cells were continuously labeled with [^{3}H]glycerol for up to 4 h in the presence or absence of 0.4 mM oleate. As expected, exogenous oleate increased cell [^{3}H]TG by 20-fold and cell [^{3}H]PC by 2-fold at the end of 4 h labeling (Fig. 3.2.4.*A*). Oleate also increased the incorporation of [^{3}H]TG and [^{3}H]PC into hB100-VLDL$_1$ by 35-fold and 21-fold, respectively (Fig. 3.2.4.*B*). In contrast, both [^{3}H]TG and [^{3}H]PC associated with hB100-VLDL$_2$ were increased only by 3-fold by oleate. These data suggested that oleate supplementation stimulates incorporation of newly synthesized

lipid into B100-$VLDL_1$. Similar results were observed for rat B100-$VLDL_1$ and -$VLDL_2$ (data not shown).

In the second experiment, we re-examined the utilization of pre-existing TG for B100-VLDL assembly with the same pulse-chase protocol (shown in Fig. 3.1.6) but using the cumulative flotation technique to separate $VLDL_1$ and $VLDL_2$. Figure 3.2.5.*A* shows that during oleate supplemented chase, cell [^{3}H]TG was increased by 4-fold and [^{3}H]PC was decreased by 30%. When lipids associated with secreted lipoproteins were examined, it was found that exogenous oleate increased secretion of [^{3}H]TG as hB100-$VLDL_1$ by 5-fold and concomitantly decreased its secretion as hB100-$VLDL_2$ by 30% (Fig. 3.2.5.*B*, *left* panels). Oleate also increased secretion of [^{3}H]PC as hB100-$VLDL_1$ by 8-fold yet had no effect on [^{3}H]PC associated with hB100-$VLDL_2$ (Fig. 3.2.5.*B*, ***right*** panels). Similar results were observed for rat B100-$VLDL_1$ and -$VLDL_2$ (data not shown). Thus, through the improved resolution of B100-VLDL particles, oleate-induced incorporation of pre-existing TG for B100-VLDL assembly became manifest. Such oleate-induced bulk TG incorporation into certain B100 fractions would have been overlooked when B100-VLDL particles (both B100-$VLDL_1$ and -$VLDL_2$) were grouped together (compare Fig. 3.2.5.*B* and Fig. 3.1.6.*B*). Taken together, these data are the first indication that bulk TG incorporation into VLDL, the hallmark for the post-translational TG-rich VLDL assembly, is also demonstrable during the assembly of B100-$VLDL_1$.

3.2.3. Post-translational assembly of triacylglycerol-rich B100-VLDL$_1$

To inquire whether B100-VLDL$_1$, like B48-VLDL, is also assembled post-translationally, we performed continuous labeling (Fig. 3.2.6.*A*) and pulse-chase experiments (Fig. 3.2.6.*B*) under conditions that were optimal for VLDL assembly (*i.e.* cells were pretreated with 0.4 mM oleate for 30 min prior to metabolic labeling). Figure 3.2.6.*A* shows that at the end of 10- or 20-min of labeling, [^{35}S]B100 was found mainly in IDL/LDL fraction with small amount in VLDL$_2$ fraction within the microsomal lumen. It also shows that [^{35}S]B100-VLDL$_1$ became detectable at 40-min of labeling. Since translation of B100 completes within 20 min (126), the delayed B100-VLDL$_1$ assembly suggests a post-translational mechanism. The post-translational assembly of VLDL$_1$ was also confirmed by pulse-chase protocol whereby the association of lumenal [^{35}S]B100 with VLDL$_1$ gradually became apparent within microsomal lumen at 15-, 45-, and 60-min of chase (Fig. 3.2.6.*B*). These results, reminiscent of the post-translational TG incorporation for B48-VLDL assembly (Fig. 3.1.8), provide evidence that B100-VLDL$_1$ assembly is achieved via a path similar to that for B48-VLDL.

3.2.4. Triacylglycerol-rich VLDL$_1$ containing carboxyl-terminally truncated apolipoprotein B

Since B100-VLDL$_1$ assembly can be achieved through a mechanism similar to that of B48-VLDL assembly, a common pool of bulk TG precursor may be utilized for both B48-VLDL and B100-VLDL$_1$ assembly. Furthermore, since apoB48 is only half of the full-length apoB, it is possible that the buoyant density of B48-VLDL is also within the range of VLDL$_1$. To test this, we examined the flotation rate of both B48-VLDL and

B37-VLDL in comparison to that of B100-$VLDL_1$. The conditioned media, obtained from oleate-fed McA-RH7777 cells expressing either human apo-B100, or -B48, or -B37, were combined, and subjected to cumulative rate flotation centrifugation. In order to monitor the flotation rate of VLDL particles, one centrifuge tube was unloaded into 12 fractions at certain intervals after the initiation of centrifugation (Fig. 3.2.7). The result shows that most of B48-VLDL and B37-VLDL particles were found in the same fractions as B100-$VLDL_1$ within the first 2 h of centrifugation (Fig. 3.2.7, *top* two panels), suggesting that these VLDL particles have a flotation rate of $VLDL_1$. However, this was not the case for B100-VLDL particles. A large portion of B100-VLDL particles (most likely $VLDL_2$) was not recovered in the top fraction until prolonged centrifugation up to 20 h (Fig. 3.2.7, ***bottom*** two panels). Thus, in comparison to B100-VLDL, B48-VLDL and B37-VLDL are relatively more homogeneous.

3.2.5. Conclusion

In conclusion, both human B100 and C-terminally truncated apoB variants (i.e. B80, B72, B64, B48, and B37) have the ability to assemble TG-rich VLDL. Formation of TG-rich B100-VLDL, i.e. B100-$VLDL_1$, can be readily revealed by cumulative rate flotation method. Assembly of B100-$VLDL_1$ and B48-VLDL share several common features: (a) Assembly is dependent upon oleate. (b) Assembly is achieved post-translationally. (c) Assembly is a process whereby bulk TG is incorporated into apoB. This reinforces the notion that incorporation of bulk TG into apoB is the hallmark for post-translational TG-rich VLDL assembly.

TABLE II.

Composition of $VLDL_1$ and $VLDL_2$ secreted from human B100-transfected McA-RH7777 cells

After being labeled with [^{35}S]methionine/cysteine or [^{3}H]glycerol for 3 h with 0.4 mM oleate, B100-$VLDL_1$ and B100-$VLDL_2$ (both human and rat B100) were recovered from fractionated media by immunoprecipitation. Radioactivity associated with [^{35}S]B100 is the mean ± S.D. from three independent experiments, and data for [^{3}H]TG and [^{3}H]PC are from a single experiment. However, similar results for [^{3}H]TG and [^{3}H]PC (presented as ratio of $VLDL_1/VLDL_2$) were obtained in an independent experiment with a different time course (2 h and 4 h) (Fig. 3.2.4.*D*). The numbers in parentheses are the ratios of [^{3}H]TG/[^{35}S]B100 and [^{3}H]PC/[^{35}S]B100.

Lipoproteins	[^{35}S]B100	[^{3}H]TG	[^{3}H]PC
		cpm × 10^{-2}/ mg cell protein	
B100-$VLDL_1$	187.1 ± 9.8	227.3 (1.2)	16.5 (0.09)
B100-$VLDL_2$	546.7 ± 41.5	81.9 (0.15)	9.0 (0.02)
$VLDL_1/VLDL_2$	0.34	2.8	1.8

FIG. 3.2.1. **Oleate-induced secretion of VLDL containing truncated human apolipoprotein B longer than apoB48.** *A*, schematic diagram of C-terminally truncated human apoBs, represented by *solid bars*. *B*, the human B64-, B72-, B80-, or B100-transfected cells were incubated with DMEM (20% serum) with (*+OA*) or without (*−OA*) 0.4 mM oleate for 6 h, and the conditioned media were fractionated by sucrose density gradient ultracentrifugation. The human apoB proteins in each fraction were analyzed by SDS-PAGE followed by immunoblotting using 1D1. Repetition of the experiments yielded similar results.

Fig. 3.2.1.

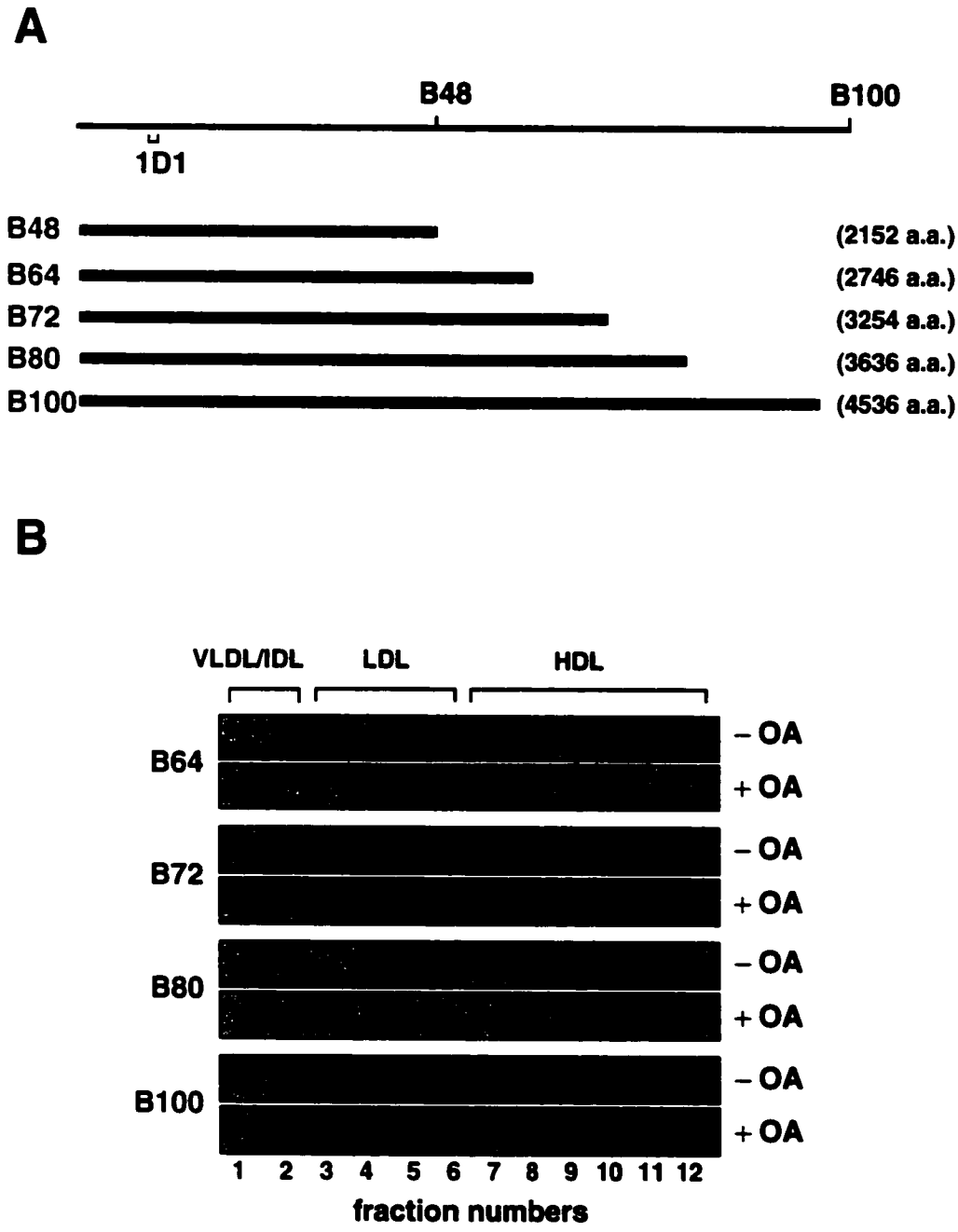
A
B48
B100
1D1
B48
B64
B72
B80
B100
(2152 a.a.)
(2746 a.a.)
(3254 a.a.)
(3636 a.a.)
(4536 a.a.)
B
VLDL/IDL
LDL
HDL
B64
B72
B80
B100
– OA
+ OA
1 2 3 4 5 6 7 8 9 10 11 12
fraction numbers

FIG. 3.2.2. **Oleate-induced secretion of B100-VLDL$_1$.** *A*, human B100-transfected cells were labeled with 400 μCi [^{35}S]methionine/cysteine in DMEM (20% serum) ± 0.4 mM oleate for 3 h. The conditioned media were fractionated by cumulative rate flotation. The [^{35}S]apoBs in each fraction were immunoprecipitated, resolved by SDS-PAGE, visualized by fluorography. The apoB48 proteins secreted from human B100-transfected cells are mainly those proteins that are derived from expression of plasmids encoding large forms of human apoBs, and the size of these protein resembles that of apoB48 (129). *B*, radioactivity associated with [^{35}S]B100 in each fraction was quantified by scintillation counting. Repetition of the experiments five times yielded similar results. *Open circle*: no oleate; *closed circle*: with oleate.

Fig. 3.2.2.

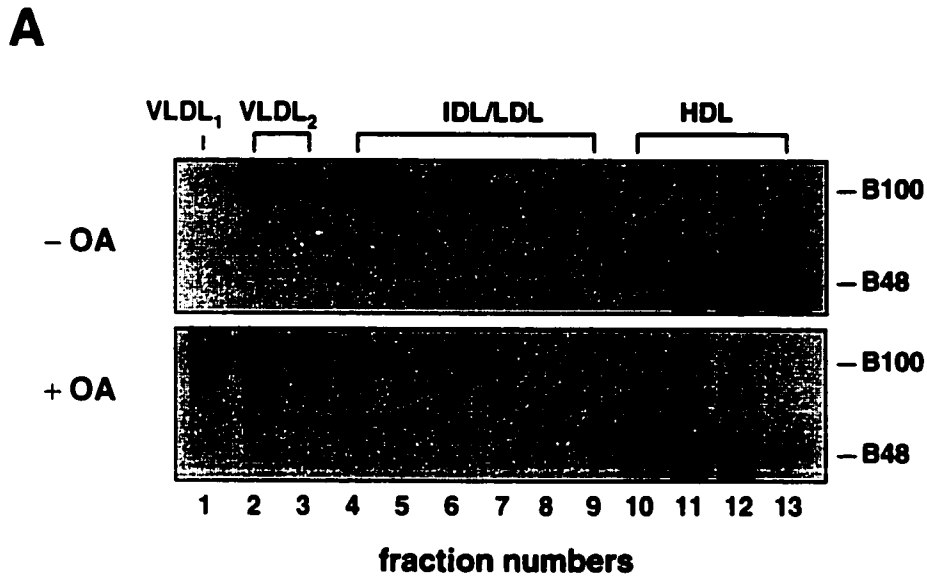
A
VLDL1
VLDL2
IDL/LDL
HDL
– OA
+ OA
– B100
– B48
– B100
– B48
1 2 3 4 5 6 7 8 9 10 11 12 13
fraction numbers
B
cpm x 10-4 / dish
0 2 4 6 8
1 2 3 4 5 6 7 8 9 10 11 12 13
fraction numbers

FIG. 3.2.3. **Gradient gel electrophoresis of secreted human B100-$VLDL_1$ and B100-$VLDL_2$.** Human B100-transfected cells were incubated with increased amount of oleate (0 - 0.4 mM, *above* each lane) for 20 h. $VLDL_1$ and $VLDL_2$ fractions were isolated from the conditioned media by cumulative rate flotation ultracentrifugation. Each fraction was resolved by gradient polyacrylamide gel (2-8 %) electrophoresis under non-denaturing conditions, followed by immunoblotting using 1D1. Positions of markers are indicated on the *left*: human LDL, 22 nm; thyroglobulin, 17 nm; ferritin, 12.2 nm. Normolipidemic LDL (*hLDL*) was used as lipoprotein standard. Repetition of the experiments yielded similar results.

Fig. 3.2.3.

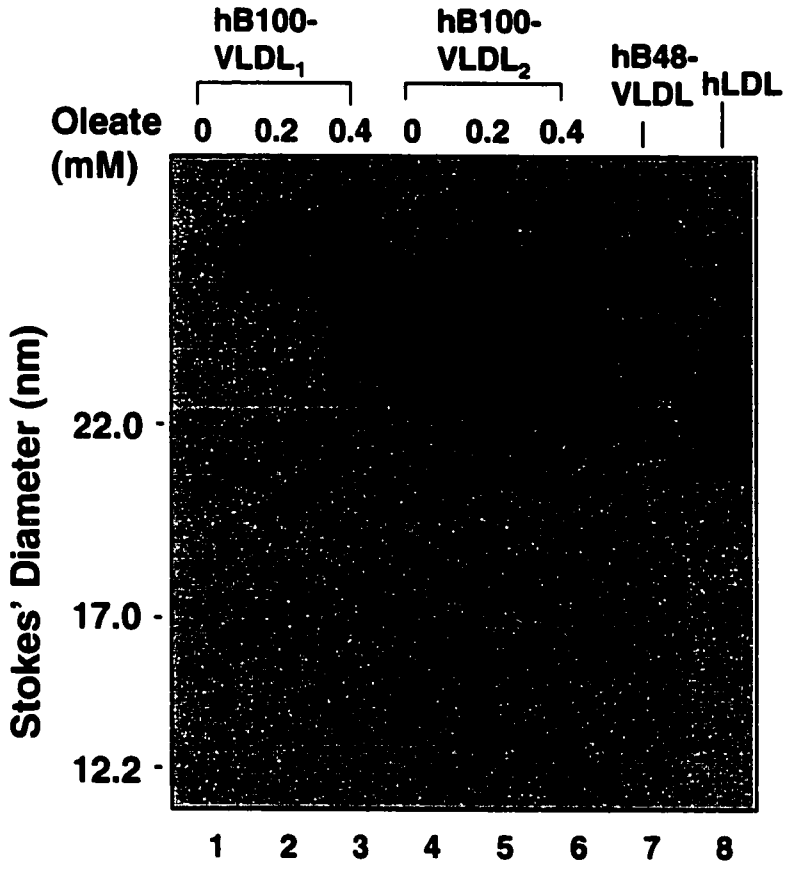
hB100-VLDL1
hB100-VLDL2
hB48-VLDL
hLDL
Oleate (mM)
0
0.2
0.4
0
0.2
0.4
Stokes' Diameter (nm)
22.0
17.0
12.2
1
2
3
4
5
6
7
8

FIG. 3.2.4. **Continuous labeling analysis of lipids associated with apoB-containing particles from human B100-transfected cells.** Human B100-transfected cells were pulsed labeled with 30 μCi [^{3}H]glycerol in the absence or presence of 0.4 mM oleate for up to 4 h. [^{3}H]glycerol-labeled cell lipids were extracted and quantified (*A*). The conditioned media were subjected to cumulative rate flotation ultracentrifugation. [^{3}H]glycerol-labeled TG and PC associated with hB100-VLDL$_1$ and hB100-VLDL$_2$ were quantified (*B*). Repetition of the experiments with different time points yielded similar kinetics profile. *Open square*: no oleate; *closed square*: with oleate.

Fig. 3.2.4.

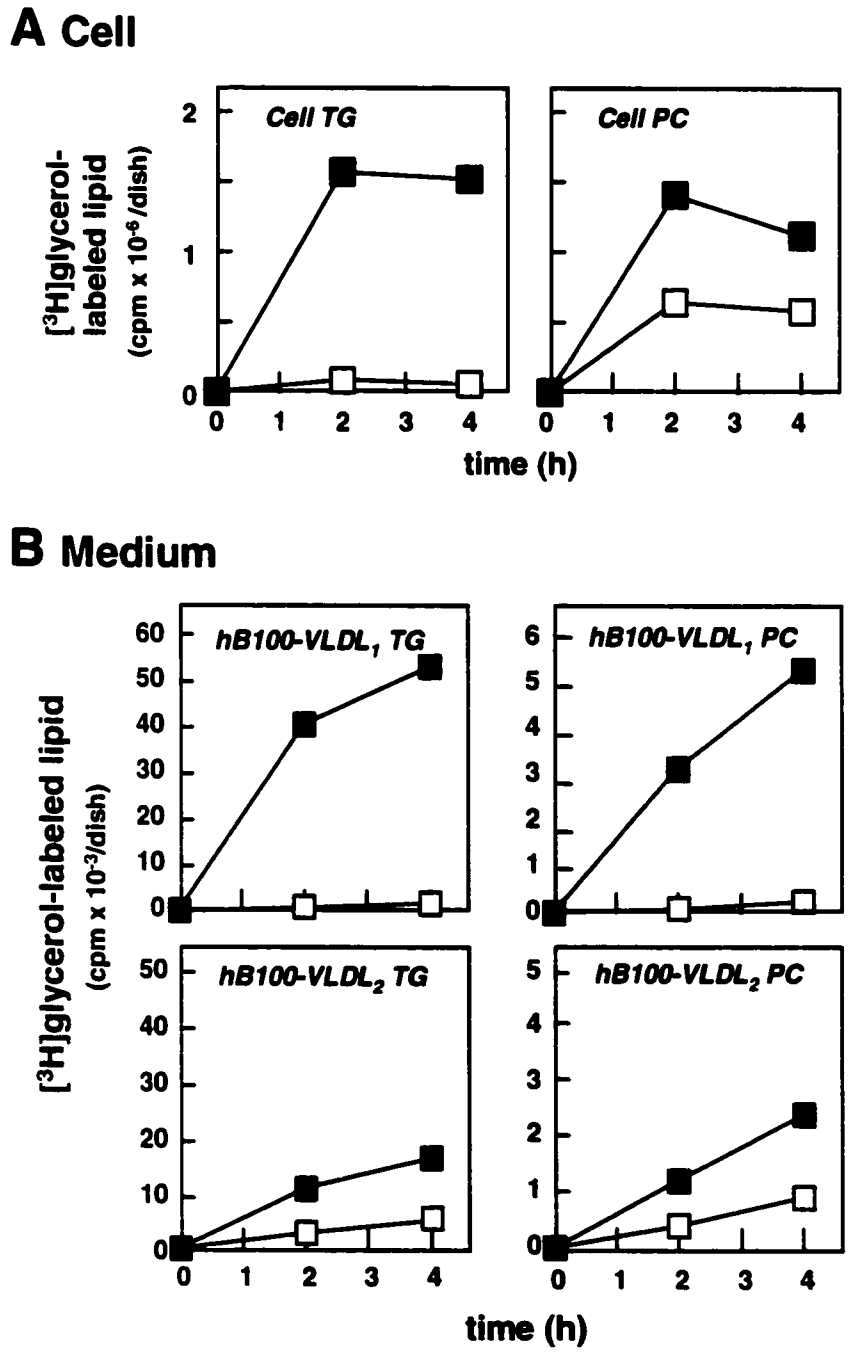
A Cell
Cell TG
Cell PC
[3H]glycerol-labeled lipid (cpm x 10-6/dish)
time (h)
B Medium
hB100-VLDL1 TG
hB100-VLDL1 PC
hB100-VLDL2 TG
hB100-VLDL2 PC
[3H]glycerol-labeled lipid (cpm x 10-3/dish)
time (h)

FIG. 3.2.5. **Pulse-chase analysis of lipids associated with apoB-containing particles from human B100-transfected cells.** Human B100-transfected cells were pulsed labeled with 10 μCi [^{3}H]oleate in the absence of oleate for 4 h, and chased in the presence or absence of 0.4 mM oleate for up to 4 h. [^{3}H]oleate-labeled cell lipids were extracted and quantified (*A*). The conditioned media were subjected to cumulative rate flotation ultracentrifugation. [^{3}H]oleate-labeled TG and PC associated with hB100-$VLDL_1$ and hB100-$VLDL_2$ were quantified (*B*). Repetition of the experiments yielded similar results. *Open square*: no oleate; *closed square*: with oleate.

Fig. 3.2.5.

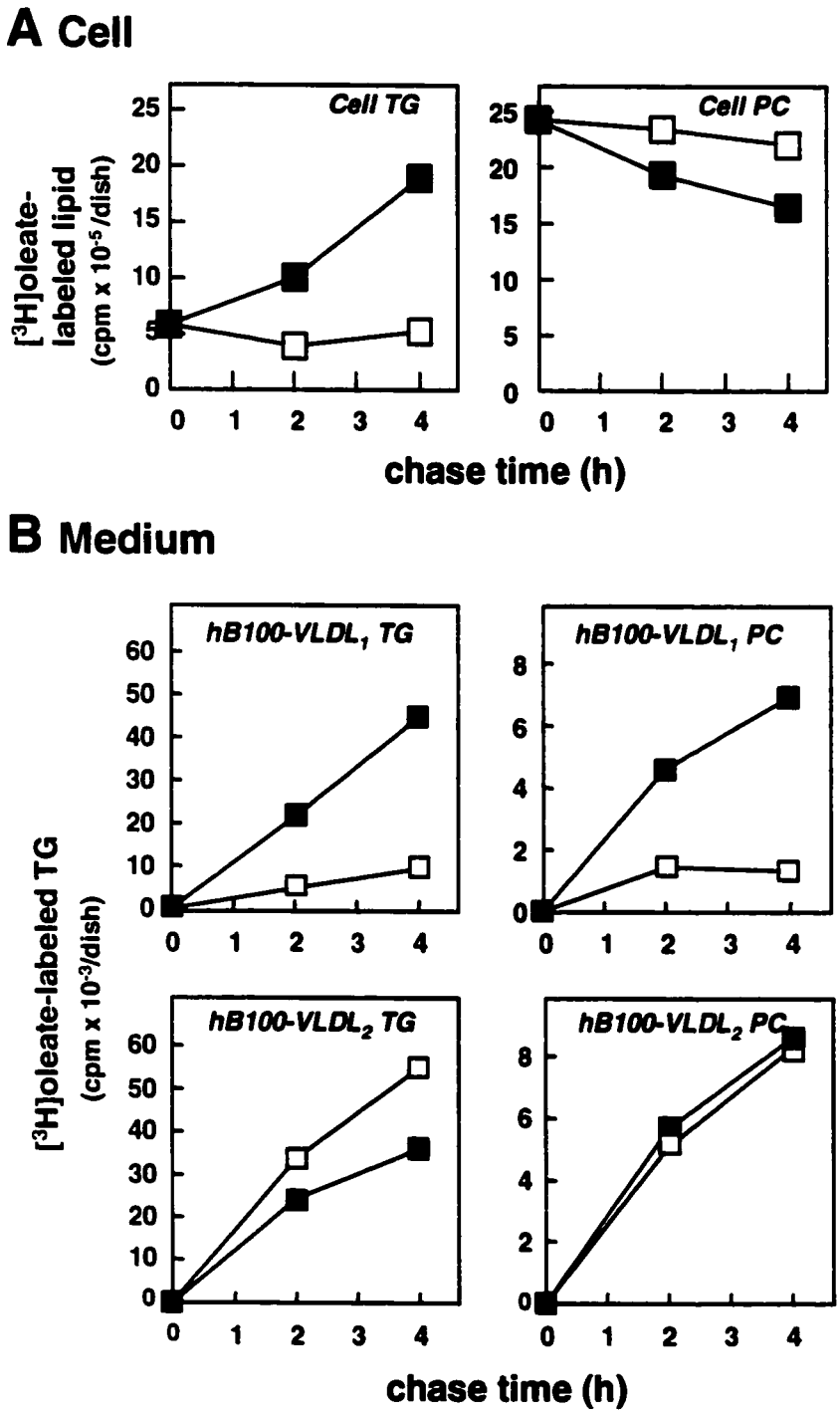
A Cell
Cell TG
Cell PC
[3H]oleate-labeled lipid (cpm x 10-5/dish)
chase time (h)
B Medium
hB100-VLDL1 TG
hB100-VLDL1 PC
hB100-VLDL2 TG
hB100-VLDL2 PC
[3H]oleate-labeled TG (cpm x 10-3/dish)
chase time (h)

FIG. 3.2.6. **Continuous labeling and pulse-chase analysis of microsomal lumenal apoB-containing lipoproteins.** Human B100-transfected cells were pretreated with DMEM (20% serum) + 0.4 mM oleate for 30 min. The cells were pulse-labeled with 800 μCi [^{35}S]methionine for up to 40 min (*A*). Alternatively, the cells were pulse-labeled with 800 μCi [^{35}S]methionine for 20 min and chased in the presence of 0.4 mM oleate for up to 60 min (*B*). Microsomal lumenal contents were released by sodium carbonate method, followed by rate flotation ultracentrifugation into 13 fractions. [^{35}S]apoBs in the top twelve fractions were subjected to immunoprecipitation, resolved by 3-15% SDS-PAGE, and visualized by fluorography. Repetition of the experiments yielded similar results.

Fig. 3.2.6.

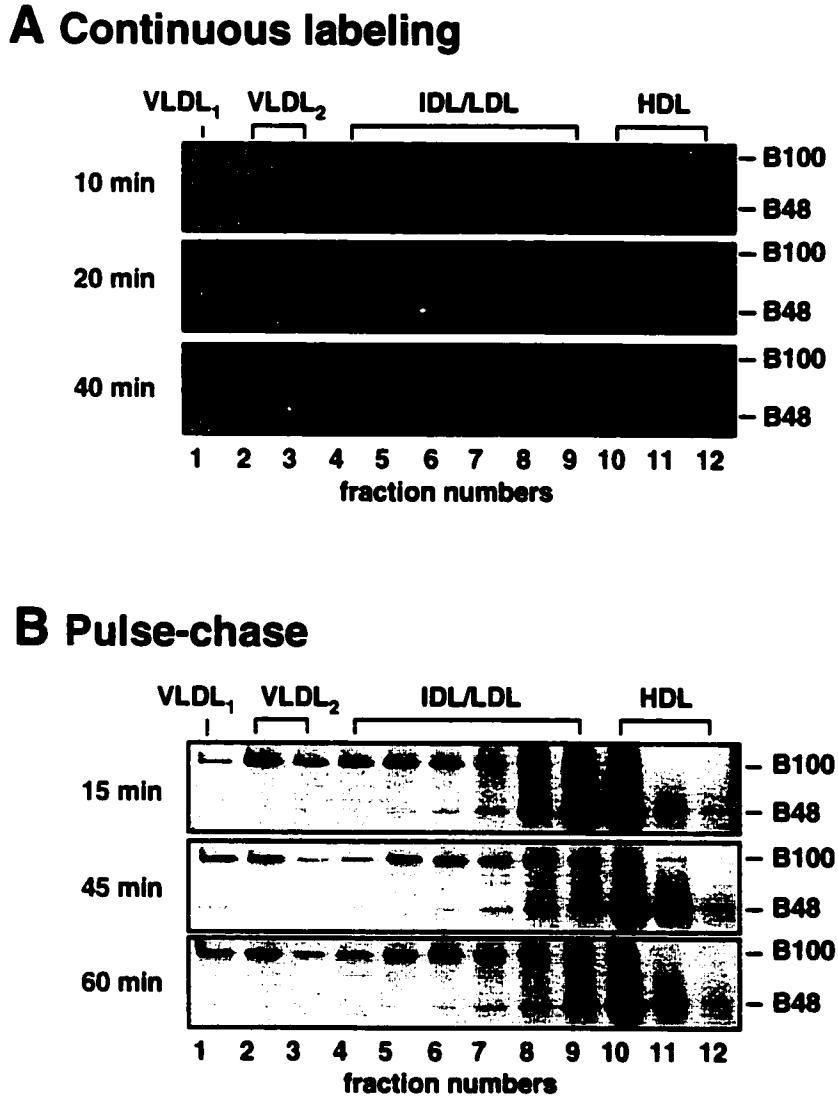
A Continuous labeling
VLDL1
VLDL2
IDL/LDL
HDL
10 min
20 min
40 min
B100
B48
1 2 3 4 5 6 7 8 9 10 11 12
fraction numbers
B Pulse-chase
15 min
45 min
60 min

FIG. 3.2.7. **Cumulative rate flotation of B37-VLDL and B48-VLDL in comparison to B100-VLDL$_1$.** Human B37-, B48-, and B100-transfected cells were incubated with DMEM (20% serum) + 0.4 mM oleate for 4 h. The conditioned media were mixed, and fractionated by cumulative rate flotation ultracentrifugation for 1 h, 2 h, 4 h and 20 h. At each time point, a centrifuge tube is unloaded into 12 fractions. The apoBs in each fraction were immunoprecipitated, resolved by SDS-PAGE, followed by immunoblotting using 1D1. The experiment was performed only once.

Fig. 3.2.7.

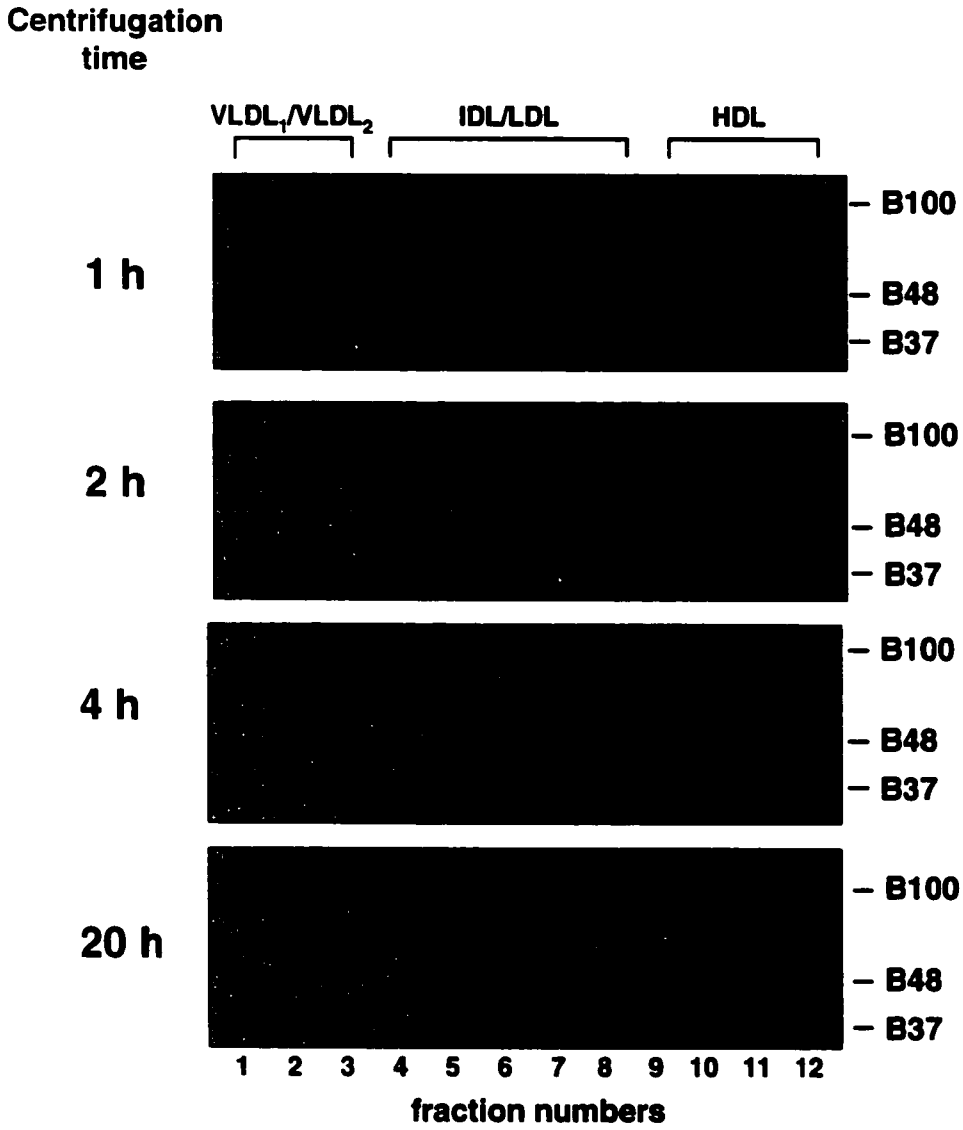
Centrifugation time
VLDL1/VLDL2
IDL/LDL
HDL
1 h
2 h
4 h
20 h
B100
B48
B37
1 2 3 4 5 6 7 8 9 10 11 12
fraction numbers

3.3. Microsomal triglyceride transfer protein is required for assembly of triacylglycerol-rich lipoproteins

We then addressed the question of whether MTP plays a role in the assembly of TG-rich VLDL. In this study, chemical inhibitors were used to specifically inactivate endogenous MTP activity in McA-RH7777 cells for the following two reasons. (a) Assembly of VLDL can not be reconstituted in heterologous cells. Although data from the reconstitution experiments clearly indicate that MTP indeed plays an important role in the assembly and secretion of lipoproteins containing apoB, cells lines used for the reconstitution experiments lacked the ability to synthesize and secrete VLDL (108). Thus, the requirement of MTP for the assembly of VLDL, particularly those TG-rich particles, could not be determined through reconstitution in heterologous cells. (b) McA-RH7777 cells retain the ability to assemble TG-rich B100-$VLDL_1$ and B48-VLDL, as described in Section 3.1. & 3.2. Particularly, the incorporation of bulk TG into apoB as a hallmark for post-translational VLDL assembly has been established, and thus can be used as an unambiguous criteria to determine the effect of MTP inactivation on TG-rich VLDL assembly.

Two inhibitors, BMS-192951 (Fig. 3.3.1.*A*) and BMS-197636 (Fig. 3.3.1.*B*), were obtained from Bristol-Myers Squibb. BMS-192951 is a photo-activated inhibitor. Once activated, it covalently binds to MTP and irreversibly inhibits MTP activity. However, the inhibition process is not acute since it generally requires one-hour preincubation followed by 15 min ultraviolet activation. In this study, BMS-192951 was mainly used to examine the role of MTP in B48-VLDL assembly. A second MTP inhibitor, BMS-

197636, was obtained in the late phase of this study. This compound has high specificity towards inhibition of MTP activity (IC_{50} = 36 nM) and apoB secretion (ED_{50} = 3 nM) (230). Unlike the photoactivated inhibitor BMS-192951, BMS-197636 does not require ultraviolet treatment, yet inhibits B100 secretion within 10 min of administration (data not shown).

3.3.1. Requirement of microsomal triglyceride transfer protein for B48-VLDL assembly

The MTP inhibitor BMS-192951, was used to inactivate endogenous MTP activity in human B48-transfected McA-RH7777 cells. BMS-192951 at 5 μM reduced the MTP activity by 65-70%. The inhibitory effect persisted for at least 8 h (Dr. H. Jamil, personal communication).

The effect of MTP inhibition on the recruitment of prelabeled TG during oleate-induced B48-VLDL assembly was determined by pulse labeling of human B48-transfected cells with [^{3}H]oleate (4 h), inactivating MTP with BMS-192951 (1¼ h), and monitoring lipoprotein secretion during oleate-supplemented chase. The turnover of prelabeled [^{3}H]TG and [^{3}H]PC in MTP-inactivated cells during oleate-supplemented chase was identical to that in untreated cells (data not shown), indicating that MTP inactivation had little effect on the total cell prelabeled lipid. However, MTP inactivation specifically abolished the recruitment of pre-existing TG for hB48-VLDL secretion (Fig. 3.3.2). At 5 μM BMS-192951, secretion of prelabeled [^{3}H]TG and [^{3}H]PC associated with hB48-VLDL was decreased by 80% and 85%, respectively, at the end of a 4-h

chase. Inhibition of MTP did not affect secretion of [^{3}H]TG associated with hB48-HDL or [^{3}H]PC with rB100-VLDL (d < 1.02 g/ml), and it only slightly (< 25%) decreased the secretion of [^{3}H]TG with rB100-VLDL or [^{3}H]PC with hB48-HDL. These results suggest that utilization of pre-existing TG for the oleate-induced B48-VLDL secretion requires normal activity of MTP.

Protein pulse-chase experiment also demonstrates that inactivation of MTP during oleate supplemented chase decreased the incorporation of [^{35}S]hB48 into VLDL by 70%, whereas MTP inhibition had little effect on secretion of [^{35}S]hB48 with HDL (Fig. 3.3.3, *A* & *B*). Incorporation of [^{35}S]rB100 into secreted VLDL decreased by 45%, as compared with cells treated with no inhibitor (Fig. 3.3.3, *A* & *B*). Inhibition of MTP did not affect secretion of endogenous rat apoAI as HDL (Fig. 3.3.3.*B*).

We then examined the effect of MTP inhibition on VLDL secretion by inactivating MTP prior to metabolic labeling of apoB and lipid. Inactivation of MTP diminished the secretion of [^{35}S]apoB proteins associated with hB48-VLDL (by 80%) or rB100-VLDL (by 90%) as compared with cells treated without inhibitor (Fig. 3.3.4). Similarly, MTP inhibition decreased secretion of [^{3}H]TG associated with hB48-VLDL (by 6-fold) or rB100-VLDL (by less than 2-fold) (Fig. 3.3.5). However, similar to our observations in pulse-chase experiments (Fig. 3.3.2 and Fig. 3.3.3), secretion of [^{35}S]B48 (Fig. 3.3.4) or [^{3}H]TG (Fig. 3.3.5) associated with hB48-HDL was unaffected by MTP inhibition. These results demonstrate further that MTP activity is required for the oleate-induced secretion of hB48-VLDL. Under these experimental conditions, incorporation of cell [^{3}H]TG was

decreased by 30% (69.8 ± 9.8% of control, n = 8) during a 4-h labeling period in the inhibitor-treated cells compared with untreated cells, whereas incorporation of cell [^{3}H]PC was not affected (103.0 ± 14.5% of control, n = 8).

Taken together from the above protein and lipid metabolic labeling experiments, the results showed that MTP plays an essential role in post-translational B48-VLDL assembly.

3.3.2. Requirement of microsomal triglyceride transfer protein for B100-VLDL$_1$ assembly

The results from the above MTP inhibitor study also indicated that the effect of BMS-192951 on the assembly of B100-VLDL (d < 1.02 g/ml) was less conclusive, since the extent of inhibition of B100-VLDL assembly by BMS-192951 varied drastically from 25% (Fig. 3.3.2) to 90% (Fig. 3.3.4). A possible explanation for this variation is that the inhibitory effect of BMS-192951 on MTP activity is not rapid enough. Therefore, suppression of B100-VLDL assembly by this inhibitor might not be revealed if the inhibitor was administered at the late stage of B100-VLDL assembly.

To test this possibility, we employed a new MTP inhibitor, BMS-197636, to inhibit MTP activity in McA-RH7777 cells since its inhibitory effect was rather fast acting (<10 minute after administration). *In vitro* MTP assay indicated that endogenous MTP activity within McA-RH7777 cells decreased with increasing dose of BMS-197636 (IC_{50} = 0.1 μM) in the culture media (Fig. 3.3.6.*A*). Since BMS-197636 is a reversible inhibitor, such

in vitro measurement is likely an underestimate of the actual inhibitory effect of the inhibitor *in vivo*. For example, treatment with 0.2 μM BMS-197636 resulted in only partial inhibition of cell-associated MTP activity (Fig. 3.3.6.*A*, *open square*), whereas adding the same concentration of BMS-197636 to the assay mixture entirely abolished MTP activity (Fig. 3.3.6.*A*, *closed square*). The effect of inactivation of MTP by BMS-197636 on B48-VLDL assembly in human B48-transfected cells was also examined. In a pulse-chase experiment, supplementation of BMS-197636 during the chase diminished [^{35}S]hB48-VLDL secretion in a dose dependent manner. Secretion of hB48-VLDL was entirely abolished at 0.2 μM of BMS-197636 (Fig. 3.3.6.*B*). In contrast, at all concentrations of BMS-197636 tested (from 0.05 to 1 μM), secretion of [^{35}S]hB48-HDL was unaffected or slightly increased as compared with control (Fig. 3.3.6.*B*). BMS-197636 had no effect on the secretion of [^{35}S]apoAI as HDL (Fig. 3.3.6.*C*). Thus, like BMS-192951, the inhibitory effect of BMS-197636 on B48-VLDL assembly is readily demonstrated.

The effect of BMS-197636 on B100-VLDL assembly in human B100-transfected cells was then examined. In a pulse chase experiment, BMS-197636 (0.2 μM) had little effect on [^{35}S]B100-VLDL (both human and rat) secretion during the oleate-supplemented chase (Fig. 3.3.7.*A*). In contrast, the effect of BMS-197636 on oleate-stimulated [^{35}S]hB72-VLDL secretion was certainly observable (Fig. 3.3.7.*B*). Thus, under the conditions that post-translational assembly/secretion of both B48-VLDL and B72-VLDL can be abolished by MTP inhibitor, post-translational assembly of B100-VLDL seems to be less sensitive to MTP inhibition, a phenomenon that is independent of

the type of MTP inhibitor used. Because of its convenience, BMS-197636 was used for the following study.

During the course of this study, we have obtained convincing evidence showing that B100-VLDL particles secreted from McA-RH7777 cells are heterogeneous, and the incorporation of bulk TG into apoB100 can only be observed in B100-$VLDL_1$ particles, but not for all B100-VLDL particles (refer to Section 3.2.). Furthermore, the kinetics for the assembly of each VLDL species is also different. Thus, it is possible that the requirement of MTP for the assembly of B100-$VLDL_1$ and -$VLDL_2$ may not be the same.

To test this possibility, we performed two lipid-labeling experiments in human B100-transfected McA-RH7777 cells (Fig. 3.3.8). Results from a lipid continuous labeling experiment showed that inactivation of MTP by BMS-197636 (0.2 μM) completely abolished secretion of both [^{3}H]TG and [^{3}H]PC associated with hB100-$VLDL_1$, while secretion of ^{3}H-labeled lipids associated with hB100-$VLDL_2$ was suppressed by the inhibitor to a less extent (Fig. 3.3.8.*A*). In a lipid pulse-chase experiment, secretion of pre-labeled [^{3}H]TG and [^{3}H]PC associated with hB100-$VLDL_1$ was also preferentially inhibited, as compared to those for hB100-$VLDL_2$ (Fig. 3.3.8.*B*). Similar results were obtained for endogenous rat B100-$VLDL_1$ and -$VLDL_2$ (data not shown). However, under no circumstances did BMS-197636 affect synthesis or accumulation of cell TG and PC (Table III). These data clearly demonstrated that the demand for MTP activity is positively correlated with the extent of B100 lipidation.

The requirement of MTP for B100-VLDL assembly could also be manifested by examining the effect of BMS-197636 on lipoprotein secretion in a protein continuous labeling experiment. With doses increasing from 0.05 to 0.5 μM, BMS-197636 not only diminished secretion of [^{35}S]B100 to <15% of control, but also decreased the size of B100-lipoproteins from VLDL to HDL (Fig. 3.3.9). The BMS-197636 doses that abolished secretion of B100-VLDL$_1$ and -VLDL$_2$ were 0.05 μM and 0.2 μM, respectively, corresponding to 62% and 50% of normal MTP activity (Fig. 3.3.6.*A*). In contrast to that of [^{35}S]B100, secretion of [^{35}S]B48 (mainly as HDL) was relatively unaffected by BMS-197636 (Fig. 3.3.9.*B*). These data showed that secretion of B100-VLDL$_1$ requires more MTP activity than that needed for B100-VLDL$_2$ secretion.

To confirm that normal MTP activity is required for B100-VLDL$_1$ assembly, we performed a pulse-chase experiment combined with subcellular fractionation (Fig. 3.3.10). Oleate-pretreated human B100-transfected cells were pulsed labeled for 20 min, and chased immediately in the presence of BMS-197636 (0.2 μM). At the beginning of the chase, only [^{35}S]B100-VLDL$_2$ and other denser particles appeared in the microsomal lumen (Fig. 3.3.10, *top* panel). Inclusion of BMS-197636 during the chase completely abolished the formation of [^{35}S]B100-VLDL$_1$ (Fig. 3.3.10, compare *middle* and *bottom* panels). These results, combined with others (Fig. 3.3.8 & 3.3.9), strongly suggested that the demand for MTP increases as B100-VLDL assembly proceeds. At the early stage of assembly, less MTP activity is required (e.g. for B100-VLDL$_2$ assembly); whereas at the later stage of assembly, more MTP activity is required (e.g. for B100-VLDL$_1$ assembly).

Thus, like B48-VLDL assembly, B100-$VLDL_1$ assembly is extremely dependent upon MTP activity.

3.3.3. Conclusion

In conclusion, post-translational assembly of TG-rich VLDL, containing either B48 or B100, requires normal MTP activity. Invariably, the incorporation of bulk TG into apoB, a hallmark for the post-translational VLDL assembly, is extremely sensitive to MTP inhibition. Furthermore, the requirement of MTP during post-translational provides additional evidence that B100-$VLDL_1$ assembly is achieved via a path similar to that for B48-VLDL.

TABLE III.

Incorporated radioactivity and mass of cell lipid in human B100-transfected McA-RH7777 cells

Cells (n= 6) were labeled with 10 μCi/ml [^{3}H]glycerol for 15, 30, 45, and 60 min under the indicated conditions. Radioactivity associated with cell [^{3}H]TG and [^{3}H]PC at each time point was quantified, and the synthetic rate was calculated from the plots of [^{3}H]TG and [^{3}H]PC versus time. Lipid mass measurement was done with cells treated with indicated conditions for 2 h. Cell TG and PC mass are presented as mean ± S.D. (n = 3). *n.d.*, not determined.

condition	lipid synthetic rate		lipid mass	
	[^{3}H]TG	[^{3}H]PC	TG	PC
	cpm × 10^{-5} / h / mg protein		*μg / mg protein*	
1. no oleate	n.d.	n.d.	5.3 ± 0.6	43.3 ± 2.5
2. + 0.4 mM oleate	5.0 ± 0.5	2.8 ± 0.7	27.9 ± 4.1	41.3 ± 2.6
3. 2. + 0.2 μM BMS-197636	5.4 ± 0.4	3.0 ± 0.6	31.4 ± 1.1	44.8 ± 4.8

FIG. 3.3.1. **Structure of MTP inhibitors.**

Fig. 3.3.1.

MTP Inhibitor BMS-192951

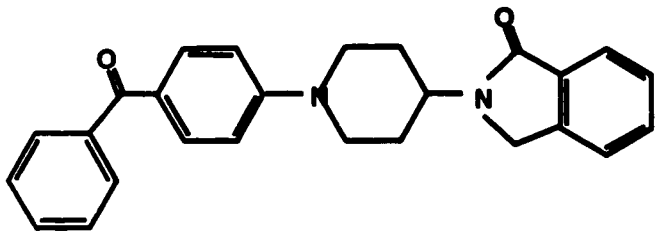

MTP Inhibitor BMS-197636

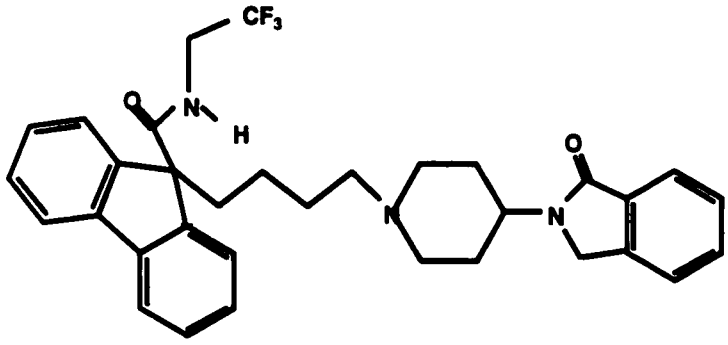

FIG. 3.3.2. **Effect of BMS-192951 on secretion of apoB-associated lipids - inhibition of MTP after metabolic labeling.** Human B48-transfected cells were labeled with 15 μCi [^{3}H]oleate for 4 h and then incubated with or without BMS-192951 (5 μM) for 1 h. Inhibition of MTP was achieved by photoactivation of the inhibitor for 15 min under 360 nm UV light. After MTP inactivation, the cells were cultured in DMEM (20% serum) + 0.4 mM oleate for up to 4 h. The media were collected at 2 h and 4 h during chase and fractionated in a sucrose density gradient. [^{3}H]Oleate-labeled TG and PC associated with hB48-VLDL, hB48-HDL and rB100-VLDL were quantified. Repetition of the experiments yielded similar results. *Open square*, control; *closed square*, MTP inhibited.

Fig. 3.3.2.

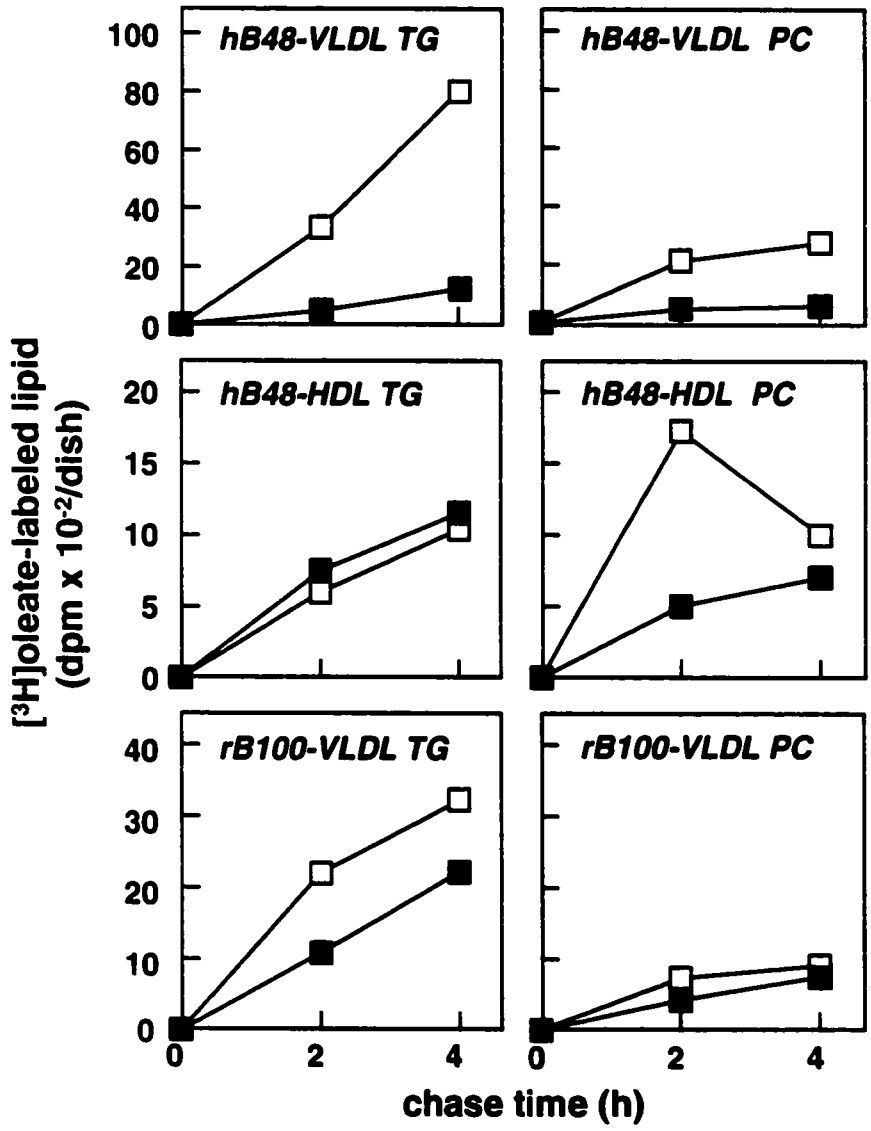
hB48-VLDL TG
hB48-VLDL PC
hB48-HDL TG
hB48-HDL PC
rB100-VLDL TG
rB100-VLDL PC
[3H]oleate-labeled lipid (dpm x 10-2/dish)
chase time (h)
0
2
4
10
20
30
40
60
80
100
5
15

FIG. 3.3.3. **Effect of BMS-192951 on secretion of apoBs - inhibition of MTP after metabolic labeling.** Human B48-transfected cells were labeled with 400 μCi [^{35}S]methionine/cysteine in DMEM (20% serum) for 2 h. After labeling, cells were incubated with DMEM (20% serum) ± BMS-192951 (5 μM) for 1 h. Inhibition of MTP was achieved by photoactivation of the inhibitor for 15 min under 360 nm UV light. Cells were then cultured with DMEM (20% serum) + 0.4 mM oleate for 4 h. The conditioned media were fractionated in a sucrose density gradient to analyze [^{35}S]apoBs. *A*, fluorograms of [^{35}S]apoBs. *B*, quantification of secretion of [^{35}S]apoBs and [^{35}S]apoAI. Each value is the average of two measurements from two independent experiments.

Fig. 3.3.3.

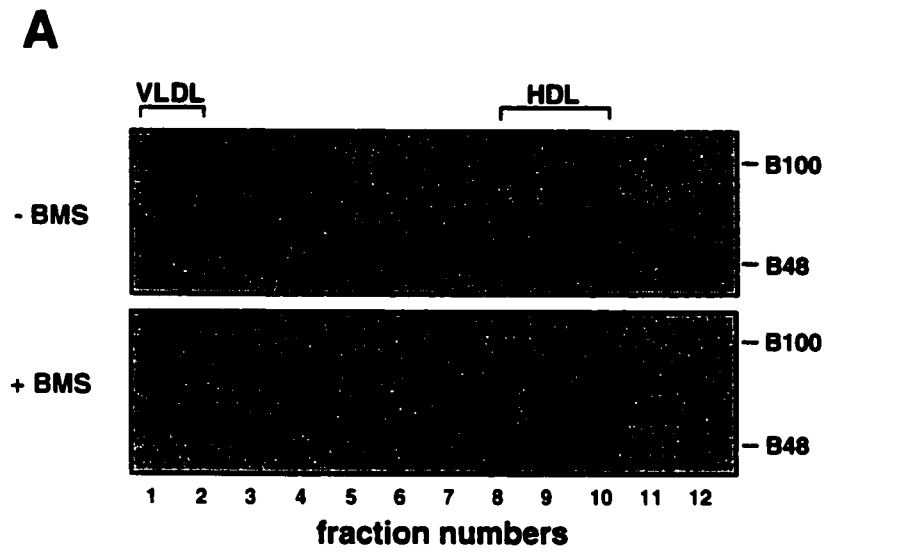
A
VLDL
HDL
- BMS
+ BMS
B100
B48
B100
B48
1 2 3 4 5 6 7 8 9 10 11 12
fraction numbers

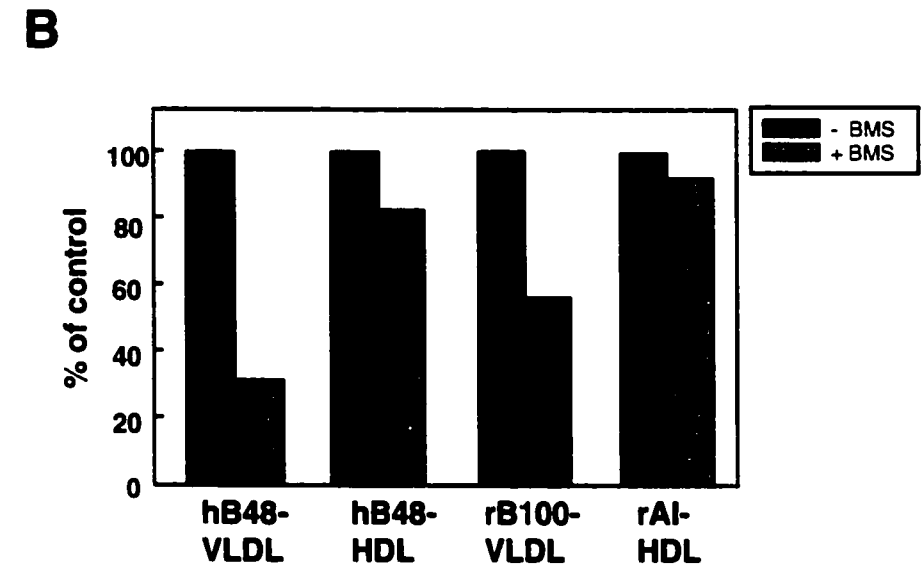
B
% of control
100
80
60
40
20
0
- BMS
+ BMS
hB48-VLDL
hB48-HDL
rB100-VLDL
rAI-HDL

FIG. 3.3.4. **Effect of BMS-192951 on secretion of apoBs - inhibition of MTP prior to metabolic labeling.** Human B48-transfected cells were incubated with DMEM (20% serum) ± BMS-192951 (5 μM) to inactivate MTP. Inhibition of MTP was achieved by photoactivation of the inhibitor for 15 min under 360 nm UV light. Cells were then labeled with 400 μCi [^{35}S]methionine/cysteine in DMEM (20% serum) + 0.4 mM oleate for up to 4 h. The conditioned media were collected at 4 h and fractionated in a sucrose density gradient. [^{35}S]ApoBs were immunoprecipitated from each fraction, resolved by SDS-PAGE. *A*, fluorograms of [^{35}S]apoBs. *B*, quantification of secretion of [^{35}S]apoBs and [^{35}S]apoAI. Each value is the average of two measurements from two independent experiments.

Fig. 3.3.4.

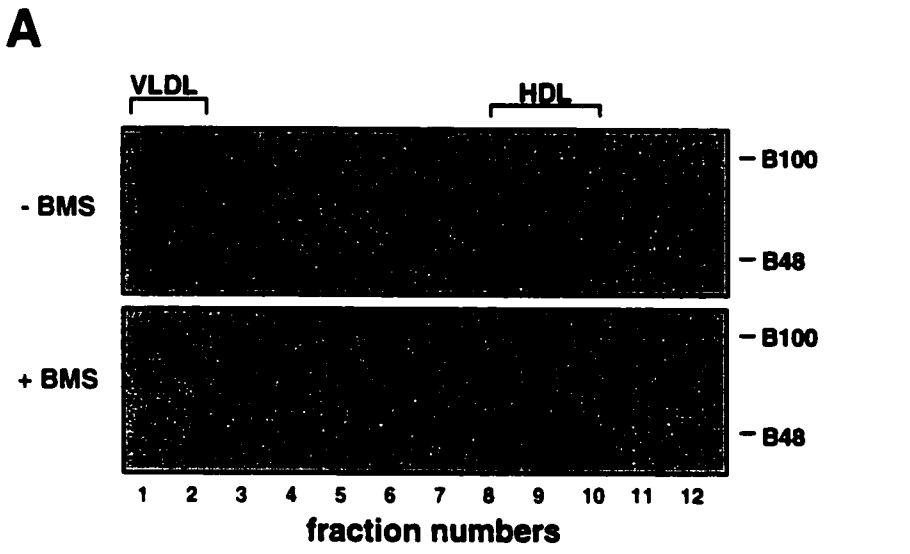
A
VLDL
HDL
- BMS
+ BMS
B100
B48
B100
B48
1 2 3 4 5 6 7 8 9 10 11 12
fraction numbers

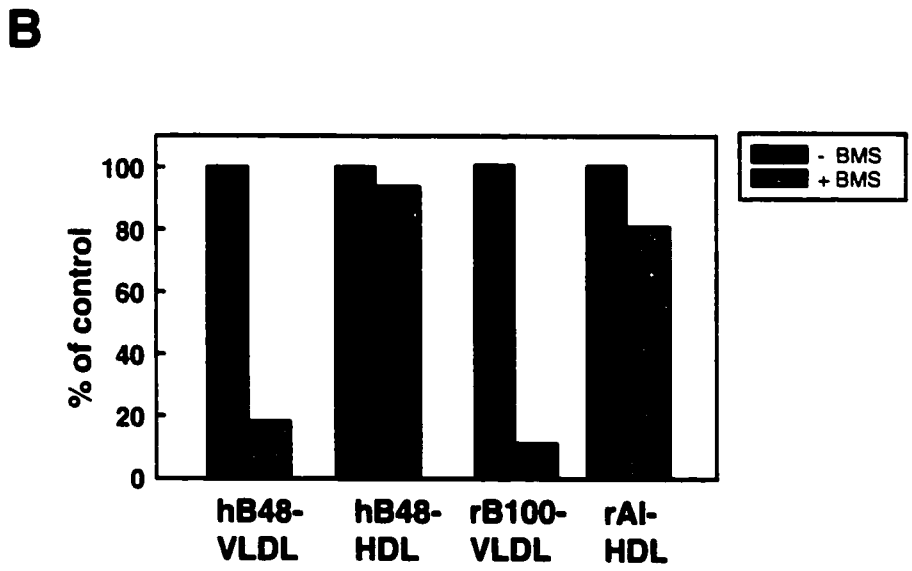
B
% of control
100
80
60
40
20
0
- BMS
+ BMS
hB48-VLDL
hB48-HDL
rB100-VLDL
rAI-HDL

FIG. 3.3.5. **Effect of BMS-192951 on secretion of apoB-associated lipids - inhibition of MTP prior to metabolic labeling.** Human B48-transfected cells were incubated with DMEM (20% serum) ± BMS-192951 (5 μM) to inactivate MTP. Inhibition of MTP was achieved by photoactivation of the inhibitor for 15 min under 360 nm UV light. Cells were then labeled with 30 μCi [^{3}H]glycerol in DMEM (20% serum) + 0.4 mM oleate for up to 4 h. The conditioned media were collected at 2 h and 4 h, fractionated in a sucrose density gradient. [^{3}H]Glycerol-labeled TG and PC associated with hB48-VLDL, hB48-HDL and rB100-VLDL were quantified. Repetition of the experiments yielded similar results. *Open square*, control; *closed square*, MTP inhibited.

Fig. 3.3.5.

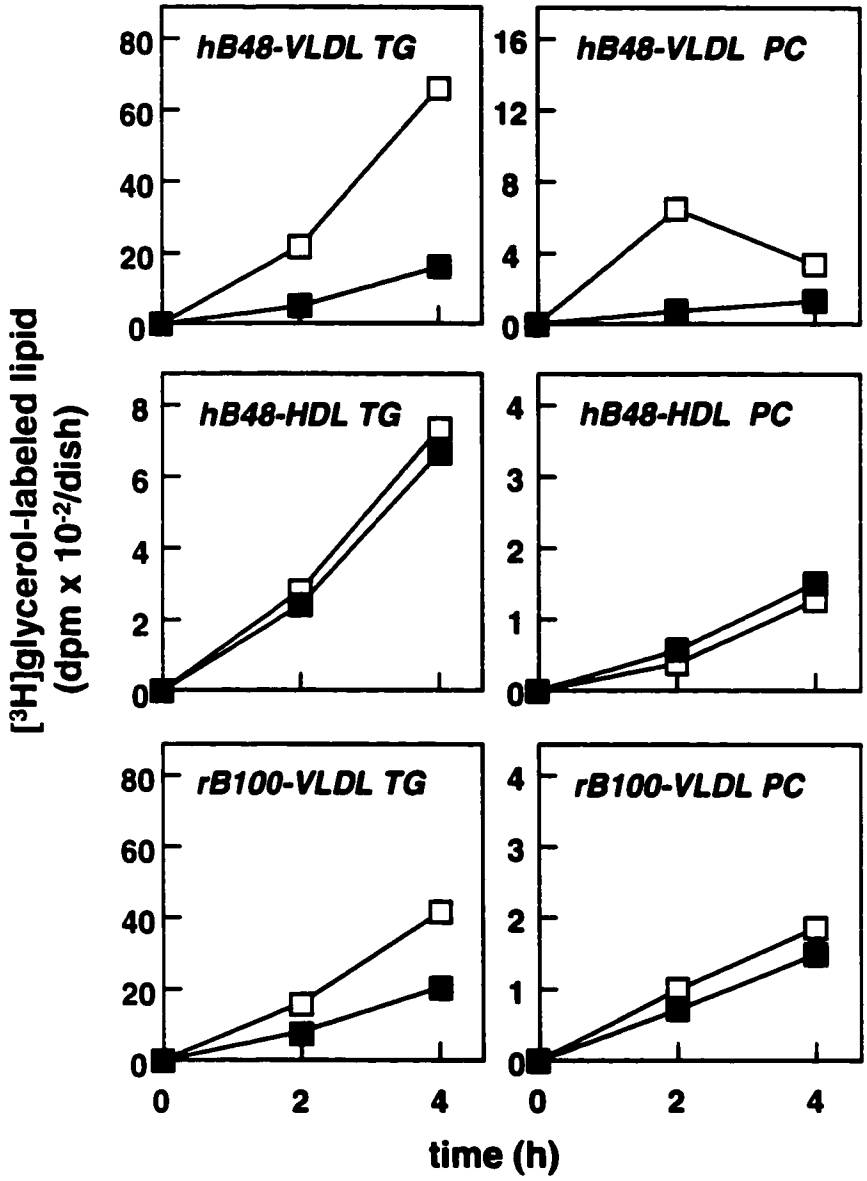
hB48-VLDL TG
hB48-VLDL PC
hB48-HDL TG
hB48-HDL PC
rB100-VLDL TG
rB100-VLDL PC
[3H]glycerol-labeled lipid (dpm x 10-2/dish)
time (h)

FIG. 3.3.6. **Effect of BMS-197636 on endogenous MTP activity and B48 secretion.** *A*, MTP activity assay. Microsomal contents were isolated from cells treated for 30 min with various doses of BMS-197636 and 0.4 mM oleate, and was used to measure the TG transfer activity (*cell*). Data are presented as % of control (n = 4). Addition of 0.2 μM BMS-197636 directly to the assay mixture abolished the TG transfer activity (*in vitro*). *B* & *C*, human B48-transfected cells were pulse-labeled with 400 μCi [^{35}S]methionine/cysteine in DMEM (20% serum) for 1 h, washed, and incubated for 4 h in DMEM (20% serum) supplemented with 0.4 mM oleate and the indicated amount of BMS-197636. The media were fractionated into VLDL (d < 1.02 g/ml) and HDL (d > 1.02 g/ml) fractions by ultracentrifugation. [^{35}S]ApoBs were recovered by immunoprecipitation and resolved by SDS-PAGE. Radioactivity associated with secreted B48 on HDL (*closed circle*) or VLDL (*open circle*) (*B*) and apoA-I on HDL (*C*) is expressed as % of signal detected in cell treated without inhibitor (*control*). Representative fluorograms of medium [^{35}S]labeled apolipoproteins at the end of 4-h incubation were shown at the *bottom* of each panel.

Fig. 3.3.6.

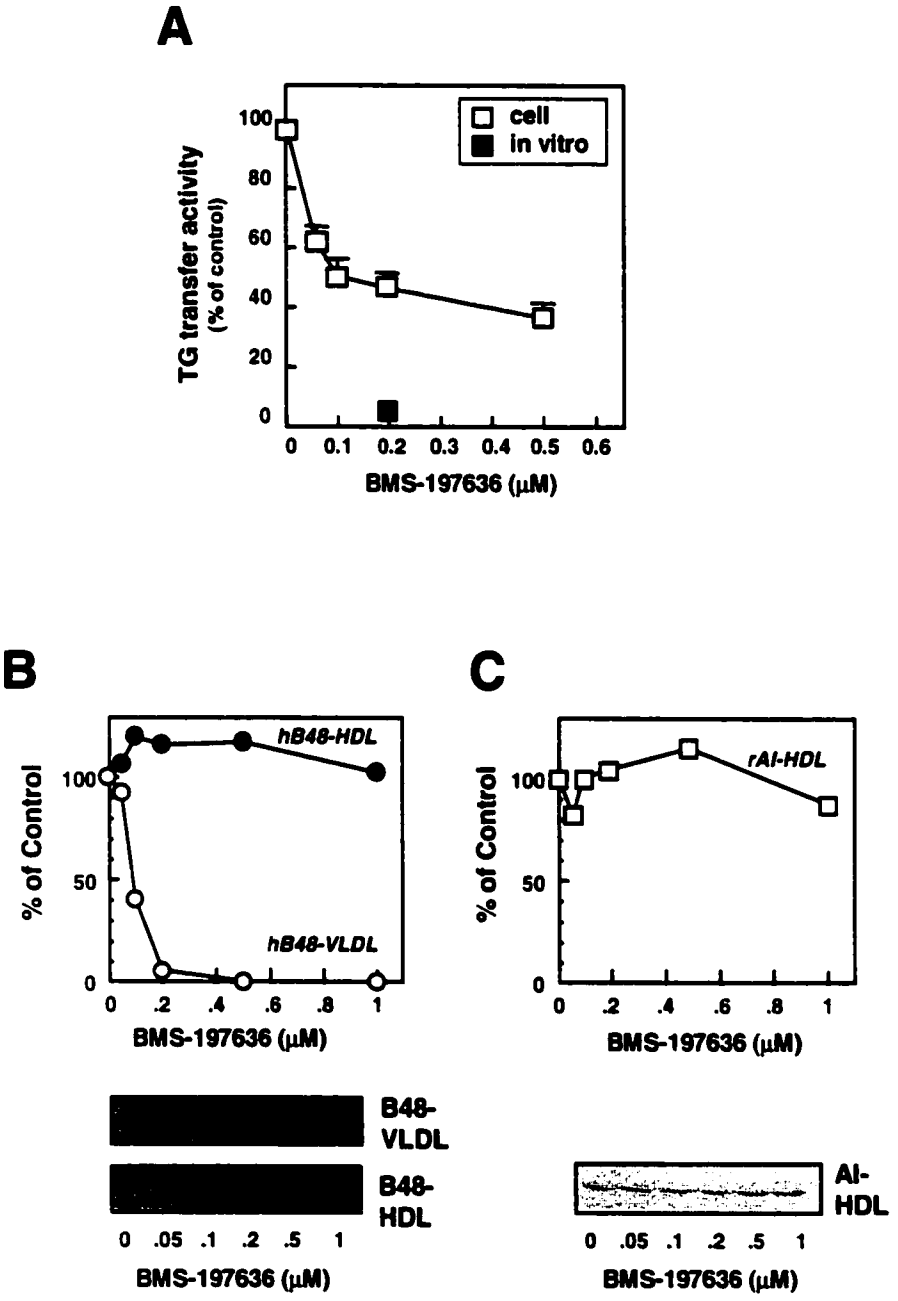
A
TG transfer activity (% of control)
cell
in vitro
BMS-197636 (μM)
B
% of Control
hB48-HDL
hB48-VLDL
BMS-197636 (μM)
B48-VLDL
B48-HDL
BMS-197636 (μM)
C
% of Control
rAI-HDL
BMS-197636 (μM)
AI-HDL
BMS-197636 (μM)

FIG. 3.3.7. **Effect of BMS-197636 on secretion of B72-VLDL and B100-VLDL.** Human B72 or B100-transfected cells were pulse-labeled with [^{35}S]methionine/cysteine for 1 h, washed and incubated for 2 h under the indicated conditions. [^{35}S]ApoBs were recovered from $d < 1.02$ and $d > 1.02$ g/ml fractions by immunoprecipitation, resolved by SDS-PAGE, and visualized by fluorography. Data were shown in duplicates.

Fig. 3.3.7.

A **B100**

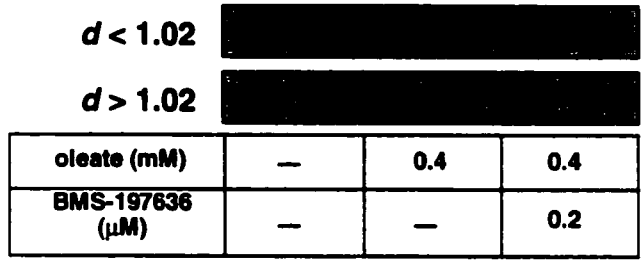

B **B72**

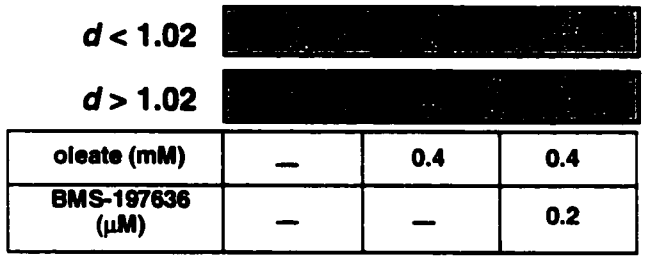

FIG. 3.3.8. **Effect of BMS-197636 on secretion of B100-associated lipids.** *A*, human B100-transfected cells were pulsed labeled with 30 μCi [^{3}H]glycerol + 0.4 mM oleate ± 0.2 μM BMS-197636 for up to 4 h. The conditioned media were fractionated by cumulative rate flotation. [^{3}H]Glycerol-labeled TG and PC associated with hB100-$VLDL_1$ and hB100-$VLDL_2$ were quantified. *B*, human B100-transfected cells were pulsed labeled with 10 μCi [^{3}H]oleate in the absence of oleate for 4 h, and chased in the presence of 0.4 mM oleate ± 0.2 μM BMS-197636 for up to 4 h. After fractionation of the conditioned media by cumulative rate flotation, [^{3}H]oleate-labeled TG and PC associated with hB100-$VLDL_1$ and hB100-$VLDL_2$ were quantified. Repetition of the experiments yielded similar results. *Open square*, control; *closed square*, MTP inhibited.

Fig. 3.3.8.

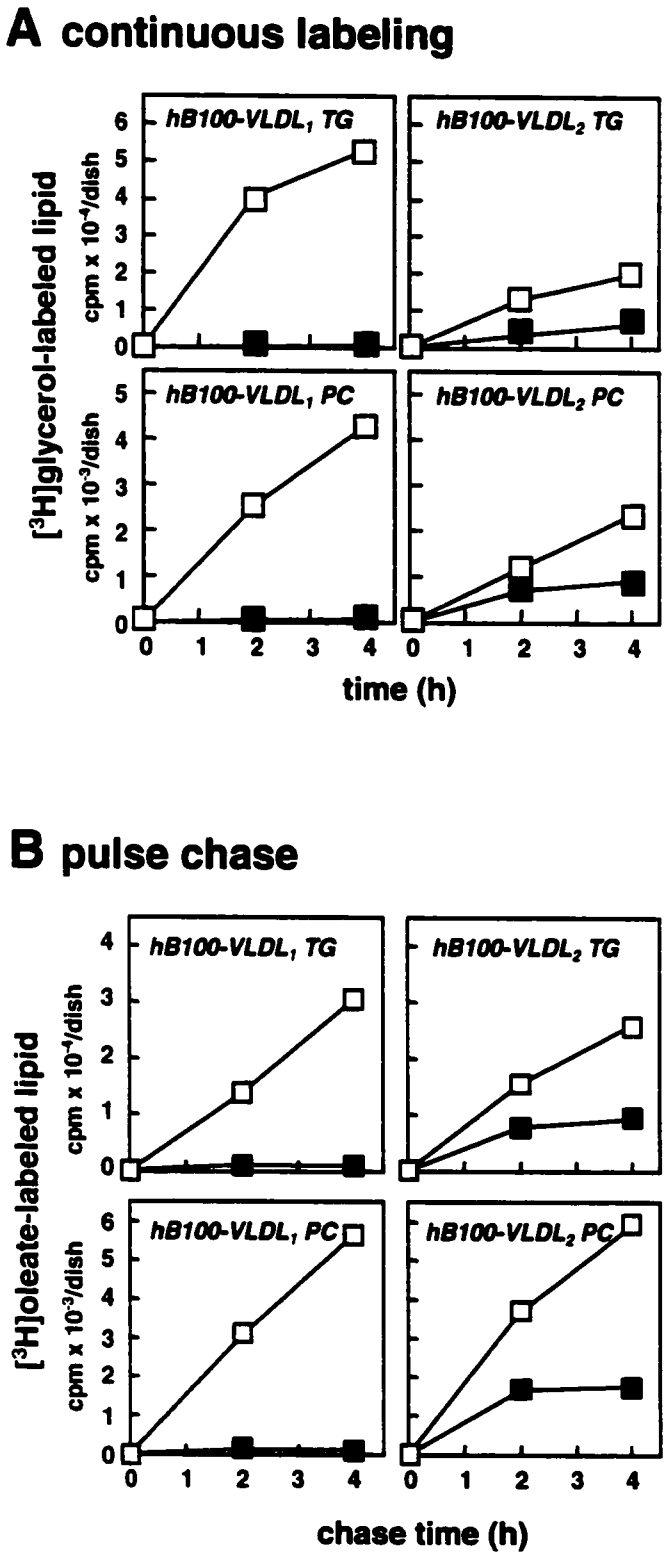
A continuous labeling
hB100-VLDL1 TG
hB100-VLDL2 TG
hB100-VLDL1 PC
hB100-VLDL2 PC
[3H]glycerol-labeled lipid
cpm x 10-4/dish
cpm x 10-3/dish
time (h)
B pulse chase
hB100-VLDL1 TG
hB100-VLDL2 TG
hB100-VLDL1 PC
hB100-VLDL2 PC
[3H]oleate-labeled lipid
cpm x 10-4/dish
cpm x 10-3/dish
chase time (h)

FIG. 3.3.9. **Effect of BMS-197636 on secretion of B100-VLDL$_1$ and B100-VLDL$_2$.** *A*, Human B100-transfected cells were labeled for 3 h with [^{35}S]methionine/cysteine in DMEM (20% serum) in the presence of 0.4 mM oleate + indicated dose of BMS-197636. The secreted [^{35}S]B100 and [^{35}S]B48 were fractionated by cumulative rate flotation. [^{35}S]ApoBs in each fraction were immunoprecipitated, resolved by SDS-PAGE, and visualized by fluorography. *B*, radioactivity associated with secreted [^{35}S]B100 and [^{35}S]B48 was quantified. Data are presented as % of control (*i.e.* no BMS-197636). Repetition of the experiments yielded similar results.

Fig. 3.3.9.

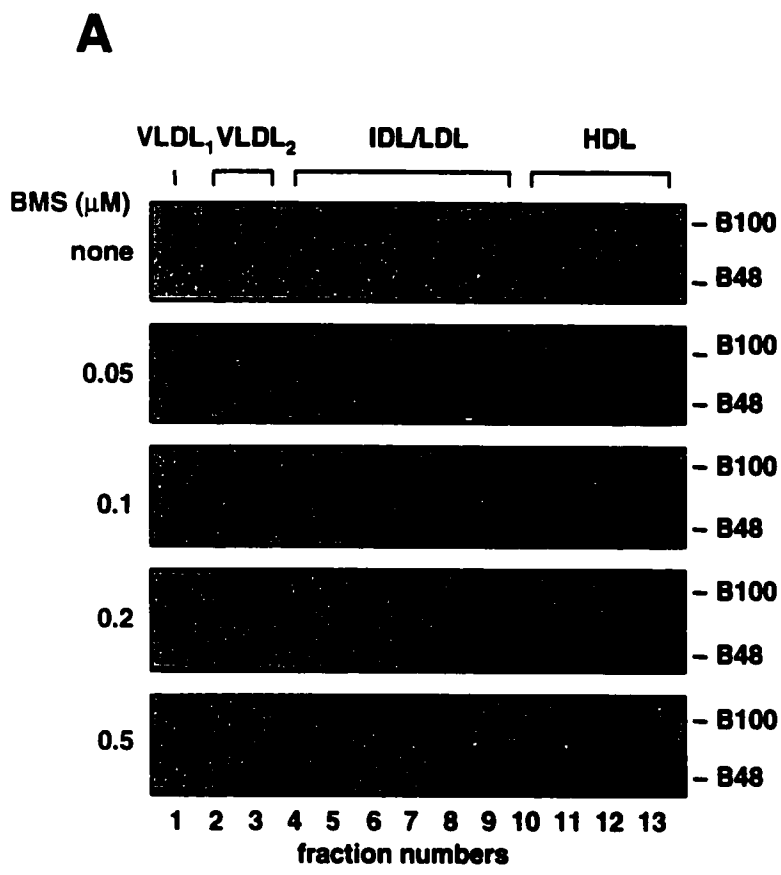
A
VLDL1 VLDL2
IDL/LDL
HDL
BMS (μM)
none
0.05
0.1
0.2
0.5
B100
B48
1 2 3 4 5 6 7 8 9 10 11 12 13
fraction numbers
B
B100
B48
apoB secretion (% of control)
100
80
60
40
20
0
0 0.1 0.2 0.3 0.4 0.5
BMS-197636 (μM)

FIG. 3.3.10. **Effect of BMS-197636 on assembly of B100-VLDL$_1$ within microsomal lumen.** Human B100-transfected cells were pretreated with 0.4 mM oleate in DMEM (20% serum) for 30 min, pulse-labeled with [^{35}S]methionine/cysteine for 20 min (*0 min* chase), and then incubated in chase medium ± 0.2 μM BMS-197636 for 60 min (*60 min* chase). The microsomal content was fractionated by cumulative rate flotation, and [^{35}S]apoBs were recovered from each fraction (except the bottom 1-ml fraction) by immunoprecipitation and analyzed by SDS-PAGE/fluorography. The experiment was repeated twice and similar results were obtained.

Fig. 3.3.10.

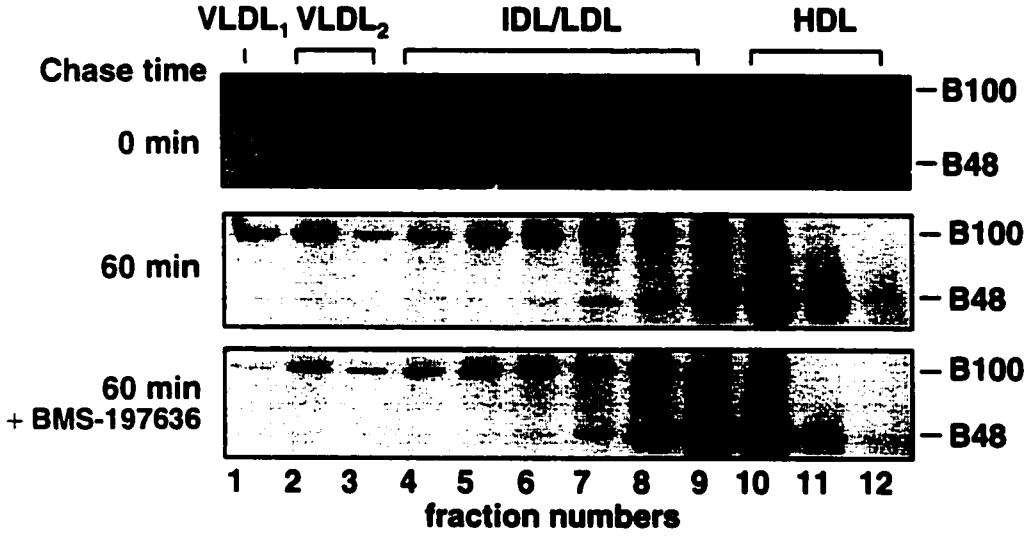
VLDL1
VLDL2
IDL/LDL
HDL
Chase time
0 min
60 min
60 min
+ BMS-197636
B100
B48
B100
B48
B100
B48
1 2 3 4 5 6 7 8 9 10 11 12
fraction numbers

3.4. Microsomal triglyceride transfer protein is required for mobilizing triacylglycerol into microsomes

Knowing that BMS-197636 did not affect either synthesis or mass of total cell lipids (Table III), we hypothesized that it may impair intracellular distribution of lipids. To test this hypothesis, we determined the effect of BMS-197636 on the distribution of lipid among different subcellular compartments. Of total microsomal TG, approximately 74% of [^{3}H] TG (Fig. 3.4.1.*A*, *top* panel) and 62% of TG mass (Fig. 3.4.1.*A*, *bottom* panel) were found in the membranes with the remainder in the lumen in oleate-treated cells. [The high proportion of membrane-associated TG in hepatic microsomes was observed previously with rat (236) and rabbit hepatocytes (157).] Treatment with BMS-197636 entirely abolished the oleate-induced accumulation of TG within microsomal lumen, and also decreased the amount of TG associated with microsomal membrane by 30%. A small (~10%) but reproducible increase in cytosolic TG by BMS-197636 treatment was observed, the quantity of which was equivalent to the decrease in total microsomal TG. BMS-197636 had little effect on the distribution of [^{3}H]PC (Fig. 3.4.1.*B*, *top* panel) or PC mass (Fig. 3.4.1.*B*, *bottom* panel) among different subcellular compartments.

The decrease in microsomal TG could either be a direct result of inhibited TG influx or else a consequence secondary to inhibited VLDL assembly. Examination of the BMS-197636 effect on TG influx showed that accumulation of [^{3}H]TG in microsomal lumen and membrane was decreased by >60% and 40%, respectively, during the first 30-min labeling (Fig. 3.4.2.*A*, *a* & *b*). Little difference in cytosolic [^{3}H]TG (Fig. 3.4.2.*A*, *c*)

and no secretion of [^{3}H]TG were observed during this period (Fig. 3.4.2.*A*, *d*). The inhibitory effect of BMS-197636 on lumenal [^{3}H]TG accumulation and on [^{3}H]TG secretion was also apparent at the end of 1 h labeling. Thus, BMS-197636 specifically impairs the accumulation and attainment of newly synthesized TG within the microsomal lumen. When [^{3}H]TG accumulation in the microsomal lumen was plotted against the dose of BMS-197636 (Fig. 3.4.2.*B*), an inverse relationship, similar to the residual MTP activity within the cells as a function of MTP inhibitor (Fig. 3.3.6.*A*), was observed. The abolished B100-VLDL$_1$ assembly/secretion (Fig. 3.3.9.*A*), coinciding with 55% decrease in lumenal [^{3}H]TG accumulation at 0.05 μM of BMS-197636 (Fig. 3.4.2.*B*), suggests strongly that the demand of MTP activity for B100-VLDL assembly correlates closely with the influx of TG into microsomal lumen.

The alternate possibility of diminished lumenal [^{3}H]TG being a consequence of impaired VLDL assembly was tested using cells treated with a low dose of BfA (0.2 μg/ml). As shown previously BfA effectively blocked bulk TG incorporation into VLDL (211), which was confirmed here by its effect on B100-VLDL assembly within the microsomal lumen (Fig. 3.4.3.*A*). Under this condition, however, influx of [^{3}H]TG into microsomes and [^{3}H]TG secretion decreased marginally as compared to control (*i.e.* no BfA) (Fig. 3.4.3.*B*, *a*, *b*, & *d*). The un-impaired accumulation of lumenal TG by BfA treatment was confirmed by prolonged lipid labeling (Fig. 3.4.3.*C*, *a*) and mass measurement (data not shown). In these cells, however, the [^{3}H]TG associated with microsomal lumen (Fig. 3.4.3.*C*, *a*) and secreted into the medium (Fig. 3.4.3.*C*, *b*) were also sensitive to BMS-197636 treatment, providing further evidence that MTP activity is

essential for TG accumulation within microsomes. Thus, the influx of TG into microsomal lumen may not be tightly coupled with VLDL assembly. Together these data suggest that the diminished lumenal [^{3}H]TG upon BMS-197636 treatment is unlikely attributable to an inhibited VLDL assembly.

We have also tested (by pulse-chase experiments) the possibility, though unlikely, that the decreased lumenal TG accumulation by BMS-197636 was the result of impaired B100 translocation across the ER membrane (Fig. 3.4.4). The experiment was done under conditions where B100-VLDL assembly was maximized (with exogenous oleate) yet degradation of B100 was minimized (with ALLN). Between control and BMS-197636 (0.2 μM)-treated cells, equal amounts of full length [^{35}S]B100 were found during 0, 15, and 30 min of chase (Fig. 3.4.4, compare *lanes 1, 4, & 7* between *A & B*). Thus, MTP inhibition *per se* does not affect apoB translation. We then determined translocation of pulse-labeled (15 min) [^{35}S]B100 during chase by trypsin digestion of the isolated microsomes. In control cells 40-50% of [^{35}S]B100 was sensitive to trypsin at 0-, 15- and 30-min of chase (Fig. 3.4.4.*A*, *lanes 2*, 5 & *8*). Under these conditions, inhibition of MTP did not have an effect on the attainment of trypsin-resistance in [^{35}S]B100 (Fig. 3.4.4.*B*, *lanes 2, 5, & 8*). [The integrity of microsomal vesicles was verified by nearly 100% trypsin-resistant of the ER resident protein disulfide isomerase (data not shown).] Fragments of apoB that were resistant to exogenous trypsin (indicated by a *bracket* on the *right* of *lanes 2* of Fig. 3.4.4.*A & B*) were observed whose intensity decreased with time (compare 0, 15 and 30 min of chase). These fragments might be derived from partially

translocated B100 as reported previously (237). Thus, decreasing MTP activity by half (at 0.2 μM of BMS-197636) did not impede B100 translation/translocation.

In conclusion, MTP is required for mobilizing bulk TG into microsomal lumen, a process that is essential for post-translational VLDL assembly. Mobilization of TG into microsomal lumen and incorporation of microsomal TG to form VLDL are two separate events.

FIG. 3.4.1. **Effect of oleate and BMS-197636 on subcellular distribution of triacylglycerol and phosphatidylcholine.** Human B100-transfected cells were pretreated for 30 min under the indicated conditions and then labeled with [^{3}H]glycerol for 2 h under the same conditions. Microsomal lumen, microsomal membrane, and cytosol were isolated. *A*, [^{3}H]TG (*top*) and TG mass (*bottom*). *B*, [^{3}H]PC (*top*) and PC mass (*bottom*). Data are presented as the average of two samples from two independent experiments.

Fig. 3.4.1.

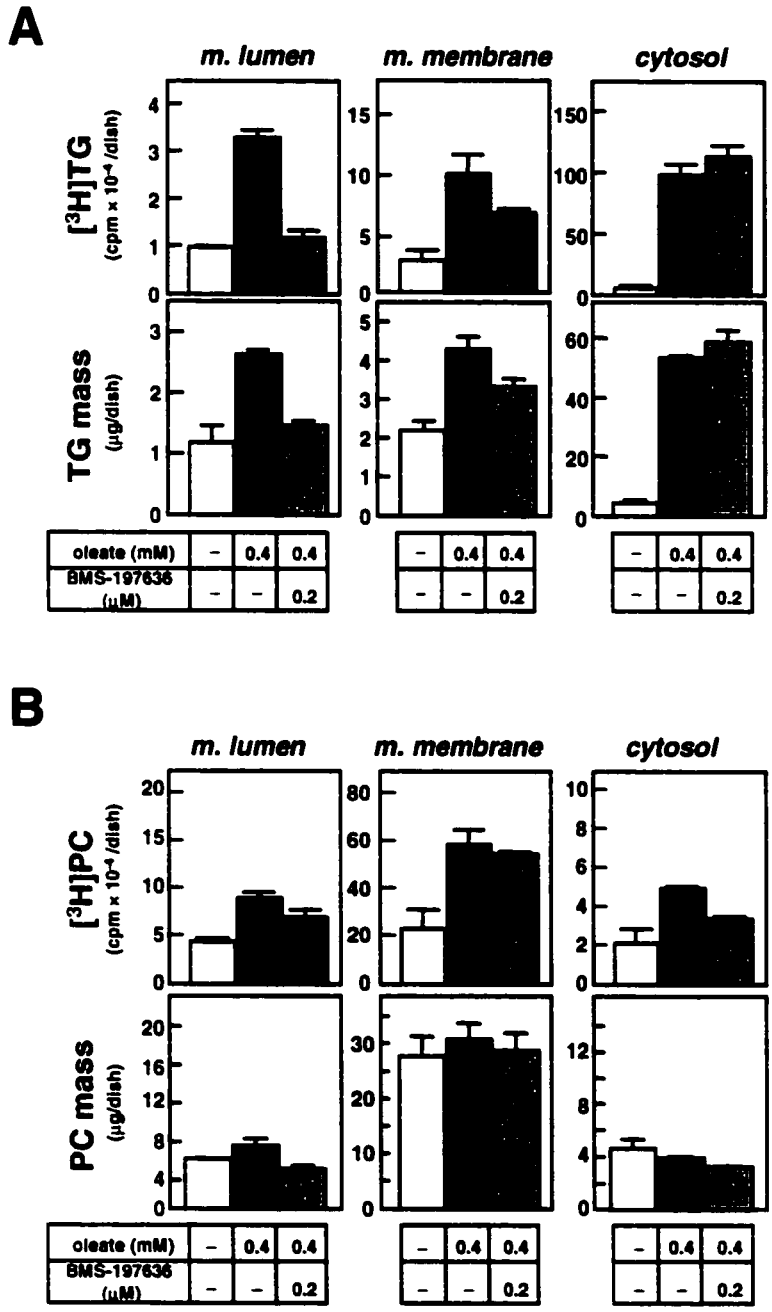
A
m. lumen
m. membrane
cytosol
[3H]TG (cpm x 10-4 /dish)
TG mass (µg/dish)
oleate (mM)
BMS-197636 (µM)
B
m. lumen
m. membrane
cytosol
[3H]PC (cpm x 10-4 /dish)
PC mass (µg/dish)
oleate (mM)
BMS-197636 (µM)

FIG. 3.4.2. **Effect of BMS-197636 on triacylglycerol distribution.** *A*, human B100-transfected cells were pretreated for 30 min with 0.4 mM oleate (*control*) or 0.4 mM oleate + 0.2 μM BMS-197636 (*+BMS*), and then labeled with [^{3}H]glycerol for up to 1 h under the same conditions. The microsomal lumen, microsomal membrane and cytosol were isolated from the cells, and lipids were extracted from each fraction. Radioactivity associated with [^{3}H]TG is presented as the average of two samples from two independent experiments. *B*, dose effect of BMS-197636 on accumulation of [^{3}H]TG in microsomes. The experiment was done as in *A*.

Fig. 3.4.2.

A

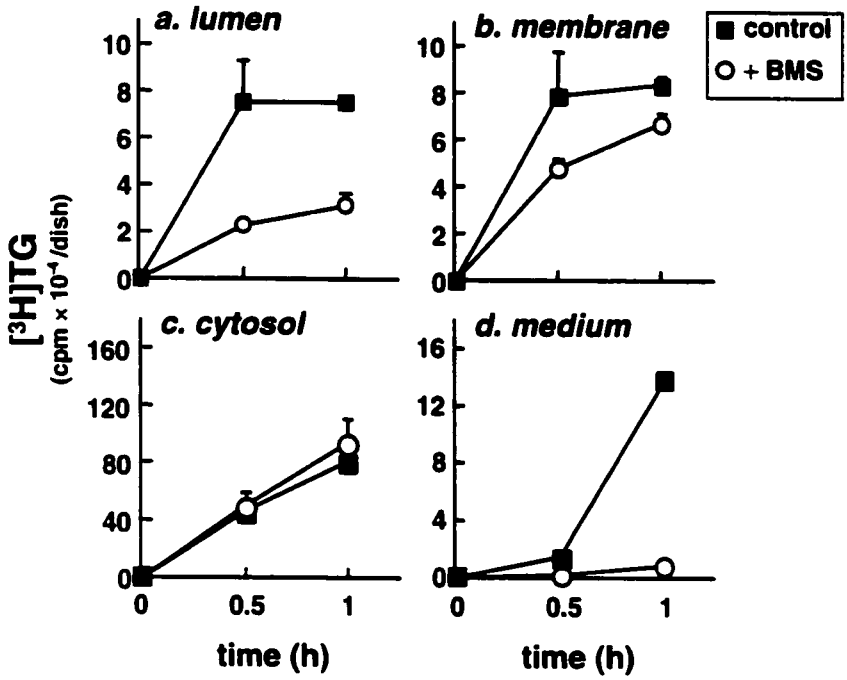

B

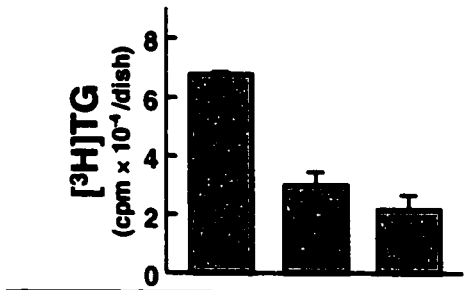

oleate (mM)	0.4	0.4	0.4
BMS-197636 (μM)	—	.05	0.2

FIG. 3.4.3. **Effect of brefeldin A on triacylglycerol distribution.** *A*, effect of 0.2 μg/ml BfA on B100-lipoproteins assembly within microsomal lumen. Human B100-transfected cells were pretreated for 30 min with 0.4 mM oleate (*control*) or 0.4 mM oleate + 0.2 μg/ml BfA (+*BfA*), and then labeled with [^{35}S]methionine/cysteine for up to 1 h under the same conditions. The microsomal content was fractionated by cumulative rate flotation, and [^{35}S]apoB was recovered from each fraction (except the bottom 1-ml fraction) by immunoprecipitation and analyzed by SDS-PAGE/fluorography. *B*, human B100-transfected cells were pretreated for 30 min with 0.4 mM oleate (*control*) or 0.4 mM oleate + 0.2 μg/ml BfA (+*BfA*), and then labeled with [^{3}H]glycerol for up to 1 h under the same conditions. The microsomal lumen, microsomal membrane and cytosol were isolated from the cells, and lipids were extracted from each fraction. Radioactivity associated with [^{3}H]TG is presented as the average of two samples from two independent experiments. *C*, dose effect of BMS-197636 on [^{3}H]TG distribution in BfA (0.2 μg/ml)-treated cells. The experiment was done as in *A*, except the cells were labeled for 2 h.

Fig. 3.4.3.

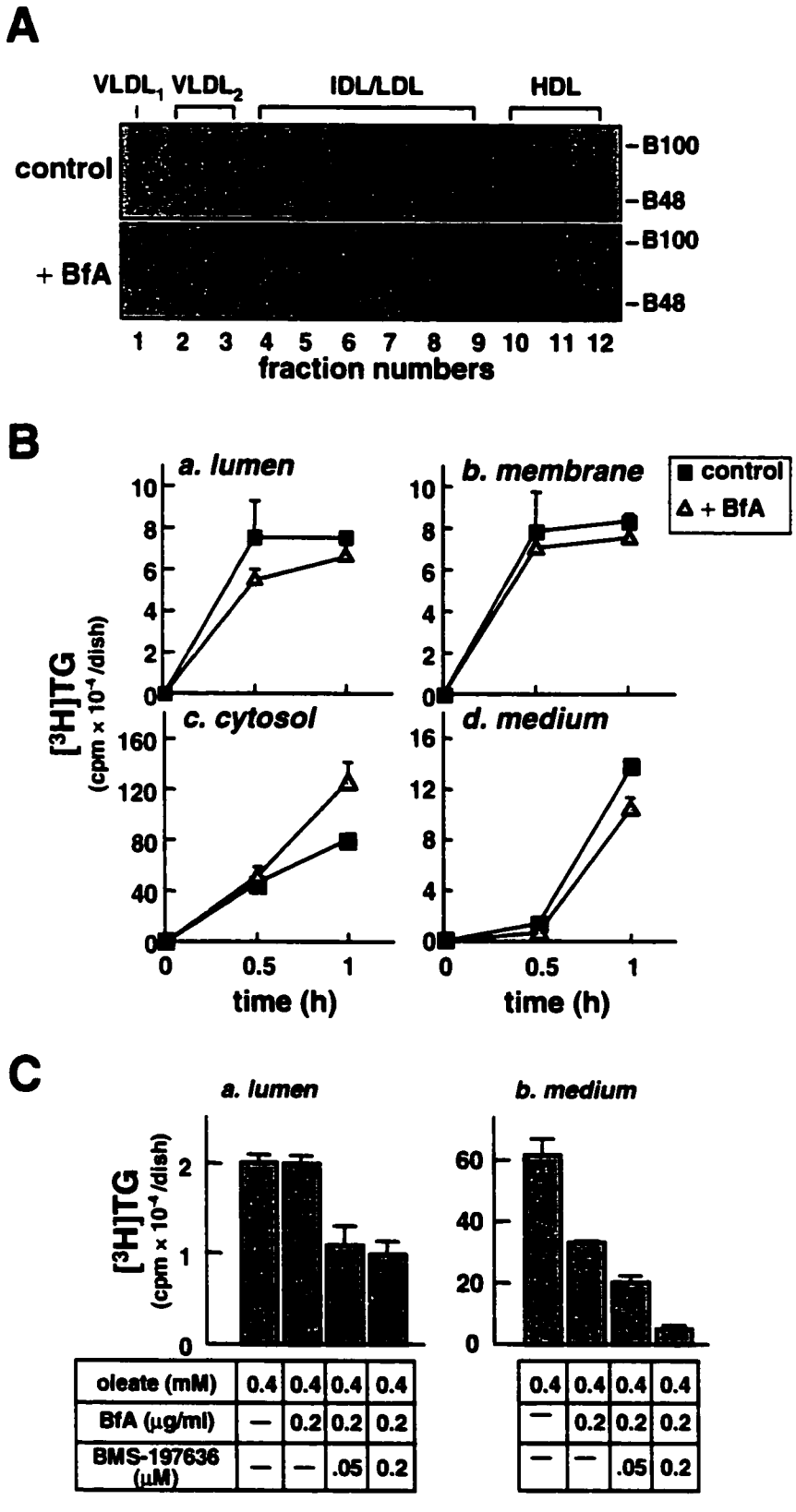
A
VLDL1
VLDL2
IDL/LDL
HDL
control
+ BfA
B100
B48
B100
B48
1 2 3 4 5 6 7 8 9 10 11 12
fraction numbers
B
a. lumen
b. membrane
c. cytosol
d. medium
control
+ BfA
[3H]TG
(cpm x 10-4/dish)
time (h)
time (h)
C
a. lumen
b. medium
[3H]TG
(cpm x 10-4/dish)
oleate (mM) 0.4 0.4 0.4 0.4
BfA (μg/ml) — 0.2 0.2 0.2
BMS-197636 (μM) — — .05 0.2
0.4 0.4 0.4 0.4
— 0.2 0.2 0.2
— — .05 0.2

FIG. 3.4.4. **Trypsin digestion of pulsed-labeled apolipoprotein B associated with microsomes.** Human B100-transfected cells were pretreated with 0.4 mM oleate, 40 μg/ml ALLN in the absence (*A*) or presence (*B*) of 0.2 μM BMS-197636 for 30 min. The cells were labeled with [^{35}S]methionine/cysteine for 15 min and chased for 0, 15, 30 min under the same conditions. Heavy microsomes were isolated, and incubated in the absence (*lanes 1, 4, & 7*) or presence (*lanes 2, 5, & 8*) of trypsin (50 μg/ml) or trypsin plus Triton X-100 (1%) (*lanes 3, 6, & 9*) for 30 min on ice. The trypsin digestion was terminated by the addition of trypsin inhibitor, and [^{35}S]apoBs were recovered by immunoprecipitation and analyzed by SDS-PAGE/fluorography. Repetition of the experiments with limited proteolysis of the total microsomes (*i.e.* heavy plus light microsomes) during chase (up to 45 min) yielded similar results.

Fig. 3.4.4.

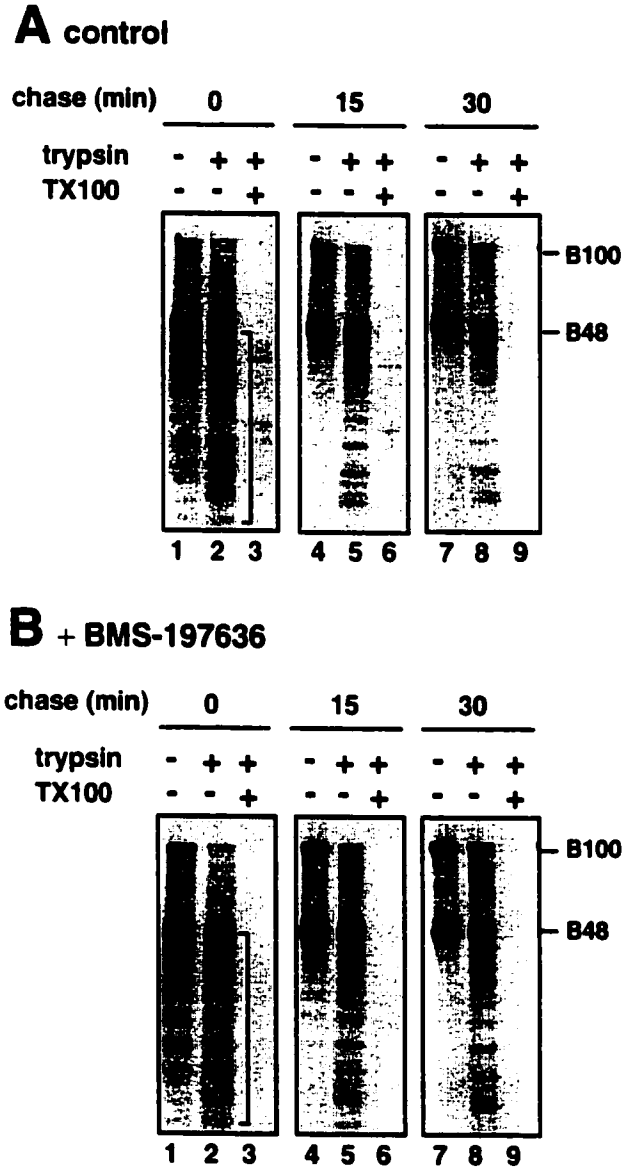
A control
chase (min)
0
15
30
trypsin
TX100
B100
B48
1 2 3 4 5 6 7 8 9
B + BMS-197636
chase (min)
0
15
30
trypsin
TX100
B100
B48
1 2 3 4 5 6 7 8 9

Chapter 4 Discussion

4.1. Structural requirement of human apolipoprotein B for hepatic assembly of very low density lipoprotein

Although it is known that apoB plays an obligatory role in hepatic VLDL assembly, the structural element(s) within apoB that is required for hepatic VLDL assembly have not been well defined. Since a mature VLDL particle can be assembled with a single copy of either apoB100 or apoB48 (the N-terminal 48% of apoB100), it is generally believed that the structural elements required for VLDL assembly reside within apoB48. Thus, in the first part of our study, we have attempted to localize structural element(s) within apoB48 that are responsible for the oleate-induced formation of VLDL in McA-RH7777 cells. The first approach that was used to localize structural elements was to systematically truncate apoB48 from the C-terminus, and to examine the effect of truncation on apoB's ability to assemble VLDL in transfected McA-RH7777 cells. Our results (Fig. 3.1.9) show that the truncated apoB variants that are equal to or longer than apoB34 can assemble VLDL, whereas apoB variants that are equal to or shorter than apoB29 can not. This result can be interpreted by two alternate, although not mutually exclusive possible mechanisms: (a) There exist putative lipid-recruiting sequences (or domains) beyond the C-terminus of 29% of apoB100 (i.e. a domain effect). (b) Alternatively, there exists a minimum length of apoB polypeptide that is sufficient for governing VLDL assembly (i.e. a length effect), which is at least longer than 29% of apoB100.

To distinguish the possibilities between the domain effect and the length effect, we have created chimeric proteins that contain human apoA-I and segments derived from apoB48. Chimera AI/B29-34 was constructed using apoA-I sequences that were fused, at their C-terminus, to a segment derived from sequences between apo-B29 and -B34 (designated AI/B29-34). Two additional chimeric proteins, designated AI/B34-37 and AI/B37-42 were constructed similarly using apoAI plus apoB segments derived from corresponding B34-37 or B37-42 sequences (79). Surprisingly, all these three AI/B chimeras turned out to be able to form discrete VLDL particles in transfected cells in the presence of exogenous oleate, whereas the control apoAI was only able to form HDL (79). These results suggest that the recruitment of large quantities of TG during VLDL assembly is not governed simply by apoB length, but is mediated by short hydrophobic sequences ranging from 152 to 237 amino acids (3-5%) of apoB100. Thus, the apoB sequences required for VLDL assembly are much shorter than was previously expected, and the ability of apoB to recruit lipids seems a domain effect.

The finding that AI/B chimeric proteins can assemble VLDL raised several questions. How can a protein containing 3-5% of the apoB sequence mediate VLDL assembly? Are there any unique features within the B29-34 segment that are responsible for the ability of apoB34 and AI/B29-34 to form VLDL? We have searched for the structural features within all three apoB segments in the AI/B chimeras (i.e. B29-34, B34-37, and B37-42). We have eliminated N-glycosylation as a requirement for VLDL assembly, since N-linked glycosylation sites are present in some (e.g. B29-34) but not the other segments (e.g. B34-37 and B37-42) (Fig. 1.1.*B*). Likewise, since cysteines (two in

B29-34, one in B34-37, and zero in B37-42) (Fig. 1.1.*C*), proline-rich clusters (one in B29-34, and zero in B34-37 or B37-42), or the postulated "pause-transfer" motifs (one in B29-34, zero in B34-37, and four in B37-42) (for "pause-transfer" motif, refer to Section 1.3.2) are not uniformly distributed among the three segments, we have concluded that none of these structural features is essential for VLDL assembly. The only common feature among the three apoB segments is their hydrophobicity. The hydropathy values, as determined by the Kyte and Doolittle algorithm (PCGene™, Intelligenetics, Inc., 15-residue window) revealed that each apoB segment generated a chimera which was more hydrophobic (grand average hydrophobicity = 6.59 for AI/B29-34, 6.20 for AI/B34-37 and 5.67 for AI/B37-42) than apoAI itself (grand average hydrophobicity = 8.06). Furthermore, according to the pentapartite model proposed by Segrest *et al.* (Fig. 1.1.*D*, (27)), each apoB segment was predicted to consist predominantly of amphipathic β strands. It is conceivable that the uniquely enriched β strands within B29-34 render the ability of apoB34 to form VLDL, whereas the presence of multiple segments enriched in β strands within apoB48 would certainly enhance the efficiency of lipid recruitment during VLDL assembly.

A point of note is that not all the amphipathic sequences within apoB are responsible for the lipid-recruiting function during VLDL assembly. For example, according to the pentapartite model (Fig. 1.1.*D*, (27)), amphipathic β strands also occur within apoB29 (between apo-B18 to -B29), but our data clearly show that apoB29 is unable to assemble VLDL (Fig. 3.1.9). Moreover, the role of other structural elements, such as amphipathic α helices, in mediating VLDL assembly remains to be defined.

Therefore, further studies are required to determine the molecular details for how some of the hydrophobic sequences within apoB48 can mediate lipid recruitment during VLDL assembly.

4.2. A unified model for the assembly of B48-VLDL and B100-VLDL

4.2.1. Novel information on the assembly of B100-VLDL

In McA-RH7777 cells, assembly of rat B48-VLDL is dependent upon exogenous oleate, and is achieved post-translationally (125). The present study has demonstrated that these features are also associated with human B48-VLDL assembly in transfected cells (Fig. 3.1.1 – 3.1.4, Fig. 3.1.8). In addition, our lipid labeling experiments clearly indicated that assembly of B48-VLDL was a process whereby bulk TG was incorporated into B48, regardless of whether bulk TG was derived from newly synthesized TG (Fig. 3.1.5) or from pre-existing TG (Fig. 3.1.6).

In contrast to that for B48-VLDL assembly, the mechanism for B100-VLDL assembly in McA-RH7777 cells was somewhat less clear. Using these cells, Borén *et al.* (125) obtained evidence showing that the rat B100-VLDL assembly could be achieved through both co-translational and post-translational pathways. Evidence in favour of the co-translational assembly model came from observations that B100-VLDL could be detected as early as three minutes after the initiation of [^{35}S]methionine labeling (125). On the other hand, the apoB100 polypeptides were also associated with dense particles resembling LDL and HDL in the microsomal lumen of McA-RH7777 cells. Pulse-chase experiments suggested that the B100-HDL/B100-LDL might serve as precursors of

B100-VLDL (125), supporting a post-translational assembly pathway. Evidence showing post-translational assembly of B100-VLDL was also presented by the same group in their subsequent investigations (161, 211). However, as to be discussed later, the published "B100-VLDL" particles were obtained as $d < 1.02$ g/ml fractions after sucrose density ultracentrifugation. These "VLDL" particles were heterogeneous in size and did not represent truly the TG-rich B100-VLDL particles.

In the current study, the mechanism responsible for the assembly of B100-VLDL has been closely examined. Although initially much attention was focused on human B48-VLDL assembly in B48-transfected McA-RH7777 cells (Section 3.1.), we nevertheless also monitored the process of endogenous rat B100-VLDL assembly and contrasted it with that of B48-VLDL assembly. In these early studies, we consistently found that the pathway for the assembly of B100-VLDL was quite different from that for B48-VLDL assembly. For example, while oleate supplementation induced a quantum leap of the particle size from B48-HDL to B48-VLDL, the change in the size of B100-VLDL upon oleate supplementation was not apparent (Fig. 3.1.4). However in these early studies, B100-VLDL was obtained simply as $d < 1.02$ g/ml fractions and their size heterogeneity was not taken into consideration.

The difference between B48-VLDL and B100-VLDL ($d < 1.02$ g/ml fraction) assembly came from the kinetics of the incorporation of pre-existing TG upon oleate supplementation. Although both newly synthesized TG (Fig. 3.1.5.*B*) and pre-existing TG (Fig. 3.1.6.*B*) could be used for B100-VLDL and B48-VLDL secretion, pre-existing

TG seemed to be preferentially incorporated into B48-VLDL upon oleate-induced VLDL secretion (Fig. 3.1.6.*B*). Thus, while there was a 6-fold increase in the incorporation of pre-existing TG into B48-VLDL, there was no difference in secretion of pre-existing TG as B100-VLDL upon oleate supplement (Fig. 3.1.6.*B*). These results led us to believe that assembly and secretion of B48-VLDL and B100-VLDL were achieved through two different pathways. The oleate-stimulated incorporation of pre-existing TG into B48-VLDL might imply that bulk TG was added to a primordial B48-HDL particle during *post-translational* VLDL assembly. In contrast, the inability of B100 to mobilize additional pre-existing TG in response to oleate might imply that B100-VLDL was assembled primarily through a *co-translational* lipidation process, and that post-translational lipid recruitment might not play a major role in B100-VLDL assembly. On the basis of these results, we proposed in our manuscript (238) that dual mechanisms operated in McA-RH7777 cells; while B48-VLDL assembly was achieved post-translationally, assembly of B100-VLDL was achieved co-translationally.

However, the putative dual mechanisms for B48-VLDL and B100-VLDL assembly did not stand up well to scrutiny in our subsequent investigations. In an attempt to determine if the apparent dual mechanisms were accounted for by apoB length (e.g. apoB48 versus apoB100), we systematically analyzed assembly/secretion of VLDL with recombinant apoB forms, namely B64, B72, and B80 (Fig. 3.2.1). We reasoned that if the apparent difference between B100-VLDL and B48-VLDL was attributable to apoB length, then examining assembly of B64-VLDL, B72-VLDL and B80-VLDL should reveal a critical length where the transition in assembly mechanisms (i.e. from post-

translational to co-translational) takes place. What we have observed was that all apoB forms can respond to oleate to form VLDL (Fig. 3.2.1). The oleate-induced enlargement of lipoprotein was readily demonstrated for B64 and B72 in a sucrose density gradient, but was less evident for B80 and B100 since these proteins were already in the VLDL fraction (d < 1.02 g/ml) even in the absence of oleate (Fig. 3.2.1). At this point, we realized that the previously used sucrose density ultracentrifugation technique, although satisfactory for revealing the two-step process for B48-VLDL assembly (79, 125, 238), did not allow detection of size changes in VLDL particles containing large apoB (*i.e.* B80 or B100). Thus, we suspected that the proposed co-translational B100-VLDL assembly mechanism was a misinterpretation of data resulting from inadequate resolution of B100-VLDL with different sizes.

Demonstration of oleate-induced enlargement in particle size during B100-VLDL assembly becomes possible with the use of cumulative rate flotation technique to separate B100-VLDL subclasses (Fig. 3.2.2, Fig. 3.2.3). Only by separating B100-$VLDL_1$ from B100-$VLDL_2$ were we able to show unequivocally that B100-$VLDL_1$ assembly shares three features common to B48-VLDL assembly: (a) is absolutely dependent on exogenous oleate (Fig. 3.2.2, Fig. 3.2.3), (b) is achieved post-translationally (Fig. 3.2.6), and (c) exhibits incorporation of bulk TG, regardless of whether bulk TG is derived from newly synthesized TG (Fig. 3.2.4.*B*) or pre-existing TG (Fig. 3.2.5.*B*). Thus, a unified model that can accommodate assembly of both B48-VLDL and B100-VLDL has emerged which invalidates our previously dual mechanisms hypothesis. A lesson learned

from this study is that novel information comes about as a result of technical development, like in most cases.

With the improved resolution of B100-VLDL by cumulative rate flotation technique, oleate-induced bulk TG incorporation, the hallmark of VLDL assembly irrespective of apoB length, becomes manifest. This novel information allows us to answer some previously puzzling questions. For example, we previously observed that exogenous oleate treatment had no effect on the secretion of pre-existing TG as B100-VLDL (Fig. 3.1.6.*B*). However, repeating the pulse-chase experiment with cumulative rate floatation technique (Fig. 3.2.5.*B*), we were able to show that exogenous oleate increased secretion of pre-existing TG as B100-$VLDL_1$ by 5-fold, and concomitantly it decreased secretion of pre-existing TG as B100-$VLDL_2$ by 30%. Thus, exogenous oleate treatment indeed causes a re-distribution of the pre-existing TG from B100-$VLDL_2$ to B100-$VLDL_1$. Since the amount of pre-existing TG associated with total B100-VLDL (i.e. B100-$VLDL_1$ + B100-$VLDL_2$) was not increased significantly by oleate treatment, as observed previously (Fig. 3.1.6.*B*), such a re-distribution of TG between small and large VLDL species was not detectable with the commonly used centrifugation techniques.

4.2.2. A common pathway for the assembly of B100-$VLDL_1$ and B48-VLDL

As mentioned above, there are three common features associated with both B100-$VLDL_1$ assembly and B48-VLDL assembly in McA-RH7777 cells. First, the assembly of VLDL is absolutely dependent on exogenous oleate (Fig. 3.1.1, Fig. 3.1.9, Fig. 3.2.1 and

Fig. 3.2.2). In the absence of oleate, only B100-$VLDL_2$ and B48-HDL are assembled in and secreted from McA-RH7777 cells. Although the precise mechanism whereby oleate can induce TG-rich VLDL assembly has not been defined, several possibilities are noteworthy. First of all, exogenous oleate stimulates TG synthesis thus providing abundant TG substrate for VLDL assembly. Conceivably and most likely, the increased TG synthesis and TG availability are prerequisites of enhanced VLDL assembly and secretion. In addition to oleate stimulating TG synthesis, the current study also demonstrates that oleate stimulates phospholipid turnover in McA-RH7777 cells (Fig. 3.1.6 and Fig. 3.2.5). Gibbons and co-workers ((193, 196), refer to Section 1.4.4) have proposed that the enhanced phospholipid turnover upon exogenous oleate may act as a critical step in channeling fatty acyl moieties for synthesis of VLDL-TGs. Second of all, fatty acyl-CoA has been implicated to play an important role in membrane vesiculation (239). Membrane vesiculation has been suggested to be an essential component of VLDL assembly (refer to Section 1.4.7). It is possible that oleate may also regulate VLDL assembly through its role in membrane vesiculation. Lastly, a rather speculative possibility is that oleate may serve as a signaling molecule in regulating gene expression of certain proteins that either directly participate in VLDL assembly process or indirectly influence the progression of VLDL maturation.

A second common feature associated with TG-rich VLDL assembly that has been revealed by the current study highlights that maturation of VLDL, either B100-$VLDL_1$ or B48-VLDL, is achieved post-translationally. Biochemical evidence supporting post-translational B48-VLDL assembly in McA-RH7777 cells comes from studies by

Olofsson and coworkers (125, 162) showing that membrane-associated B48-HDL is the precursor for B48-VLDL formation. In rat hepatocytes, formation of B48-VLDL is achieved at least 15-20 min after synthesis of B48 (154). The current study shows that the assembly of B100-VLDL$_1$ in microsomal lumen is undetectable until 15-20 min after apoB100 synthesis (Fig. 3.2.6). These data combined support the notion that formation of B100-VLDL$_1$ and B48-VLDL may share the same pathway. To date, identification of the precursor of B100-VLDL$_1$ remains to be a challenging task. It has been suggested that the membrane-associated B100-HDL within microsomes may serve as precursor(s) for total B100-VLDL (161).

Post-translational VLDL assembly implies that there is a temporal delay from the moment when apoB translation is complete to the moment when VLDL matures. The molecular events underlying such a delay remain to be determined. It is possible that such a temporal delay is required for spatial transition of primordial particles from the site of apoB translation/translocation to the site of VLDL assembly. Additionally, this temporal delay may be required for spatial transit of lipid entities from the site of synthesis to the site of VLDL assembly. Currently, the exact subcellular compartment where VLDL assembly occurs is not clear (refer to Section 1.4.1.). Future protein pulse-chase experiments, combined with subcellular fractionation, may provide some clues about the subcellular location where maturation of VLDL takes place. Alternatively, the temporal delay may be attributable to the time required for a conformational change of newly synthesized apoB100 that allows the protein to become assembly competent, as proposed by Olofsson and associates (161). To date, experimental evidence for such a

conformational change of apoB is lacking. Apparently, more studies are needed to determine the fate of the newly synthesized apoB during the temporal delay.

The current study also demonstrates the third feature that oleate-induced incorporation of bulk TG into apoB is a common path for TG-rich VLDL assembly. Thus, assembly of B48-VLDL is accompanied with a 15-fold increase in TG content per particle as compared to that of B48-HDL, whereas B100-$VLDL_1$ contains 8-fold more TG than B100-$VLDL_2$. The incorporation of bulk TG into apoB is the governing factor for the expansion of neutral lipid core of LpB, and is therefore the hallmark for post-translational VLDL assembly.

On the basis of these three common features for the assembly of B100-$VLDL_1$ and B48-VLDL, a unified model for TG-rich VLDL assembly in McA-RH7777 cells has been advanced. ApoB is associated with a small amount of lipid to form a primordial particle during or immediately after apoB translation. Subsequently, in the presence of oleate, the primordial particle undergoes a second lipidation stage, expanding its core by recruitment of bulk TG, to form TG-rich VLDL. A central question associated with this model, however, concerns the mechanism by which bulk TG is sequestered into the microsomes and subsequently incorporated into apoB (irrespective of the apoB length) during the post-translational VLDL assembly (see below).

4.3. The post-translational very low density lipoprotein assembly depends upon normal activity of microsomal triglyceride transfer protein

An important finding in this study is that normal MTP is indispensable for the post-translational VLDL assembly. In human B48-transfected McA-RH7777 cells, under conditions where endogenous MTP activity was reduced by 65% by chemical inhibitors, secretion of either newly synthesized or pre-labeled hB48 and TG as hB48-VLDL was abolished, whereas their secretion as hB48-HDL was unaffected (Fig. 3.3.2 – Fig. 3.3.5). Similarly, in human B100-transfected McA-RH7777 cells, secretion of B100 (both human and rat) and TG as B100-$VLDL_1$ was extremely sensitive to MTP inhibition (Fig. 3.3.8 and Fig. 3.3.9.*A*). At 0.05 μM BMS-197636, corresponding to 60% of normal MTP activity (Fig. 3.3.6.*A*), the largest B100-VLDL particle that could be secreted was $VLDL_2$ but not $VLDL_1$ (Fig. 3.3.9.*A*). Thus, the requirement of MTP activity is determined by the amount of TG to be utilized for lipoprotein assembly. The greater amount of TG to be recruited, the more MTP activity is required, and the more sensitive towards MTP inhibition.

Demonstration of the requirement of MTP activity for post-translational VLDL assembly by no means denies the crucial role of MTP in the initial stage of apoB-lipoprotein formation. Using heterologous cells co-transfected with apoB and MTP or using hepatic cells treated with specific MTP inhibitors, several laboratories including ours have demonstrated that MTP activity is essential for the elongation of apoB polypeptide chains during translation (126), for the translocation of apoB across the endoplasmic reticulum membrane (108), and for the assembly and secretion of products

of the first step (62, 108-111). Furthermore, under conditions where MTP activity was decreased lower than 40% of control (0.5 μM BMS-197636, Fig. 3.3.6.*A*), the only observed B100-lipoproteins in media were those of HDL size (Fig. 3.3.9.*A*). The enlargement of secreted particles, shown as a gradual conversion of B100-HDL to B100-$VLDL_2$ (Fig. 3.3.9.*A*), is correlated closely with increased residual MTP activity (Fig. 3.3.6.*A*). These data clearly indicate that the requirement of MTP activity at the initial stage of apoB-containing lipoprotein assembly is also correlated positively with the extent of lipid recruitment.

4.4. Requirement of microsomal triglyceride transfer protein for mobilization of triacylglycerol into microsomes

Another important observation made in this study is that the accumulation and attainment of TG within microsomal lumen is a function of MTP activity. Experimental evidence supporting this conclusion includes (a) measurement of metabolically labeled TG (Fig. 3.4.1.*A* & Fig. 3.4.2.*A*) and of TG mass (Fig. 3.4.1.*A*), and (b) demonstration of a direct correlation between the attainment of lumenal TG and the MTP activity (Fig. 3.4.2.*B*). In principle, the steady state level of lumenal TG is determined by the rate of influx of TG through mobilization and the efflux via secretion. Since MTP inactivation inhibits TG secretion yet it does not inhibit TG synthesis, the decreased influx of TG is the most likely explanation for the diminished lumenal TG content. Thus, we propose that MTP is *the* protein factor that mobilizes TG into the microsomal lumen.

Although the origin of TG that is mobilized by MTP into the microsomal lumen was not determined in the current study, we speculate that the donor for MTP-mediated TG transfer is most likely the ER membrane. Regardless of whether TG is derived from *de novo* synthesis or from hydrolysis-reesterification of a storage pool (refer to Section 1.4.4), the ER membrane is the site where active TG synthesis takes place. Thus, the ER membrane is a dynamic TG donor, which continuously provides a supply of TG for MTP-mediated lipid transfer to the acceptor membrane, resulting in a net TG mass transport from the ER membrane to the microsomal lumen.

However, the ER membrane is not a TG storage pool. When the MTP-mediated TG mobilization is blocked by MTP inhibitor, we did not observe an increase in the TG mass or radiolabeled TG counts associated with the microsomal membrane. Instead, we observed a small (10%) but reproducible increase in cytosolic TG, the quantity of which was equivalent to the decrease in total microsomal TG (Fig. 3.4.1.*A*, Fig. 3.4.2.*A*). This is consistent with previous observations in liver-specific MTP-knockout mice (8) and MTP-inhibitor treated rabbit (230), where a large amount of TG accumulates in the cytosol with prolonged MTP inactivation. It is possible that an excessive amount of TG on the ER membrane, supposedly being mobilized by MTP into the microsomal lumen, is shunted to the cytosolic TG pool when MTP activity is inhibited. In that sense, MTP acts as a switch at the bifurcation of the intracellular TG partitioning between microsomal lumen and cytosol.

The current study also demonstrates that accumulation of lumenal TG may occur independently of VLDL assembly in McA-RH7777 cells (Fig. 3.4.3 *A&B*). These two uncoupled events can become manifest by treating cells with BfA. At a low dose of BfA, assembly of TG-rich VLDL is abolished, yet TG mobilization into microsomal lumen can still be observed. This suggests that TG may exist within the lumen even in the absence of VLDL assembly. Interestingly, observation of "TG particles" within the secretory compartments has been reported recently in mice enterocytes where apoB expression is abolished by genetic inactivation (203). Our data are in accord with this observation and provide indirect evidence that the MTP-mediated TG mobilization may lead to the formation of apoB-free "TG particles" (156). A point of note is that in mice in which hepatic MTP was inactivated by gene targeting, lipid droplets were completely absent within the secretory compartment (8). These *in vitro* and *in vivo* findings together argue strongly that accumulation of bulk TG within microsomes is associated with normal MTP activity, and apoB-free "TG particles" may act as the acceptor for MTP-mediated TG transfer in microsomes.

A major challenge ahead though is to characterize these "TG particles" biochemically and to demonstrate that they are indeed precursors for VLDL assembly. Identification of protein factors that associate with these "TG particles" will probably provide some clues. We speculate that exchangeable apolipoproteins, such as apoCIII, apoE, or apoAI, may be the candidate proteins associated with "TG particles". Secretion of VLDL-like particles containing apoE and/or apoAI, but essentially no apoB, from McA-RH7777 cells has been reported previously (79). Whether these VLDL-like

particles are derived from the apoB-free "TG particles" in the microsomal lumen remains to be tested. Interestingly, it has been shown that overexpression of apoCIII (240) or apoE (241) in transgenic mice stimulates VLDL production. It is possible that the major function of these exchangeable apolipoproteins is to stabilize "TG particles" prior to their incorporation into mature VLDL.

The core difficulty with all VLDL assembly models harks back to the old question concerning the path that is taken by bulk TG before eventually being incorporated into apoB. The current studies indicate that MTP may play a role in mobilizing TG into the microsomes. However, they did not address the question of whether MTP activity is required for incorporation of the microsomal TG into VLDL. It is clear that the demand for MTP is much greater for the assembly of TG-rich VLDL than for the assembly of a more dense particle. For instance, $VLDL_1$ assembly was abolished at 0.05 μM of BMS-197636, 4-times lower than the dose needed to abolish $VLDL_2$ assembly (Fig. 3.3.9.*A*). These results are nicely in accord with our observations that formation of B48-VLDL also exhibits higher demand for MTP activity than that of B48-HDL (Fig. 3.3.2 – Fig. 3.3.5). In addition, measurement of the residual MTP activity in BMS-197636-treated cells has shown a positive correlation between MTP activity and lumenal TG content in microsomes (Fig. 3.3.6.*A* & Fig. 3.4.2.*B*). These combined observations suggest the existence of a particular "threshold" MTP activity for the maintenance of sufficient lumenal TG, which is required for efficient assembly of TG-rich VLDL.

Lastly, a noteworthy but less conclusive result from this study is the role of the

BfA-sensitive factor in TG-rich VLDL assembly. In this study, we observed that the low dose of BfA does not affect TG accumulation in microsomal lumen, yet abolishes TG-rich VLDL assembly, suggesting that the BfA-sensitive factor may play an important role in the fusion of microsomal "TG-particles" into the apoB primordial particle to form mature VLDL. Interestingly, hepatocytes treated with BfA seem to be phenotypically similar to fatty-hepatocytes isolated from orotic acid-fed rats, in which apoE- or apoC-containing TG-rich lipoproteins, not mature VLDL, accumulate in the ER lumen ((220), refer to Section 1.4.8.). It is tempting to speculate that the BfA- and orotic acid-inhibited VLDL assembly is mediated through the same mechanism involving the suppression of a GTP-binding protein. More studies are required to identify the protein factor(s) that promote the incorporation of microsomal TG into mature VLDL.

4.5. The debate over the requirement of MTP for the post-translational VLDL assembly

The current study clearly demonstrates that the demand for MTP activity is much greater for the post-translational TG-rich VLDL assembly than for the primordial particle formation, regardless the assembly being B100-VLDL$_1$ or B48-VLDL. Our finding of the *in vivo* function of MTP was subsequently confirmed by studies with Caco2 cells (209) and with primary rat hepatocytes (242).

However, our conclusion(s) are not in accord with the conclusion of Gordon *et al.* (113), suggesting that MTP activity is not required for the second step of apoB48-VLDL assembly. In a recent report, the notion that MTP inhibition did not affect post-

translational B100-VLDL assembly was reinforced (161). In that study, McA-RH7777 cells cultured under basal condition (DMEM + 20% serum) were treated with high dose BfA to arrest B100-lipoprotein assembly at the HDL stage. By removing BfA from and supplementing oleate into the medium, secretion of B100-lipoproteins resumed. Inhibition of MTP at this stage decreased secretion of total B100 by 25%, but it did not block conversion of the B100-HDL into B100-VLDL ($d < 1.02$ g/ml) (161). Thus, it was concluded that the post-translational B100-VLDL assembly is achieved through a process insensitive to MTP inhibition. However, three caveats associated with these experiments are noteworthy and could potentially jeopardize the conclusion. First, the reported "B100-VLDL" whose assembly was insensitive to MTP inhibition is not B100-$VLDL_1$. It is apparent from the current work that under basal culture condition without exogenous oleate, only a low level of TG accumulates within the microsomal lumen and only B100-$VLDL_2$ and B100-IDL/LDL are produced (Fig. 3.2.2). Even in the presence of exogenous oleate, accumulation of TG within microsomal lumen (Fig. 3.4.1.*A* & Fig. 3.4.2.*A*) or assembly of B100-$VLDL_1$ (Fig. 3.3.10) does not occur if the activity of MTP is inhibited. Second, the report was unaware that the demand for MTP is determined by the amount of TG loaded into B100-lipoprotein. It is clear from the present study that assembly of small B100-lipoproteins is much more resistant to MTP inhibition than that of B100-$VLDL_1$. Since accumulation of TG within microsomal lumen is shown to be unaffected by BfA treatment (Fig. 3.4.3.*B*), conceivably the reported "B100-VLDL" formation after BfA removal could result from recruitment of residual microsomal TG into B100-IDL/LDL and B100-$VLDL_2$ particles. Third, conclusion that MTP inhibition has no effect on VLDL assembly was drawn solely on the basis of measuring B100 associated with

VLDL without considering the amount of TG incorporated. It is evident from the current study that B100-VLDL secreted from McA-RH7777 cells upon oleate treatment is heterogeneous, and that the majority of secreted TG is associated with a small portion of B100 (~25% of total) in the $VLDL_1$ fraction (Table II). Thus, the requirement of MTP activity for B100-$VLDL_1$ assembly would not be revealed unless the bulk TG incorporation is measured. For these reasons, caution must be exercised in concluding that MTP activity is not required for bulk lipid incorporation during B100-VLDL assembly.

4.6. Concluding remarks and future considerations

The major findings of this study are: (a) Human recombinant apoB100 and apoB48, like their rat counterparts, can assemble TG-rich VLDL in McA-RH7777 cells. The minimum length of apoB that is required to assemble TG-rich VLDL is apoB34. (b) Assembly of B100-$VLDL_1$ and B48-VLDL in McA-RH7777 cells is achieved through the same pathway. This is manifested by the fact that in both cases, assembly of VLDL is achieved post-translationally, is absolutely dependent upon oleate, and is a process marked by bulk TG incorporation into apoB. (c) The demand for MTP activity is much greater for the post-translational TG-rich VLDL assembly than for the primordial particle formation. (d) Mechanistically, MTP plays an important role in mobilizing TG into microsomal lumen, a process that is a prerequisite for VLDL maturation.

Hepatic VLDL assembly is a complicated process involving multiple protein and lipid factors. What we have learnt from the current study represents only a fraction of

what we would like to know about the assembly process. The questions remaining to be addressed include: What is the origin of TG utilized for VLDL assembly? What is the exact route by which bulk TG is incorporated into apoB within microsomes? Identification of additional protein factors that regulate TG mobilization and TG incorporation into mature VLDL will definitely help us to understand the VLDL maturation process. Nevertheless, the current study has shown that McA-RH7777 cells expressing human apoB proteins can serve as a useful cell model for future studies of assembly and secretion of TG-rich VLDL.

References

1. Havel, R. J. and J. P. Kane. 1995. Introduction: Structure and metabolism of plasma lipoproteins. In *The metabolic and molecular bases of inherited disease.* 7 ed. Edited by C. R. Scriver, A. L. Beaudet, W. S. Sly, and D. Valle. McGraw-Hill, New York. pp. 1841-1851.

2. Brown, M. S. and J. L. Goldstein. 1986. A receptor-mediated pathway for cholesterol homeostasis. *Science* **232**: 34-47.

3. Linton, M. F., R. V. Farese, Jr., and S. G. Young. 1993. Familial hypobetalipoproteinemia. *J. Lipid Res.* **34**: 521-541.

4. Kim, E. and S. G. Young. 1998. Genetically modified mice for the study of apolipoprotein B. *J. Lipid Res.* **39**: 703-723.

5. Wetterau, J. R., L. P. Aggerbeck, M.-E. Bouma, C. Eisenberg, A. Munck, M. Hermier, J. Schmitz, G. Gay, D. J. Rader, and R. E. Gregg. 1992. Absence of microsomal triglyceride transfer protein in individuals with abetalipoproteinemia. *Science* **258**: 999-1001.

6. Kane, J. P. and R. J. Havel. 1995. Disorders of the biogenesis and secretion of lipoproteins containing the B apolipoproteins. In *The metabolic and molecular bases of inherited disease.* 7 ed. Edited by C. R. Scriver, A. L. Beaudet, W. S. Sly, and D. Valle. McGraw-Hill, New York. pp. 1853-1885.

7. Chang, B. H., W. Liao, L. Li, M. Nakamuta, D. Mack, and L. Chan. 1999. Liver-specific inactivation of the abetalipoproteinemia gene completely abrogates very low density lipoprotein/low density lipoprotein production in a viable conditional knockout mouse. *J. Biol. Chem.* **274**: 6051-6055.

8. Raabe, M., M. M. Véniant, M. A. Sullivan, C. H. Zlot, J. Björkegren, L. B. Nielsen, J. S. Wong, R. L. Hamilton, and S. G. Young. 1999. Analysis of the role of microsomal triglyceride transfer protein in the liver of tissue-specific knockout mice. *J. Clin. Invest.* **103**: 1287-1298.

9. Elovson, J., J. E. Chatterton, G. T. Bell, V. N. Schumaker, Reuben, M.A., D. L. Puppione, J. R. Reeve, Jr., and N. L. Young. 1988. Plasma very low density lipoproteins contain a single molecule of apolipoprotein B. *J. Lipid Res.* **29**: 1461-1473.

10. Hussain, M. M., R. K. Kancha, Z. Zhou, J. Luchoomun, H. Zu, and A. Bakillah. 1996. Chylomicron assembly and catabolism: role of apolipoproteins and receptors. *Biochim. Biophys. Acta* **1300**: 151-170.

11. Powell, L. M., S. C. Wallis, R. J. Pease, Y. H. Edwards, T. J. Knott, and J. Scott. 1987. A novel form of tissue-specific RNA processing produces apolipoprotein-B48 in intestine. *Cell* **50**: 831-840.

12. Chen, S. H., G. Habib, C. Y. Yang, Z. W. Gu, B. R. Lee, S. A. Weng, S. R. Silberman, S. J. Cai, J. P. Deslypere, M. Rosseneu, A. M. Gotto, Jr., W. H. Li, and L. Chan. 1987. Apolipoprotein B-48 is the product of a messenger RNA with an organ- specific in-frame stop codon. *Science* **238**: 363-366.

13. Lusis, A. J., R. West, M. Mehrabian, M. A. Reuben, R. C. LeBoeuf, J. S. Kaptein, D. F. Johnson, V. N. Schumaker, M. P. Yuhasz, and M. C. Schotz. 1985. Cloning and expression of apolipoprotein B, the major protein of low and very low density lipoproteins. *Proc. Natl. Acad. Sci. U. S. A.* **82**: 4597-4601.

14. Knott, T. J., R. J. Pease, L. M. Powell, S. C. Wallis, S. C. Rall, Jr., T. L. Innerarity, B. Blackhart, W. H. Taylor, Y. Marcel, and R. Milne. 1986. Complete protein sequence and identification of structural domains of human apolipoprotein B. *Nature* **323**: 734-738.

15. Yang, C. Y., S. H. Chen, S. H. Gianturco, W. A. Bradley, J. T. Sparrow, M. Tanimura, W. H. Li, D. A. Sparrow, H. DeLoof, M. Rosseneu, F.-S. Lee, Z.-W. G. A. M. Gu, Jr., and L. Chan. 1986. Sequence, structure, receptor-binding domains and internal repeats of human apolipoprotein B-100. *Nature* **323**: 738-742.

16. Law, S. W., S. M. Grant, K. Higuchi, A. Hospattankar, K. Lackner, N. Lee, and H. B. Brewer, Jr. 1986. Human liver apolipoprotein B-100 cDNA: complete nucleic acid and derived amino acid sequence. *Proc. Natl. Acad. Sci. U. S. A.* **83**: 8142-8146.

17. Cladaras, C., M. Hadzopoulou-Cladaras, R.T. Nolte, D. Atkinson, and V. I. Zannis. 1986. The complete sequence and structural analysis of human apolipoprotein B-100: relationship between apoB-100 and apoB-48 forms. *EMBO J.* **5**: 3495-3507.

18. Yang, C. Y., Z. W. Gu, S. A. Weng, T. W. Kim, S. H. Chen, H. J. Pownall, P. M. Sharp, S. W. Liu, W. H. Li, A. M. Gotto, Jr., and L. Chan. 1989. Structure of apolipoprotein B-100 of human low density lipoproteins. *Arteriosclerosis* **9**: 96-108.

19. Struck, D. K., P. B. Siuta, M. D. Lane, and W. J. Lennarz. 1978. Effect of tunicamycin on the secretion of serum proteins by primary cultures of rat and chick hepatocytes. Studies on transferrin, very low density lipoprotein, and serum albumin. *J. Biol. Chem.* **253**: 5332-5337.

20. Vukmirica, J., T. Nishimaki-Mogami, R. S. McLeod, and Z. Yao. 1999. Functional analysis of the role of N-linked glycosylation of apoB in lipoprotein assembly and secretion. *Circulation* **100, Suppl.**, I-746 (Abstract)

21. Yang, C. Y., T. W. Kim, S. A. Weng, B. R. Lee, M. L. Yang, and A. M. Gotto, Jr. 1990. Isolation and characterization of sulfhydryl and disulfide peptides of human apolipoprotein B-100. *Proc. Natl. Acad. Sci. U. S. A.* **87**: 5523-5527.

22. Huang, X. F. and G. S. Shelness. 1997. Identification of cysteine pairs within the amino-terminal 5% of apolipoprotein B essential for hepatic lipoprotein assembly and secretion. *J. Biol. Chem.* **272**: 31872-31876.

23. Tran, K., J. Borén, J. Macri, Y. Wang, R. McLeod, Avramoglu, RK, K. Adeli, and Z. Yao. 1998. Functional analysis of disulfide linkages clustered within the amino terminus of human apolipoprotein B. *J. Biol. Chem.* **273**: 7244-7251.

24. Mahley, R. W. 1988. Apolipoprotein E: cholesterol transport protein with expanding role in cell biology. *Science* **240**: 622-630.

25. Law, A. and J. Scott. 1990. A cross-species comparison of the apolipoprotein B domain that binds to the LDL receptor. *J. Lipid Res.* **31**: 1109-1120.

26. Chan, L. 1992. Apolipoprotein B, the major protein component of triglyceride-rich and low density lipoproteins. *J. Biol. Chem.* **267**: 25621-25624.

27. Segrest, J. P., M. K. Jones, V. K. Mishra, G. M. Anantharamaiah, and D. W. Garber. 1994. ApoB-100 has a pentapartite structure composed of three amphipathic alpha-helical domains alternating with two amphipathic beta-strand domains. Detection by the computer program LOCATE. *Arterioscler Thromb.* **14**: 1674-1685.

28. Segrest, J. P., M. K. Jones, V. K. Mishra, V. Pierotti, S. H. Young, J. Borén, T. L. Innerarity, and N. Dashti. 1998. Apolipoprotein B-100: conservation of lipid-associating amphipathic secondary structural motifs in nine species of vertebrates. *J. Lipid Res.* **39**: 85-102.

29. Chauhan, V., X. Wang, T. Ramsamy, R. W. Milne, and D. L. Sparks. 1998. Evidence for lipid-dependent structural changes in specific domains of apolipoprotein B100. *Biochemistry* **37**: 3735-3742.

30. Chatterton, J. E., M. L. Phillips, L. K. Curtiss, R. W. Milne, Y. L. Marcel, and V. N. Schumaker. 1991. Mapping apolipoprotein B on the low density lipoprotein surface by immunoelectron microscopy. *J. Biol. Chem.* **266**: 5955-5962.

31. Chatterton, J. E., M. L. Phillips, L. K. Curtiss, R. Milne, J. C. Fruchart, and V. N. Schumaker. 1995. Immunoelectron microscopy of low density lipoproteins yields a ribbon and bow model for the conformation of apolipoprotein B on the lipoprotein surface. *J. Lipid Res.* **36**: 2027-2037.

32. Wetterau, J. R. and D. B. Zilversmit. 1984. A triglyceride and cholesteryl ester transfer protein associated with liver microsomes. *J. Biol. Chem.* **259**: 10863-10866.

33. Wetterau, J. R. and D. B. Zilversmit. 1986. Localization of intracellular triacylglycerol and cholesteryl ester transfer activity in rat tissues. *Biochim. Biophys. Acta* **875**: 610-617.

34. Wetterau, J. R. and D. B. Zilversmit. 1985. Purification and characterization of microsomal triglyceride and cholesteryl ester transfer protein from bovine liver microsomes. *Chemistry & Physics of Lipids* **38**: 205-222.

35. Wetterau, J. R., K. A. Combs, S. N. Spinner, and B. J. Joiner. 1990. Protein disulfide isomerase is a component of the microsomal triglyceride transfer protein complex. *J. Biol. Chem.* **265**: 9801-9807.

36. Freedman, R. B., T. R. Hirst, and M. F. Tuite. 1994. Protein disulphide isomerase: building bridges in protein folding. *Trends Biochem. Sci.* **19**: 331-336.

37. Lamberg, A., M. Jauhiainen, J. Metso, C. Ehnholm, C. C. Shoulders, J. Scott, T. Pihlajaniemi, and K. I. Kivirikko. 1996. The role of protein disulphide isomerase in the microsomal triacylglycerol transfer protein does not reside in its isomerase activity. *Biochem. J.* **315**: 533-536.

38. Ricci, B., D. Sharp, E. O'Rourke, B. Kienzle, L. Blinderman, D. Gordon, C. Smith-Monroy, G. Robinson, R. E. Gregg, and D. J. Rader. 1995. A 30-amino acid truncation of the microsomal triglyceride transfer protein large subunit disrupts its interaction with protein disulfide-isomerase and causes abetalipoproteinemia. *J. Biol. Chem.* **270**: 14281-14285.

39. Pihlajaniemi, T., T. Helaakoski, K. Tasanen, R. Myllyla, M. L. Huhtala, J. Koivu, and K. I. Kivirikko. 1987. Molecular cloning of the beta-subunit of human prolyl 4-hydroxylase. This subunit and protein disulphide isomerase are products of the same gene. *EMBO J.* **6**: 643-649.

40. Pelham, H. R. 1995. Sorting and retrieval between the endoplasmic reticulum and Golgi apparatus. *Curr. Opin. Cell Biol.* **7**: 530-535.

41. Sharp, D., L. Blinderman, K. A. Combs, B. Kienzle, B. Ricci, K. Wager-Smith, C. M. Gil, C. W. Turck, M. E. Bouma, D. J. Rader, L. P. Aggerbeck, R. E. Gregg, D. A. Gordon, and J. R. Wetterau. 1993. Cloning and gene defects in microsomal triglyceride transfer protein associated with abetalipoproteinaemia. *Nature* **365**: 65-69.

42. Atzel, A. and J. R. Wetterau. 1993. Mechanism of microsomal triglyceride transfer protein catalyzed lipid transport. *Biochemistry* **32**: 10444-10450.

43. Jamil, H., J. K. Dickson, Jr., C.-H. Chu, M. W. Lago, J. K. Rinehart, S. A. Biller, Gregg, RE, and J. R. Wetterau. 1995. Microsomal triglyceride transfer protein. Specificity of lipid binding and transport. *J. Biol. Chem.* **270**: 6549-6554.

44. Baker, M. E. 1988. Is vitellogenin an ancestor of apolipoprotein B-100 of human low-density lipoprotein and human lipoprotein lipase? *Biochem. J.* **255**: 1057-1060.

45. Shoulders, C. C., T. M. Narcisi, J. Read, A. Chester, D. J. Brett, J. Scott, T. A. Anderson, D. G. Levitt, and L. J. Banaszak. 1994. The abetalipoproteinemia gene is a member of the vitellogenin family and encodes an alpha-helical domain. *Nat. Struct. Biol.* **1**: 285-286.

46. Mann, C. J., T. A. Anderson, J. Read, S. A. Chester, G. B. Harrison, S. Kochl, Ritchie, P.J., P. Bradbury, F. S. Hussain, J. Amey, B. Vanloo, M. Rosseneu, R. Infante, J. M. Hancock, D. G. Levitt, L. J. Banaszak, J. Scott, and C. C. Shoulders. 1999. The structure of vitellogenin provides a molecular model for the assembly and secretion of atherogenic lipoproteins. *J. Mol. Biol.* **285**: 391-408.

47. Segrest, J. P., M. K. Jones, and N. Dashti. 1999. N-terminal domain of apolipoprotein B has structural homology to lipovitellin and microsomal triglyceride transfer protein. A "lipid pocket" model for self-assembly of apob-containing lipoprotein particles. *J. Lipid Res.* **40**: 1401-1416.

48. Brown, M. S., J. Herz, and J. L. Goldstein. 1997. LDL-receptor structure. Calcium cages, acid baths and recycling receptors. *Nature* **388**: 629-630.

49. Byrne, B. M., M. Gruber, and G. Ab. 1989. The evolution of egg yolk proteins. *Prog. Biophys. Mol. Biol.* **53**: 33-69.

50. Bujo, H., M. Hermann, K. A. Lindstedt, J. Nimpf, and W. J. Schneider. 1997. Low density lipoprotein receptor gene family members mediate yolk deposition. *J. Nutr.* **127**: 801S-804S.

51. Raag, R., K. Appelt, N. H. Xuong, and L. Banaszak. 1988. Structure of the lamprey yolk lipid-protein complex lipovitellin- phosvitin at 2.8 A resolution. *J. Mol. Biol.* **200**: 553-569.

52. Banaszak, L., W. Sharrock, and P. Timmins. 1991. Structure and function of a lipoprotein: lipovitellin. *Annu. Rev. Biophys. Biophys. Chem.* **20**: 221-246.

53. Timmins, P. A., B. Poliks, and L. Banaszak. 1992. The location of bound lipid in the lipovitellin complex. *Science* **257**: 652-655.

54. Anderson, T. A., D. G. Levitt, and L. J. Banaszak. 1998. The structural basis of lipid interactions in lipovitellin, a soluble lipoprotein. *Structure.* **6**: 895-909.

55. Rehberg, E. F., M. E. Samson-Bouma, B. Kienzle, L. Blinderman, H. Jamil, J. R. Wetterau, L. P. Aggerbeck, and D. A. Gordon. 1996. A novel abetalipoproteinemia genotype. Identification of a missense mutation in the 97-kDa subunit of the microsomal triglyceride transfer protein that prevents complex formation with protein disulfide isomerase. *J. Biol. Chem.* **271**: 29945-29952.

56. Wu, X., M. Zhou, L.-S. Huang, J. Wetterau, and H. N. Ginsberg. 1996. Demonstration of a physical interaction between microsomal triglyceride transfer protein and apolipoprotein B during the assembly of ApoB-containing lipoproteins. *J. Biol. Chem.* **271**: 10277-10281.

57. Linnik, K. M. and H. Herscovitz. 1998. Multiple molecular chaperones interact with apolipoprotein B during its maturation. The network of endoplasmic reticulum-resident chaperones (ERp72, GRP94, calreticulin, and BiP) interacts with apolipoprotein b regardless of its lipidation state. *J. Biol. Chem.* **273**: 21368-21373.

58. Hussain, M. M., A. Bakillah, and H. Jamil. 1997. Apolipoprotein B binding to microsomal triglyceride transfer protein decreases with increases in length and lipidation: implications in lipoprotein biosynthesis. *Biochemistry* **36**: 13060-13067.

59. Bakillah, A., H. Jamil, and M. M. Hussain. 1998. Lysine and arginine residues in the N-terminal 18% of apolipoprotein B are critical for its binding to microsomal triglyceride transfer protein. *Biochemistry* **37**: 3727-3734.

60. Hussain, M. M., A. Bakillah, N. Nayak, and G. S. Shelness. 1998. Amino acids 430-570 in apolipoprotein B are critical for its binding to microsomal triglyceride transfer protein. *J. Biol. Chem.* **273**: 25612-25615.

61. Bradbury, P., C. J. Mann, S. Kochl, T. A. Anderson, S. A. Chester, J. M. Hancock, P. J. Ritchie, J. Amey, G. B. Harrison, D. G. Levitt, L. J. Banaszak, J. Scott, and C. C. Shoulders. 1999. A common binding site on the microsomal triglyceride transfer protein for apolipoprotein B and protein disulfide isomerase. *J. Biol. Chem.* **274**: 3159-3164.

62. Nicodeme, E., F. Benoist, R. McLeod, Z. Yao, J. Scott, C. C. Shoulders, and T. Grand-Perret. 1999. Identification of domains in apolipoprotein B100 that confer a high requirement for the microsomal triglyceride transfer protein. *J. Biol. Chem.* **274**: 1986-1993.

63. Boström, K., J. Borén, M. Wettesten, A. Sjoberg, G. Bondjers, O. Wiklund, P. Carlsson, and S.-O. Olofsson. 1988. Studies on the assembly of apo B-100-containing lipoproteins in HepG2 cells. *J. Biol. Chem.* **263**: 4434-4442.

64. Pullinger, C. R., J. D. North, B. B. Teng, V. A. Rifici, A. E. Ronhild de Brito, and J. Scott. 1989. The apolipoprotein B gene is constitutively expressed in HepG2 cells: regulation of secretion by oleic acid, albumin, and insulin, and measurement of the mRNA half-life. *J. Lipid Res.* **30**: 1065-1077.

65. Dashti, N., D. L. Williams, and P. Alaupovic. 1989. Effects of oleate and insulin on the production rates and cellular mRNA concentrations of apolipoproteins in HepG2 cells. *J. Lipid Res.* **30**: 1365-1373.

66. Davis, R. A. 1993. The endoplasmic reticulum is the site of lipoprotein assembly and regulation of secretion. *Sub-Cellular Biochemistry* **21**: 169-187.

67. Bonnardel, J. A. and R. A. Davis. 1995. In HepG2 cells, translocation, not degradation, determines the fate of the de novo synthesized apolipoprotein B. *J. Biol. Chem.* **270**: 28892-28896.

68. Pilon, M. and R. Schekman. 1999. Protein translocation: how Hsp70 pulls it off. *Cell* **97**: 679-682.

69. Corsi, A. K. and R. Schekman. 1996. Mechanism of polypeptide translocation into the endoplasmic reticulum. *J. Biol. Chem.* **271**: 30299-30302.

70. Boström, K., M. Wettesten, J. Borén, G. Bondjers, O. Wiklund, and S.-O. Olofsson. 1986. Pulse-chase studies of the synthesis and intracellular transport of apolipoprotein B-100 in Hep G2 cells. *J. Biol. Chem.* **261**: 13800-13806.

71. Borén, J., M. Wettesten, A. Sjoberg, T. Thorlin, G. Bondjers, O. Wiklund, and S.-O. Olofsson. 1990. The assembly and secretion of apoB 100 containing lipoproteins in Hep G2 cells. Evidence for different sites for protein synthesis and lipoprotein assembly. *J. Biol. Chem.* **265**: 10556-10564.

72. Bamberger, M. J. and M. D. Lane. 1990. Possible role of the Golgi apparatus in the assembly of very low density lipoprotein. *Proc. Natl. Acad. Sci. U. S. A.* **87**: 2390-2394.

73. Davis, R. A., R. N. Thrift, C. C. Wu, and K. E. Howell. 1990. Apolipoprotein B is both integrated into and translocated across the endoplasmic reticulum membrane. Evidence for two functionally distinct pools. *J. Biol. Chem.* **265**: 10005-10011.

74. Davis, R. A., S. M. Dluz, J. K. Leighton, and V. A. Brengaze. 1989. Increased translatable mRNA and decreased lipogenesis are responsible for the augmented secretion of lipid-deficient apolipoprotein E by hepatocytes from fasted rats. *J. Biol. Chem.* **264**: 8970-8977.

75. Davis, R. A., A. B. Prewett, D. C. Chan, J. J. Thompson, Borchardt, RA, and W. R. Gallaher. 1989. Intrahepatic assembly of very low density lipoproteins: immunologic characterization of apolipoprotein B in lipoproteins and hepatic membrane fractions and its intracellular distribution. *J. Lipid Res.* **30**: 1185-1196.

76. Dixon, J. L., R. Chattapadhyay, T. Huima, C. M. Redman, and Banerjee. 1992. Biosynthesis of lipoprotein: location of nascent apoAI and apoB in the rough endoplasmic reticulum of chicken hepatocytes. *J. Cell Biol.* **117**: 1161-1169.

77. Wilkinson, J., J. A. Higgins, P. H. Groot, E. Gherardi, and D. E. Bowyer. 1992. Membrane-bound apolipoprotein B is exposed at the cytosolic surface of liver microsomes. *FEBS Lett.* **304**: 24-26.

78. Wilkinson, J., J. A. Higgins, P. Groot, E. Gherardi, and D. Bowyer. 1993. Topography of apolipoprotein B in subcellular fractions of rabbit liver probed with a panel of monoclonal antibodies. *J. Lipid Res.* **34**: 815-825.

79. McLeod, R. S., Y. Wang, S. Wang, A. Rusiñol, P. Links, and Z. Yao. 1996. Apolipoprotein B sequence requirements for hepatic very low density lipoprotein assembly. Evidence that hydrophobic sequences within apolipoprotein B48 mediate lipid recruitment. *J. Biol. Chem.* **271**: 18445-18455.

80. Zhou, M., X. Wu, L. S. Huang, and H. N. Ginsberg. 1995. Apoprotein B100, an inefficiently translocated secretory protein, is bound to the cytosolic chaperone, heat shock protein 70. *J. Biol. Chem.* **270**: 25220-25224.

81. Shelness, G. S., K. C. Morris-Rogers, and M. F. Ingram. 1994. Apolipoprotein B48-membrane interactions. Absence of transmembrane localization in nonhepatic cells. *J. Biol. Chem.* **269**: 9310-9318.

82. Ingram, M. F. and G. S. Shelness. 1996. Apolipoprotein B-100 destined for lipoprotein assembly and intracellular degradation undergoes efficient translocation across the endoplasmic reticulum membrane. *J. Lipid Res.* **37**: 2202-2214.

83. Leiper, J. M., G. B. Harrison, J. Bayliss, J. D. Scott, and R. J. Pease. 1996. Systematic expression of the complete coding sequence of apoB-100 does not reveal transmembrane determinants. *J. Lipid Res.* **37**: 2215-2231.

84. Sass, H. J., G. Buldt, E. Beckmann, F. Zemlin, M. van Heel, E. Zeitler, J. P. Rosenbusch, D. L. Dorset, and A. Massalski. 1989. Densely packed beta-structure at the protein-lipid interface of porin is revealed by high-resolution cryo-electron microscopy. *J. Mol. Biol.* **209**: 171-175.

85. Small, D. M. and D. Atkinson. 1997. The first beta sheet region of apoB (apoB21-41) is an amphipathic ribbon 50-60Å wide and 200Å long, which initiates triglyceride binding and assembly of nascent lipoproteins. *Circulation* **96, Suppl.**, 1-I (Abstract)

86. Liang, J., X. Wu, H. Jiang, M. Zhou, H. Yang, P. Angkeow, L. S. Huang, S. L. Sturley, and H. Ginsberg. 1998. Translocation efficiency, susceptibility to proteasomal degradation, and lipid responsiveness of apolipoprotein B are determined by the presence of beta sheet domains. *J. Biol. Chem.* **273**: 35216-35221.

87. Cavallo, D., R. S. McLeod, D. Rudy, A. Aiton, Z. Yao, and K. Adeli. 1998. Intracellular translocation and stability of apolipoprotein B are inversely proportional to the length of the nascent polypeptide. *J. Biol. Chem.* **273**: 33397-33405.

88. Sturley, S. L., P. J. Talmud, R. Brasseur, M. R. Culbertson, S. E. Humphries, and A. D. Attie. 1994. Human apolipoprotein B signal sequence variants confer a secretion-defective phenotype when expressed in yeast. *J. Biol. Chem.* **269**: 21670-21675.

89. Görlich, D. and T. A. Rapoport. 1993. Protein translocation into proteoliposomes reconstituted from purified components of the endoplasmic reticulum membrane. *Cell* **75**: 615-630.

90. Görlich, D., E. Hartmann, S. Prehn, and T. A. Rapoport. 1992. A protein of the endoplasmic reticulum involved early in polypeptide translocation. *Nature* **357**: 47-52.

91. Görlich, D., S. Prehn, E. Hartmann, K. U. Kalies, and T. A. Rapoport. 1992. A mammalian homolog of SEC61p and SECYp is associated with ribosomes and nascent polypeptides during translocation. *Cell* **71**: 489-503.

92. Hanein, D., K. E. Matlack, B. Jungnickel, K. Plath, K. U. Kalies, K. R. Miller, T. A. Rapoport, and C. W. Akey. 1996. Oligomeric rings of the Sec61p complex induced by ligands required for protein translocation. *Cell* **87**: 721-732.

93. Beckmann, R., D. Bubeck, R. Grassucci, P. Penczek, A. Verschoor, G. Blobel, and J. Frank. 1997. Alignment of conduits for the nascent polypeptide chain in the ribosome- Sec61 complex. *Science* **278**: 2123-2126.

94. Hamman, B. D., L. M. Hendershot, and A. E. Johnson. 1998. BiP maintains the permeability barrier of the ER membrane by sealing the lumenal end of the translocon pore before and early in translocation. *Cell* **92**: 747-758.

95. Chuck, S. L., Z. Yao, B. D. Blackhart, B. J. McCarthy, and V. R. Lingappa. 1990. New variation on the translocation of proteins during early biogenesis of apolipoprotein B. *Nature* **346**: 382-385.

96. Chuck, S. L. and V. R. Lingappa. 1992. Pause transfer: a topogenic sequence in apolipoprotein B mediates stopping and restarting of translocation. *Cell* **68**: 9-21.

97. Chuck, S. L. and V. R. Lingappa. 1993. Analysis of a pause transfer sequence from apolipoprotein B. *J. Biol. Chem.* **268**: 22794-22801.

98. Kivlen, M. H., C. A. Dorsey, V. R. Lingappa, and R. S. Hegde. 1997. Asymmetric distribution of pause transfer sequences in apolipoprotein B-100. *J. Lipid Res.* **38**: 1149-1162.

99. Pease, R. J., G. B. Harrison, and J. Scott. 1991. Cotranslocational insertion of apolipoprotein B into the inner leaflet of the endoplasmic reticulum. *Nature* **353**: 448-450.

100. Pease, R. J., J. M. Leiper, G. B. Harrison, and J. Scott. 1995. Studies on the translocation of the amino terminus of apolipoprotein B into the endoplasmic reticulum. *J. Biol. Chem.* **270**: 7261-7271.

101. Hegde, R. S. and V. R. Lingappa. 1996. Sequence-specific alteration of the ribosome-membrane junction exposes nascent secretory proteins to the cytosol. *Cell* **85**: 217-228.

102. Hegde, R. S., S. Voigt, T. A. Rapoport, and V. R. Lingappa. 1998. TRAM regulates the exposure of nascent secretory proteins to the cytosol during translocation into the endoplasmic reticulum. *Cell* **92**: 621-631.

103. Ginsberg, H. N. 1995. Synthesis and secretion of apolipoprotein B from cultured liver cells. *Curr. Opin. Lipidol.* **6**: 275-280.

104. Thrift, R. N., J. Drisko, S. Dueland, J. D. Trawick, and R. A. Davis. 1992. Translocation of apolipoprotein B across the endoplasmic reticulum is blocked in a nonhepatic cell line. *Proc. Natl. Acad. Sci. U. S. A.* **89**: 9161-9165.

105. Du, E. Z., J. Kurth, S. L. Wang, P. Humiston, and R. A. Davis. 1994. Proteolysis-coupled secretion of the N terminus of apolipoprotein B. Characterization of a transient, translocation arrested intermediate. *J. Biol. Chem.* **269**: 24169-24176.

106. Du, E. Z., S. L. Wang, H. J. Kayden, R. Sokol, L. K. Curtiss, and R. A. Davis. 1996. Translocation of apolipoprotein B across the endoplasmic reticulum is blocked in abetalipoproteinemia. *J. Lipid Res.* **37**: 1309-1315.

107. Fleming, J. F., G. M. Spitsen, T. Y. Hui, L. Olivier, E. Z. Du, M. Raabe, and R. A. Davis. 1999. Chinese hamster ovary cells require the coexpression of microsomal triglyceride transfer protein and cholesterol 7alpha-hydroxylase for the assembly and secretion of apolipoprotein B-containing lipoproteins. *J. Biol. Chem.* **274** : 9509-9514.

108. Wang, S., R. S. McLeod, D. A. Gordon, and Z. Yao. 1996. The microsomal triglyceride transfer protein facilitates assembly and secretion of apolipoprotein B-containing lipoproteins and decreases cotranslational degradation of apolipoprotein B in transfected COS-7 cells. *J. Biol. Chem.* **271**: 14124-14133.

109. Patel, S. B. and S. M. Grundy. 1996. Interactions between microsomal triglyceride transfer protein and apolipoprotein B within the endoplasmic reticulum in a heterologous expression system. *J. Biol. Chem.* **271**: 18686-18694.

110. Leiper, J. M., J. D. Bayliss, R. J. Pease, D. J. Brett, J. Scott, and C. C. Shoulders. 1994. Microsomal triglyceride transfer protein, the abetalipoproteinemia gene product, mediates the secretion of apolipoprotein B-containing lipoproteins from heterologous cells. *J. Biol. Chem.* **269**: 21951-21954.

111. Gordon, D. A., H. Jamil, D. Sharp, D. Mullaney, Z. Yao, R. E. Gregg, and J. Wetterau. 1994. Secretion of apolipoprotein B-containing lipoproteins from HeLa cells is dependent on expression of the microsomal triglyceride transfer protein and is regulated by lipid availability. *Proc. Natl. Acad. Sci. U. S. A.* **91**: 7628-7632.

112. Jamil, H., D. A. Gordon, D. C. Eustice, C. M. Brooks, J. K. Dickson, Jr., Y. Chen, B. Ricci, C.-H. Chu, T. W. Harrity, C. P. Ciosek, Jr., S. A. Biller, R. E. Gregg, and J. R. Wetterau. 1996. An inhibitor of the microsomal triglyceride transfer protein inhibits apoB secretion from HepG2 cells. *Proc. Natl. Acad. Sci. U. S. A.* **93**: 11991-11995.

113. Gordon, D. A., H. Jamil, R. E. Gregg, S.-O. Olofsson, and J. Borén. 1996. Inhibition of the microsomal triglyceride transfer protein blocks the first step of apolipoprotein B lipoprotein assembly but not the addition of bulk core lipids in the second step. *J. Biol. Chem.* **271**: 33047-33053.

114. Mitchell, D. M., M. Zhou, R. Pariyarath, H. Wang, J. D. Aitchison, H. N. Ginsberg, and E. A. Fisher. 1998. Apoprotein B100 has a prolonged interaction with the translocon during which its lipidation and translocation change from dependence on the microsomal triglyceride transfer protein to independence. *Proc. Natl. Acad. Sci. U. S. A.* **95**: 14733-14738.

115. Gordon, D. A., J. R. Wetterau, and R. E. Gregg. 1995. Microsomal triglyceride transfer protein: a protein required for the assembly of lipoprotein particles. *Trends in Cell Biol.* **5**: 317-321.

116. Herscovitz, H., A. Kritis, I. Talianidis, E. Zanni, V. Zannis, and D. M. Small. 1995. Murine mammary-derived cells secrete the N-terminal 41% of human apolipoprotein B on high density lipoprotein-sized lipoproteins containing a triacylglycerol-rich core. *Proc. Natl. Acad. Sci. U. S. A.* **92**: 659-663.

117. Rusiñol, A. E., H. Jamil, and J. E. Vance. 1997. In vitro reconstitution of assembly of apolipoprotein B48-containing lipoproteins. *J. Biol. Chem.* **272**: 8019-8025.

118. Yao, Z. and D. E. Vance. 1989. Head group specificity in the requirement of phosphatidylcholine biosynthesis for very low density lipoprotein secretion from cultured hepatocytes. *J. Biol. Chem.* **264**: 11373-11380.

119. Vance, J. E. 1991. Secretion of VLDL, but not HDL, by rat hepatocytes is inhibited by the ethanolamine analogue N-monomethylethanolamine. *J. Lipid Res.* **32**: 1971-1982.

120. Rusiñol, A. E., E. Y. Chan, and J. E. Vance. 1993. Movement of apolipoprotein B into the lumen of microsomes from hepatocytes is disrupted in membranes enriched in phosphatidylmonomethylethanolamine. *J. Biol. Chem.* **268**: 25168-25175.

121. Rusiñol, A. E. and J. E. Vance. 1995. Inhibition of secretion of truncated apolipoproteins B by monomethylethanolamine is independent of the length of the apolipoprotein. *J. Biol. Chem.* **270**: 13318-13325.

122. Rusiñol, A. E., R. S. Hegde, S. L. Chuck, V. R. Lingappa, and J. E. Vance. 1998. Translocational pausing of apolipoprotein B can be regulated by membrane lipid composition. *J. Lipid Res.* **39**: 1287-1294.

123. Borén, J., L. Graham, M. Wettesten, J. Scott, A. White, and S.-O. Olofsson. 1992. The assembly and secretion of ApoB 100-containing lipoproteins in Hep G2 cells. ApoB 100 is cotranslationally integrated into lipoproteins. *J. Biol. Chem.* **267** : 9858-9867.

124. Spring, D. J., L. W. Chen-Liu, J. E. Chatterton, J. Elovson, and V. N. Schumaker. 1992. Lipoprotein assembly. Apolipoprotein B size determines lipoprotein core circumference. *J. Biol. Chem.* **267**: 14839-14845.

125. Borén, J., S. Rustaeus, and S.-O. Olofsson. 1994. Studies on the assembly of apolipoprotein B-100- and B-48-containing very low density lipoproteins in McA-RH7777 cells. *J. Biol. Chem.* **269**: 25879-25888.

126. Benoist, F. and T. Grand-Perret. 1997. Co-translational degradation of apolipoprotein B100 by the proteasome is prevented by microsomal triglyceride transfer protein. Synchronized translation studies on HepG2 cells treated with an inhibitor of microsomal triglyceride transfer protein. *J. Biol. Chem.* **272**: 20435-20442.

127. Graham, D. L., T. J. Knott, T. C. Jones, R. J. Pease, C. R. Pullinger, and J. Scott. 1991. Carboxyl-terminal truncation of apolipoprotein B results in gradual loss of the ability to form buoyant lipoproteins in cultured human and rat liver cell lines. *Biochemistry* **30**: 5616-5621.

128. Yao, Z., B. D. Blackhart, M. F. Linton, S. M. Taylor, S. G. Young, and B. J. McCarthy. 1991. Expression of carboxyl-terminally truncated forms of human apolipoprotein B in rat hepatoma cells. Evidence that the length of apolipoprotein B has a major effect on the buoyant density of the secreted lipoproteins. *J. Biol. Chem.* **266**: 3300-3308.

129. McLeod, R. S., Y. Zhao, S. L. Selby, J. Westerlund, and Z. Yao. 1994. Carboxyl-terminal truncation impairs lipid recruitment by apolipoprotein B100 but does not affect secretion of the truncated apolipoprotein B-containing lipoproteins. *J. Biol. Chem.* **269**: 2852-2862.

130. Borén, J., M. Wettesten, S. Rustaeus, M. Andersson, and S.-O. Olofsson. 1993. The assembly and secretion of apoB-100-containing lipoproteins. *Biochem. Soc. Trans.* **21**: 487-493.

131. Gretch, D. G., S. L. Sturley, L. Wang, B. A. Lipton, A. Dunning, K. A. A. Grunwald, J. R. Wetterau, Z. Yao, P. Talmud, and A. D. Attie. 1996. The amino terminus of apolipoprotein B is necessary but not sufficient for microsomal triglyceride transfer protein responsiveness. *J. Biol. Chem.* **271**: 8682-8691.

132. Herscovitz, H., M. Hadzopoulou-Cladaras, M. T. Walsh, Cladaras, V. I. Zannis, and D. M. Small. 1991. Expression, secretion, and lipid-binding characterization of the N-terminal 17% of apolipoprotein B. *Proc. Natl. Acad. Sci. U. S. A.* **88**: 7313-7317.

133. Shelness, G. S. and J. T. Thornburg. 1996. Role of intramolecular disulfide bond formation in the assembly and secretion of apolipoprotein B-100-containing lipoproteins. *J. Lipid Res.* **37**: 408-419.

134. Borchardt, R. A. and R. A. Davis. 1987. Intrahepatic assembly of very low density lipoproteins. Rate of transport out of the endoplasmic reticulum determines rate of secretion. *J. Biol. Chem.* **262**: 16394-16402.

135. Furukawa, S., N. Sakata, H. N. Ginsberg, and J. L. Dixon. 1992. Studies of the sites of intracellular degradation of apolipoprotein B in Hep G2 cells. *J. Biol. Chem.* **267**: 22630-22638.

136. Sato, R., T. Imanaka, A. Takatsuki, and T. Takano. 1990. Degradation of newly synthesized apolipoprotein B-100 in a pre-Golgi compartment. *J. Biol. Chem.* **265**: 11880-11884.

137. Yeung, S. J., S. H. Chen, and L. Chan. 1996. Ubiquitin-proteasome pathway mediates intracellular degradation of apolipoprotein B. *Biochemistry* **35**: 13843-13848.

138. Fisher, E. A., M. Zhou, D. M. Mitchell, X. Wu, S. Omura, H. Wang, A. L. Goldberg, and H. N. Ginsberg. 1997. The degradation of apolipoprotein B100 is mediated by the ubiquitin-proteasome pathway and involves heat shock protein 70. *J. Biol. Chem.* **272**: 20427-20434.

139. Chen, Y., F. Le Caherec, and S. L. Chuck. 1998. Calnexin and other factors that alter translocation affect the rapid binding of ubiquitin to apoB in the Sec61 complex. *J. Biol. Chem.* **273**: 11887-11894.

140. Liao, W., S. C. Yeung, and L. Chan. 1998. Proteasome-mediated degradation of apolipoprotein B targets both nascent peptides cotranslationally before translocation and full-length apolipoprotein B after translocation into the endoplasmic reticulum. *J. Biol. Chem.* **273**: 27225-27230.

141. Coux, O., K. Tanaka, and A. L. Goldberg. 1996. Structure and functions of the 20S and 26S proteasomes. *Annu. Rev. Biochem.* **65**: 801-847.

142. Omura, S., T. Fujimoto, K. Otoguro, K. Matsuzaki, R. Moriguchi, H. Tanaka, and Y. Sasaki. 1991. Lactacystin, a novel microbial metabolite, induces neuritogenesis of neuroblastoma cells. *J. Antibiot. (Tokyo)* **44**: 113-116.

143. Rock, K. L., C. Gramm, L. Rothstein, K. Clark, R. Stein, L. Dick, D. Hwang, and A. L. Goldberg. 1994. Inhibitors of the proteasome block the degradation of most cell proteins and the generation of peptides presented on MHC class I molecules. *Cell* **78**: 761-771.

144. Cavallo, D., D. Rudy, A. Mohammadi, J. Macri, and K. Adeli. 1999. Studies on degradative mechanisms mediating post-translational fragmentation of

apolipoprotein B and the generation of the 70-kDa fragment. *J. Biol. Chem.* **274**: 23135-23143.

145. Zhou, M., E. A. Fisher, and H. N. Ginsberg. 1998. Regulated Co-translational ubiquitination of apolipoprotein B100. A new paradigm for proteasomal degradation of a secretory protein. *J. Biol. Chem.* **273**: 24649-24653.

146. Adeli, K., J. Macri, A. Mohammadi, M. Kito, R. Urade, and Cavallo. 1997. Apolipoprotein B is intracellularly associated with an ER-60 protease homologue in HepG2 cells. *J. Biol. Chem.* **272**: 22489-22494.

147. Moberly, J. B., T. G. Cole, D. H. Alpers, and G. Schonfeld. 1990. Oleic acid stimulation of apolipoprotein B secretion from HepG2 and Caco-2 cells occurs post-transcriptionally. *Biochim. Biophys. Acta* **1042**: 70-80.

148. Dixon, J. L., S. Furukawa, and H. N. Ginsberg. 1991. Oleate stimulates secretion of apolipoprotein B-containing lipoproteins from Hep G2 cells by inhibiting early intracellular degradation of apolipoprotein B. *J. Biol. Chem.* **266**: 5080-5086.

149. Sakata, N., X. Wu, J. L. Dixon, and H. N. Ginsberg. 1993. Proteolysis and lipid-facilitated translocation are distinct but competitive processes that regulate secretion of apolipoprotein B in Hep G2 cells. *J. Biol. Chem.* **268**: 22967-22970.

150. Lindgren, F. T., L. C. Jensen, and F. T. Hatch. 1972. The isolation and quantitation analysis of serum lipoprotein. In *Blood Lipid and Lipoproteins: Quantitation, Composition and Metabolism.* pp. 181-274.

151. Packard, C. J., A. Munro, A. R. Lorimer, Gotto, AM, and J. Shepherd. 1984. Metabolism of apolipoprotein B in large triglyceride-rich very low density lipoproteins of normal and hypertriglyceridemic subjects. *J. Clin. Invest.* **74**: 2178-2192.

152. Packard, C. J. and J. Shepherd. 1997. Lipoprotein heterogeneity and apolipoprotein B metabolism. *Arterioscler. Thromb. Vasc. Biol.* **17**: 3542-3556.

153. Rusiñol, A., H. Verkade, and J. E. Vance. 1993. Assembly of rat hepatic very low density lipoproteins in the endoplasmic reticulum. *J. Biol. Chem.* **268**: 3555-3562.

154. Swift, L. L. 1995. Assembly of very low density lipoproteins in rat liver: a study of nascent particles recovered from the rough endoplasmic reticulum. *J. Lipid Res.* **36**: 395-406.

155. Jones, A. L., N. B. Ruderman, and M. G. Herrera. 1967. Electron microscopic and biochemical study of lipoprotein synthesis in the isolated perfused rat liver. *J. Lipid Res.* **8**: 429-446.

156. Alexander, C. A., R. L. Hamilton, and R. J. Havel. 1976. Subcellular localization of B apoprotein of plasma lipoproteins in rat liver. *J. Cell Biol.* **69**: 241-263.

157. Cartwright, I. J. and J. A. Higgins. 1995. Intracellular events in the assembly of very-low-density-lipoprotein lipids with apolipoprotein B in isolated rabbit hepatocytes. *Biochem. J.* **310**: 897-907.

158. Higgins, J. A. 1988. Evidence that during very low density lipoprotein assembly in rat hepatocytes most of the triacylglycerol and phospholipid are packaged with apolipoprotein B in the Golgi complex. *FEBS Lett.* **232**: 405-408.

159. Cartwright, I. J. and J. A. Higgins. 1992. Quantification of apolipoprotein B-48 and B-100 in rat liver endoplasmic reticulum and Golgi fractions. *Biochem. J.* **285**: 153-159.

160. Bamberger, M. J. and M. D. Lane. 1988. Assembly of very low density lipoprotein in the hepatocyte. Differential transport of apoproteins through the secretory pathway. *J. Biol. Chem.* **263**: 11868-11878.

161. Rustaeus, S., P. Stillemark, K. Lindberg, D. Gordon, and S.-O. Olofsson. 1998. The microsomal triglyceride transfer protein catalyzes the post-translational assembly of apolipoprotein B-100 very low density lipoprotein in McA-RH7777 cells. *J. Biol. Chem.* **273**: 5196-5203.

162. Stillemark, P., S. Rustaeus, J. Borén, K.-A. Karlsson, T. Larsson, and S.-O. Olofsson. 1998. Studies on the assembly of apo-B48 VLDL in McA-RH7777 cells. *Circulation* **98, Suppl.**, I-390 (Abstract)

163. Gibbons, G. F. 1990. Assembly and secretion of hepatic very-low-density lipoprotein. *Biochem. J.* **268**: 1-13.

164. Hellerstein, M. K., M. Christiansen, S. Kaempfer, C. Kletke, K. Wu, J. S. Reid, K. Mulligan, N. S. Hellerstein, and C. H. Shackleton. 1991. Measurement of de novo hepatic lipogenesis in humans using stable isotopes. *J. Clin. Invest.* **87**: 1841-1852.

165. Duerden, J. M. and G. F. Gibbons. 1990. Storage, mobilization and secretion of cytosolic triacylglycerol in hepatocyte cultures. The role of insulin. *Biochem. J.* **272**: 583-587.

166. Wiggins, D. and G. F. Gibbons. 1992. The lipolysis/esterification cycle of hepatic triacylglycerol. Its role in the secretion of very-low-density lipoprotein and its response to hormones and sulphonylureas. *Biochem. J.* **284**: 457-462.

167. Nestel, P. J., W. E. Connor, M. F. Reardon, S. Connor, S. Wong, and R. Boston. 1984. Suppression by diets rich in fish oil of very low density lipoprotein production in man. *J. Clin. Invest.* **74**: 82-89.

168. Wong, S. H., P. J. Nestel, R. P. Trimble, G. B. Storer, R. J. Illman, and D. L. Topping. 1984. The adaptive effects of dietary fish and safflower oil on lipid and lipoprotein metabolism in perfused rat liver. *Biochim. Biophys. Acta* **792**: 103-109.

169. Parks, J. S., F. L. Johnson, M. D. Wilson, and L. L. Rudel. 1990. Effect of fish oil diet on hepatic lipid metabolism in nonhuman primates: lowering of secretion of hepatic triglyceride but not apoB. *J. Lipid Res.* **31**: 455-466.

170. Parks, J. S. and L. L. Rudel. 1990. Effect of fish oil on atherosclerosis and lipoprotein metabolism. *Atherosclerosis* **84**: 83-94.

171. Harris, W. S. 1989. Fish oils and plasma lipid and lipoprotein metabolism in humans: a critical review. *J. Lipid Res.* **30**: 785-807.

172. Wang, H., X. Chen, and E. A. Fisher. 1993. N-3 fatty acids stimulate intracellular degradation of apoprotein B in rat hepatocytes. *J. Clin. Invest.* **91**: 1380-1389.

173. Lang, C. A. and R. A. Davis. 1990. Fish oil fatty acids impair VLDL assembly and/or secretion by cultured rat hepatocytes. *J. Lipid Res.* **31**: 2079-2086.

174. Homan, R., J. E. Grossman, and H. J. Pownall. 1991. Differential effects of eicosapentaenoic acid and oleic acid on lipid synthesis and secretion by HepG2 cells. *J. Lipid Res.* **32**: 231-241.

175. Brown, A. M., J. Castle, A. M. Hebbachi, and G. F. Gibbons. 1999. Administration of n-3 fatty acids in the diets of rats or directly to hepatocyte cultures results in different effects on hepatocellular ApoB metabolism and secretion. *Arterioscler. Thromb. Vasc. Biol.* **19**: 106-114.

176. Hebbachi, A. M. and G. F. Gibbons. 1997. The effect of dietary n-3 fatty acids on the assembly and secretion of very low density lipoprotein by isolated rat hepatocytes. *Biochem. Soc. Trans.* **25**: S683.

177. Brown, A. M., P. W. Baker, and G. F. Gibbons. 1997. Changes in fatty acid metabolism in rat hepatocytes in response to dietary n-3 fatty acids are associated with changes in the intracellular metabolism and secretion of apolipoprotein B-48. *J. Lipid Res.* **38**: 469-481.

178. Geelen, M. J., W. J. Schoots, C. Bijleveld, and A. C. Beynen. 1995. Dietary medium-chain fatty acids raise and (n-3) polyunsaturated fatty acids lower hepatic triacylglycerol synthesis in rats. *J. Nutr.* **125**: 2449-2456.

179. Harris, W. S., W. E. Connor, D. R. Illingworth, D. W. Rothrock, and D. M. Foster. 1990. Effects of fish oil on VLDL triglyceride kinetics in humans. *J. Lipid Res.* **31**: 1549-1558.

180. Mooney, R. A. and M. D. Lane. 1981. Formation and turnover of triglyceride-rich vesicles in the chick liver cell. Effects of cAMP and carnitine on triglyceride mobilization and conversion to ketones. *J. Biol. Chem.* **256**: 11724-11733.

181. Yang, L. Y., A. Kuksis, J. J. Myher, and G. Steiner. 1995. Origin of triacylglycerol moiety of plasma very low density lipoproteins in the rat: structural studies. *J. Lipid Res.* **36**: 125-136.

182. Yang, L. Y., A. Kuksis, J. J. Myher, and G. Steiner. 1996. Contribution of de novo fatty acid synthesis to very low density lipoprotein triacylglycerols: evidence from mass isotopomer distribution analysis of fatty acids synthesized from [$^2H_6$]ethanol. *J. Lipid Res.* **37**: 262-274.

183. Gibbons, G. F., S. M. Bartlett, C. E. Sparks, and J. D. Sparks. 1992. Extracellular fatty acids are not utilized directly for the synthesis of very-low-density lipoprotein in primary cultures of rat hepatocytes. *Biochem. J.* **287**: 749-753.

184. Francone, O. L., A. D. Kalopissis, and G. Griffaton. 1989. Contribution of cytoplasmic storage triacylglycerol to VLDL-triacylglycerol in isolated rat hepatocytes. *Biochim. Biophys. Acta* **1002**: 28-36.

185. Lehner, R. and R. Verger. 1997. Purification and characterization of a porcine liver microsomal triacylglycerol hydrolase. *Biochemistry* **36**: 1861-1868.

186. Lehner, R., Z. Cui, and D. E. Vance. 1999. Subcellullar localization, developmental expression and characterization of a liver triacylglycerol hydrolase. *Biochem. J.* **338**: 761-768.

187. Pease, R. J., D. Wiggins, E. D. Saggerson, J. Tree, and G. F. Gibbons. 1999. Metabolic characteristics of a human hepatoma cell line stably transfected with hormone-sensitive lipase. *Biochem. J.* **341**: 453-460.

188. Lankester, D. L., A. M. Brown, and V. A. Zammit. 1998. Use of cytosolic triacylglycerol hydrolysis products and of exogenous fatty acid for the synthesis of triacylglycerol secreted by cultured rat hepatocytes. *J. Lipid Res.* **39**: 1889-1895.

189. Thrift, R. N., T. M. Forte, B. E. Cahoon, and V. G. Shore. 1986. Characterization of lipoproteins produced by the human liver cell line, Hep G2, under defined conditions. *J. Lipid Res.* **27**: 236-250.

190. Gibbons, G. F., R. Khurana, A. Odwell, and M. C. Seelaender. 1994. Lipid balance in HepG2 cells: active synthesis and impaired mobilization. *J. Lipid Res.* **35**: 1801-1808.

191. Kondrup, J., S. E. Damgaard, and P. Fleron. 1979. Metabolism of palmitate in perfused rat liver. Computer models of subcellular triacylglycerol metabolism. *Biochem. J.* **184**: 73-81.

192. Owen, M. R., C. C. Corstorphine, and V. A. Zammit. 1997. Overt and latent activities of diacylglycerol acytransferase in rat liver microsomes: possible roles in very-low-density lipoprotein triacylglycerol secretion. *Biochem. J.* **323**: 17-21.

193. Gibbons, G. F. and D. Wiggins. 1995. The enzymology of hepatic very-low-density lipoprotein assembly. *Biochem. Soc. Trans.* **23**: 495-500.

194. Zammit, V. A. 1996. Role of insulin in hepatic fatty acid partitioning: emerging concepts. *Biochem. J.* **314**: 1-14.

195. Cases, S., S. J. Smith, Y. W. Zheng, H. M. Myers, S. R. Lear, E. Sande, S. Novak, C. Collins, C. B. Welch, A. J. Lusis, S. K. Erickson, and R. V. Farese, Jr. 1998. Identification of a gene encoding an acyl CoA:diacylglycerol acyltransferase, a key enzyme in triacylglycerol synthesis. *Proc. Natl. Acad. Sci. U. S. A.* **95**: 13018-13023.

196. Wiggins, D. and G. F. Gibbons. 1996. Origin of hepatic very-low-density lipoprotein triacylglycerol: the contribution of cellular phospholipid. *Biochem. J.* **320**: 673-679.

197. Gavino, V. C., J. S. Miller, J. M. Dillman, G. E. Milo, and D. G. Cornwell. 1981. Polyunsaturated fatty acid accumulation in the lipids of cultured fibroblasts and smooth muscle cells. *J. Lipid Res.* **22**: 57-62.

198. Rosenthal, M. D. 1980. Selectivity in incorporation, utilization and retention of oleic and linoleic acids by human skin fibroblasts. *Lipids* **15**: 838-848.

199. Spring, D. J., S. M. Lee, D. L. Puppione, M. Phillips, J. Elovson, and V. N. Schumaker. 1992. Identification of a neutral lipid core in a transiently expressed and secreted lipoprotein containing an apoB-48-like apolipoprotein. *J. Lipid Res.* **33**: 233-240.

200. Vermeulen, P. S., S. Lingrell, Z. Yao, and D. E. Vance. 1997. Phosphatidylcholine biosynthesis is required for secretion of truncated apolipoprotein Bs from McArdle RH7777 cells only when a neutral lipid core is formed. *J. Lipid Res.* **38**: 447-458.

201. Coleman, R. and R. M. Bell. 1978. Evidence that biosynthesis of phosphatidylethanolamine, phosphatidylcholine, and triacylglycerol occurs on the cytoplasmic side of microsomal vesicles. *J. Cell Biol.* **76**: 245-253.

202. Scow, R. O. and E. J. Blanchette-Mackie. 1985. Why fatty acids flow in cell membranes. *Prog. Lipid Res.* **24**: 197-241.

203. Hamilton, R. L., J. S. Wong, C. M. Cham, L. B. Nielsen, and S. G. Young. 1998. Chylomicron-sized lipid particles are formed in the setting of apolipoprotein B deficiency. *J. Lipid Res.* **39**: 1543-1557.

204. Cartwright, I. J., J. A. Higgins, J. Wilkinson, S. Bellavia, J. S. Kendrick, and J. M. Graham. 1997. Investigation of the role of lipids in the assembly of very low density lipoproteins in rabbit hepatocytes. *J. Lipid Res.* **38**: 531-545.

205. Small, D. M. 1997. Physical behavior of lipase substrates. *Methods Enzymol.* **286**: 153-167.

206. Broadway, N. M. and E. D. Saggerson. 1995. Microsomal carnitine acyltransferases. *Biochem. Soc. Trans.* **23**: 490-494.

207. Broadway, N. M. and E. D. Saggerson. 1995. Solubilization and separation of two distinct carnitine acyltransferases from hepatic microsomes: characterization of the malonyl-CoA-sensitive enzyme. *Biochem. J.* **310**: 989-995.

208. Abumrad, N., C. Harmon, and A. Ibrahimi. 1998. Membrane transport of long-chain fatty acids: evidence for a facilitated process. *J. Lipid Res.* **39**: 2309-2318.

209. van Greevenbroek, M. M., M. G. Robertus-Teunissen, D. W. Erkelens, and T. W. de Bruin. 1998. Participation of the microsomal triglyceride transfer protein in lipoprotein assembly in Caco-2 cells: interaction with saturated and unsaturated dietary fatty acids. *J. Lipid Res.* **39**: 173-185.

210. Raabe, M., L. M. Flynn, C. H. Zlot, J. S. Wong, M. M. Véniant, R. L. Hamilton, and S. G. Young. 1998. Knockout of the abetalipoproteinemia gene in mice: reduced lipoprotein secretion in heterozygotes and embryonic lethality in homozygotes. *Proc. Natl. Acad. Sci. U. S. A.* **95**: 8686-8691.

211. Rustaeus, S., K. Lindberg, J. Borén, and S.-O. Olofsson. 1995. Brefeldin A reversibly inhibits the assembly of apoB containing lipoproteins in McA-RH7777 cells. *J. Biol. Chem.* **270**: 28879-28886.

212. Klausner, R. D., J. G. Donaldson, and J. Lippincott-Schwartz. 1992. Brefeldin A: insights into the control of membrane traffic and organelle structure. *J. Cell Biol.* **116**: 1071-1080.

213. Standerfer, S. B. and P. Handler. 1955. Fatty liver induced by orotic acid feeding. *Proc. Soc. Exp. Biol. Med.* **90**: 270-271.

214 Von Euler, L. H. and H. G. Windmueller. 1967. Fatty liver in the rat after intravenous infusion of orotic acid. *Proc. Soc. Exp. Biol. Med.* **125**: 1251-1254.

215. Windmueller, H. G. 1964. An orotic acid-induced, adenine-reversed inhibition of hepatic lipoprotein secretion in the rat. *J. Biol. Chem.* **239**: 530-537.

216. Windmueller, H. G. and R. I. Levy. 1967. Total inhibition of hepatic beta-lipoprotein production in the rat by orotic acid. *J. Biol. Chem.* **242**: 2246-2254.

217. Novikoff, A. B., P. S. Roheim, and N. Quintana. 1966. Changes in rat liver cells induced by orotic acid feeding. *Laboratory Investigation* **15**: 27-49.

218. Jatlow, P., W. R. Adams, and R. E. Handschumacher. 1965. Pathogenesis of orotic acid-induced fatty change in the rat liver. Light and electron microscopic studies. *Am. J. Pathol.* **47**: 125-145.

219. Pottenger, L. A. and G. S. Getz. 1971. Serum lipoprotein accumulation in the livers of orotic acid-fed rats. *J. Lipid Res.* **12**: 450-459.

220. Hay, R., R. Fleming, W. O'Connell, J. Kirschner, and W. Oppliger. 1988. Apolipoproteins of the orotic acid fatty liver: implications for the biogenesis of plasma lipoproteins. *J. Lipid Res.* **29**: 981-995.

221. Pottenger, L. A., L. E. Frazier, L. H. DuBien, G. S. Getz, and R. W. Wissler. 1973. Carbohydrate composition of lipoprotein apoproteins isolated from rat plasma and from the livers of rats fed orotic acid. *Biochem. Biophys. Res. Commun.* **54**: 770-776.

222. Rajalakshmi, S., W. R. Adams, and R. E. Handschumacher. 1969. Isolation and characterization of low density structures from orotic acid-induced fatty livers. *J. Cell Biol.* **41**: 625-636.

223. Novikoff, P. M., P. S. Roheim, A. B. Novikoff, and D. Edelstein. 1974. Production and prevention of fatty liver in rats fed clofibrate and orotic acid diets containing sucrose. *Laboratory Investigation* **30**: 732-750.

224. Hamilton, R. L., L. S. Guo, T. E. Felker, Y. S. Chao, and R. J. Havel. 1986. Nascent high density lipoproteins from liver perfusates of orotic acid-fed rats. *J. Lipid Res.* **27**: 967-978.

225. Cartwright, I. J., A. M. Hebbachi, and J. A. Higgins. 1993. Transit and sorting of apolipoprotein B within the endoplasmic reticulum and Golgi compartments of isolated hepatocytes from normal and orotic acid-fed rats. *J. Biol. Chem.* **268**: 20937-20952.

226. Handschumacher, R. E., W. A. Creasey, J. J. Jaffe, C. A. Pasternak, and L. Hankin. 1960. Biochemical and nutritional studies on the induction of fatty livers by dietary orotic acid. *Proc. Natl. Acad. Sci. U. S. A.* **46**: 178-186.

227. Windmueller, H. G. and A. E. Spaeth. 1966. Perfusion in situ with tritium oxide to measure hepatic lipogenesis and lipid secretion. Normal and orotic acid-fed rats. *J. Biol. Chem.* **241**: 2891-2899.

228. Kane, J. P., D. A. Hardman, and H. E. Paulus. 1980. Heterogeneity of apolipoprotein B: isolation of a new species from human chylomicrons. *Proc. Natl. Acad. Sci. U. S. A.* **77**: 2465-2469.

229. Yao, Z. and R. S. McLeod. 1994. Synthesis and secretion of hepatic apolipoprotein B-containing lipoproteins. *Biochim. Biophys. Acta Lipids Lipid Metab.* **1212**: 152-166.

230. Wetterau, J. R., R. E. Gregg, T. W. Harrity, C. Arbeeny, M. Cap, F. Connolly, C.-H. Chu, R. J. George, D. A. Gordon, H. Jamil, K. G. Jolibois, L. K. Kunselman, S.-J. Lan, T. J. Maccagnan, B. Ricci, M. Yan, D. Young, Y. Chen, O. M. Fryszman, J. V. Logan, C. L. Musial, M. A. Poss, J. A. Robl, L. M. Simpkins, W. A. Slusarchyk, R. Sulsky, P. Taunk, D. R. Magnin, J. A. Tino, R. M. Lawrence, J. K. Dickson, Jr., and S. A. Biller. 1998. An MTP inhibitor that normalizes atherogenic lipoprotein levels in WHHL rabbits. *Science* **282**: 751-754.

231. Selby, S. L. and Z. Yao. 1995. Level of apolipoprotein B mRNA has an important effect on the synthesis and secretion of apolipoprotein B-containing lipoproteins - Studies on transfected hepatoma cell lines expressing recombinant human apolipoprotein B. *Arterioscler. Thromb. Vasc. Biol.* **15**: 1900-1910.

232. Pease, R. J., R. W. Milne, W. K. Jessup, A. Law, P. Provost, J. C. Fruchart, R. T. Dean, Y. L. Marcel, and J. Scott. 1990. Use of bacterial expression cloning to localize the epitopes for a series of monoclonal antibodies against apolipoprotein B100. *J. Biol. Chem.* **265**: 553-568.

233. Lowry, O. H., N. J. Rosebrough, A. L. Farr, and R. J. Randall. 1955. Protein measurement with the Folin phenol reagent. *J. Biol. Chem.* **193**: 265-275.

234. Neri, B. P. and C. S. Frings. 1973. Improved method for determination of triglycerides in serum. *Clin. Chem.* **19**: 1201-1202.

235. Hussain, M. M., Y. Zhao, R. K. Kancha, B. D. Blackhart, and Z. Yao. 1995. Characterization of recombinant human apoB-48-containing lipoproteins in rat hepatoma McA-RH7777 cells transfected with apoB-48 cDNA. Overexpression of apoB-48 decreases synthesis of endogenous apoB-100. *Arterioscler. Thromb. Vasc. Biol.* **15**: 485-494.

236. Higgins, J. A. and J. L. Hutson. 1984. The roles of Golgi and endoplasmic reticulum in the synthesis and assembly of lipoprotein lipids in rat hepatocytes. *J. Lipid Res.* **25**: 1295-1305.

237. Macri, J. and K. Adeli. 1997. Studies on intracellular translocation of apolipoprotein B in a permeabilized HepG2 system. *J. Biol. Chem.* **272**: 7328-7337.

238. Wang, Y., R. S. McLeod, and Z. Yao. 1997. Normal activity of microsomal triglyceride transfer protein is required for the oleate-induced secretion of very low density lipoproteins containing apolipoprotein B from McA-RH7777 cells. *J. Biol. Chem.* **272**: 12272-12278.

239. Moss, J. and M. Vaughan. 1998. Molecules in the ARF orbit. *J. Biol. Chem.* **273**: 21431-21434.

240. Aalto-Setala, K., E. A. Fisher, X. Chen, T. Chajek-Shaul, T. Hayek, R. Zechner, A. Walsh, R. Ramakrishnan, H. N. Ginsberg, and J. L. Breslow. 1992. Mechanism of hypertriglyceridemia in human apolipoprotein (apo) CIII transgenic mice.

Diminished very low density lipoprotein fractional catabolic rate associated with increased apo CIII and reduced apo E on the particles. *J. Clin. Invest.* **90**: 1889-1900.

241. Huang, Y., X. Q. Liu, S. C. Rall, Jr., J. M. Taylor, A. von Eckardstein, G. Assmann, and R. W. Mahley. 1998. Overexpression and accumulation of apolipoprotein E as a cause of hypertriglyceridemia. *J. Biol. Chem.* **273**: 26388-26393.

242. Hebbachi, A. M., A. M. Brown, and G. F. Gibbons. 1999. Suppression of cytosolic triacylglycerol recruitment for very low density lipoprotein assembly by inactivation of microsomal triglyceride transfer protein results in a delayed removal of apoB-48 and apoB-100 from microsomal and Golgi membranes of primary rat hepatocytes. *J. Lipid Res.* **40**: 1758-1768.

243. Davis, R.A. and J.E. Vance. 1996. Structure, assembly and secretion of plasma lipoproteins. In *Biochemistry of lipids, lipoproteins and membranes.* 3 ed. Edited by D. E. Vance, and J.E. Vance. Elsevier Science B.V. pp. 473-493.

244. Yao, Z., and D.E. Vance. 1988. The active synthesis of phosphatidylcholine is required for very low density lipoprotein secretion from rat hepatocytes. *J. Biol. Chem.* **263**: 2998-3004.

Curriculum Vitae
Yuwei Wang

Date of Birth: August 4, 1969

Gender: Male

Home address: 511 Courtland Place,
Ottawa, Ontario,
Canada K2C 3T7

Work address: Lipoprotein and Atherosclerosis Group,
University of Ottawa Heart Institute, H447
40 Ruskin Street,
Ottawa, Ontario
Canada K1Y 4W7
Phone: (613)-798-5555 ext. 8712
Fax: (613)-761-5281
e-mail: ywang@ottawaheart.ca

Education:

1987-1990	MD program, Shanghai Medical University, Shanghai, China
1990-1993	BSc (Honors), Biochemistry, University of Manitoba, Winnipeg, Manitoba
1993-1994	MSc candidate, Biochemistry, University of Alberta, Edmonton, Alberta
1994-1999	PhD candidate, Biochemistry, University of Ottawa, Ottawa, Ontario

Distinctions and Awards:

1988-1990	Shanghai Medical University Medical Training Scholarship
1990-1992	Reverend Joseph Hogg Scholarship (University of Manitoba)
1991-1992	A.N. Campbell Scholarship (University of Manitoba)
1993	Graduation with first class honors in Science (University of Manitoba)
1993	University of Manitoba Graduate Fellowship
1995-1998	Heart and Stroke Foundation of Canada Research Traineeship
1995-1999	University of Ottawa Excellence Scholarship
1997-1999	Natural Sciences and Engineering Research Council of Canada Postgraduate Scholarship
1999	University of Ottawa Doctoral Research Scholarship

Professional Societies:

1994-	Member, Canadian Society of Biochemistry and Molecular Biology
1997-	Member, American Society for Cell Biology

Publications:

A. Refereed papers:

1. McLeod, R.S., **Wang, Y.,** Wang, S., Rusiñol, A., Links, P., Yao, Z. (1996) Apolipoprotein B sequence requirements for hepatic very low density lipoprotein assembly. *J. Biol. Chem.* **271**, 18445-18455.

2. **Wang, Y.**, McLeod, R.S., Yao, Z. (1997) Normal activity of microsomal triglyceride transfer protein is required for the oleate-induced secretion of very low density lipoproteins containing apolipoprotein B from McA-RH7777 Cells. *J. Biol. Chem.* **272**, 12272-12278.
3. Avramoglu, R. K., Nimpf, J., Ko, K., **Wang, Y.**, FitzGerald, D., and Yao, Z. (1998) Functional expression of the chicken LDL receptor-related protein in a mutant CHO cell line restores toxicity of Pseudomonas exotoxin A and degradation of α_2-macroglobulin. *J. Biol. Chem.* **273**, 6057-6065.
4. Tran, K., Borén, J., Macri, J., **Wang, Y.**, McLeod, R. S., Avramoglu, R. K., Adeli, K., and Yao, Z. (1998) Functional analysis of disulfide linkages clustered within the amino terminus of human apolipoprotein B. *J. Biol. Chem.* **273**, 7244-7251.
5. **Wang, Y.**, Tran, K., and Yao, Z. (1999) The activity of microsomal triglyceride transfer protein is essential for accumulation of triglyceride within microsomes in McA-RH7777 cells. A unified model for the assembly of very low density lipoproteins. *J. Biol. Chem.* **274**, 27793-27800.
6. Tran, K., **Wang, Y.**, and Yao, Z. The Ca^{2+}-independent phospholipase A_2 is required for the assembly and secretion of triglyceride-rich lipoproteins from rat hepatoma McA-RH7777 cells. (manuscript submitted to *J. Biol. Chem.*)

B. Conference abstracts:

1. **Wang, Y.**, McLeod, R.S., Wang, S., and Yao, Z. (1995) Characterization of protein and lipid origin of apoB48-containing VLDL in transfected hepatoma McA-RH7777 cells. (Canadian Lipoprotein Conference, Jasper, Alberta)
2. **Wang, Y.**, McLeod, R.S., and Yao, Z. (1995) Secretion of hepatic very low density lipoprotein is mediated by apoB sequences enriched in amphipathic β-strands. *Can. J. Cardiol.* 11 Suppl. E: 126E. (Canadian Cardiovascular Society 48th Annual Meeting, Toronto, Ontario)
3. **Wang, Y.**, Wang, X., Franklin, V., and Yao, Z. (1995) The second step assembly of hepatic apolipoprotein B48-containing very low density lipoprotein does not utilize newly synthesized triglycerides. *Circulation* **92(8)** Suppl. I-227. (American Heart Association 68th Scientific Sessions, Anaheim, California)
4. McLeod, R.S., **Wang, Y.**, Wang, S., Franklin, V., and Yao, Z. (1995) Assembly of hepatic very low density lipoprotein is mediated by sequences within the amphipathic β-strand cluster of human apolipoprotein B48. *Circulation* **92(8)** Suppl. I-228. (American Heart Association 68th Scientific Sessions, Anaheim, California)
5. **Wang, Y.**, and Yao, Z. (1996) Distinct lipid and protein requirements for the hepatic assembly and secretion of apoB48-VLDL and apoB100-VLDL: studies of rat hepatoma McA-RH7777 cells transfected with recombinant human apoB cDNA. (Canadian Lipoprotein Conference, Ottawa, Ontario)
6. Avramoglu, R.K., **Wang, Y.**, Ko, K., and Yao, Z. (1996) Factor(s) involved in the surface presentation of LDL receptor-related protein (LRP): studies of COS-7 cells transfected with the chicken LRP cDNA. (Canadian Lipoprotein Conference, Ottawa, Ontario)
7. Avramoglu, R.K., **Wang, Y.**, Nimpf, J., Ko, K., and Yao, Z. (1996) Expression of somatic LDL receptor-related protein (LRP) of chicken. *Molecular Biology of the Cell* **7**, Suppl. 430a. (6th International Congress on Cell Biology and 36th American Society for Cell Biology Annual Meeting, San Francisco, California)
8. **Wang, Y.**, and Yao, Z. (1997) Assembly of large very low density lipoproteins is accomplished through a two-step lipidation process. (University of Ottawa Heart Institute Research Day, Ottawa, Ontario)

9. Avramoglu, R. K., Nimpf, J., Ko, K., **Wang, Y.**, FitzGerald, D., and Yao, Z. (1997) Functional expression of the chicken LDL receptor related protein in a mutant CHO cell line restores sensitivity to Pseudomonas exotoxin. (The 40th Annual Meeting of Canadian Federation of Biological Societies, Quebec City, Quebec)
10. McLeod, R. S., **Wang, Y.**, and Yao, Z. (1997) Microsomal triglyceride transfer protein activity is required for the second step in VLDL formation in rat hepatoma cells. (The 40th Annual Meeting of Canadian Federation of Biological Societies, Quebec City, Quebec)
11. Yao, Z., McLeod, R.S., and **Wang, Y.** (1997) Inhibition of microsomal triglyceride transfer protein (MTP) decreases secretion of oleate-induced triglyceride-rich very low density lipoproteins (VLDL) from hepatoma cells. *Atherosclerosis* 134, 356. (the 11th International Symposium on Atherosclerosis, Paris, France)
12. **Wang, Y.**, Ooi, T. C., and Yao, Z. (1997) Utilization of hepatic storage triglycerides for the assembly of large apoB100-VLDL (S_f> 100) requires microsomal triglyceride transfer protein activity. (The Kern Aspen Lipid Conference, Aspen, Colorado)
13. Tran, K. T., Borén, J., **Wang, Y.**, McLeod, R. S., Avramoglu, R. K., and Yao, Z. (1997) Functional analysis of disulfide linkages clustered within the amino terminus of human apolipoprotein B. (The Kern Aspen Conference, Aspen, Colorado)
14. Tran, K. T., Borén, J., **Wang, Y.**, McLeod, R. S., Avramoglu, R. K., and Yao, Z. (1997) The disulfide bonds that are clustered within the N-terminus of human apoB are essential for lipoprotein assembly and apoB secretion. *Circulation* **96,** Suppl. I-227. (American Heart Association 70th Scientific Sessions, Orlando, Florida)
15. Avramoglu, R. K., Nimpf, J., Ko, K. W. S., McLeod, R. S., **Wang, Y.**, FitzGerald, D. J., and Yao, Z. (1997) Functional expression of recombinant chicken LDL receptor-related protein mutants in a deficient cell line. *Molecular Biology of the Cell* **8,** Suppl. 80a. (7th International Congress on Cell Biology and 37th American Society for Cell Biology Annual Meeting, Washington D.C.)
16. **Wang, Y.**, Tran, K., and Yao, Z. (1998) Appropriate lipid mobilization within microsome is crucial for hepatic very low density lipoproteins (VLDL) assembly. (University of Ottawa Heart Institute Research Day, Ottawa, Ontario)
17. Tran, K., **Wang, Y.**, and Yao, Z. (1998) Phospholipid turnover mediated by the calcium-independent phospholipase A_2 is required for assembly and secretion of triglyceride-rich lipoproteins from rat hepatoma McA-RH7777 cells. (FASEB Summer Research Conferences 1998, Saxtons River, Vermont)
18. **Wang, Y.**, Tran, K., and Yao, Z. (1998) MTP is required for sequestration of lipid into microsomal lumen but not for translation/translocation of apoB. (The 23rd Annual Canadian Lipoprotein Conference, Muskoka, Ontario)
19. Tran, K., **Wang, Y.**, and Yao, Z. (1998) Phospholipid turnover mediated by iPLA$_2$ is associated with assembly/secretion of VLDL. (The 23rd Annual Canadian Lipoprotein Conference, Muskoka, Ontario)
20. **Wang, Y.**, Tran, K., Ooi, T.C., and Yao, Z. (1998) New insights into directional lipid mobilization mediated by microsomal triglyceride transfer protein (MTP) and a brefeldin A (BfA) sensitive factor during B100-VLDL assembly. *Circulation* **98,** Suppl. I-178. (American Heart Association 71th Scientific Sessions, Dallas, Texas)
21. Tran, K., **Wang, Y.**, and Yao, Z. (1998) Phospholipid turnover mediated by the novel calcium-independent phospholipase A_2 is required for assembly and secretion of triglyceride-rich lipoproteins. *Circulation* **98,** Suppl. I-178. (American Heart Association 71th Scientific Sessions, Dallas, Texas)

A Statement of Contribution of Collaborators

For all the experimental works I presented in this thesis, I have taken charge of all the experimental designs, conducted the experiments, interpreted the data, and drawn the figures.

I acknowledge these collaborators' participation in conducting the following experiments:

Collaborator	Experimental results shown in
Xingyu Wang	Fig. 3.1.7.
Roger McLeod and Shelley Wang	Fig. 3.2.1.
Roger McLeod	Fig. 3.3.6.
Khai Tran	Fig. 3.4.1.- Fig. 3.4.4.